



# Kent Academic Repository

**Rose, Madison (2023) *Taxonomic and functional interpretation of associated cercopithecoid carpal bones (KB 5378) from Kromdraai B, South Africa.* Master of Science by Research (MScRes) thesis, University of Kent,.**

## Downloaded from

<https://kar.kent.ac.uk/99784/> The University of Kent's Academic Repository KAR

## The version of record is available from

## This document version

UNSPECIFIED

## DOI for this version

## Licence for this version

CC BY (Attribution)

## Additional information

## Versions of research works

### Versions of Record

If this version is the version of record, it is the same as the published version available on the publisher's web site. Cite as the published version.

### Author Accepted Manuscripts

If this document is identified as the Author Accepted Manuscript it is the version after peer review but before type setting, copy editing or publisher branding. Cite as Surname, Initial. (Year) 'Title of article'. To be published in *Title of Journal*, Volume and issue numbers [peer-reviewed accepted version]. Available at: DOI or URL (Accessed: date).

## Enquiries

If you have questions about this document contact [ResearchSupport@kent.ac.uk](mailto:ResearchSupport@kent.ac.uk). Please include the URL of the record in KAR. If you believe that your, or a third party's rights have been compromised through this document please see our [Take Down policy](https://www.kent.ac.uk/guides/kar-the-kent-academic-repository#policies) (available from <https://www.kent.ac.uk/guides/kar-the-kent-academic-repository#policies>).

**Title:** Taxonomic and functional interpretation of associated cercopithecoid carpal bones (KB 5378) from Kromdraai B, South Africa

**Authors:** Madison Rose<sup>1</sup>

**Affiliations:** 1 School of Anthropology and Conservation, University of Kent, Canterbury, UK

### **Abstract**

A partial carpus belonging to a large, South African Pliocene cercopithecoid was excavated from Kromdraai B (Gauteng, South Africa) between 1977 and 1981 alongside associated, late juvenile metacarpals 1-5 and several manual phalanges (KB 5378). Included in the KB 5378 carpus is a partial scaphoid, lunate, os centrale, trapezium, trapezoid, capitate, and hamate. Here I describe each carpal quantitatively and qualitatively in comparison to a sample of extant anthropoid primates to gain an understanding of both functional morphology and taxonomy of the KB 5378 fossils. Overall, the carpal morphology reflects that of a generalized quadruped with potential specializations for terrestrial, digitigrade locomotion. The absolute size of the carpus and metacarpals indicate that they are likely from the same individual but are more similar in size to that of *Papio* or *Parapapio* rather than the larger *Gorgopithecus major*, as previously suggested.

### Introduction

Understanding primate evolution requires drawing inferences about behavior, and particularly locomotion, from fossilized remains of the skeleton. The bones of the forearm, carpus (wrist) and hand have been used to reconstruct locomotor behavior in numerous fossil primates (Etter, 1973; Hamrick, 1996; Lovejoy et al., 2009; Marzke, 1983; McCrossin et al., 1998; O'Connor, 1975; Patel, 2010a, b; Schmitt, 2003; Vanhoof et al., 2021) based on morphological variation in extant primates (Daver 2012; Patel 2010a; Patel, 2010b; Richmond 2006; Vanhoof.et al. 2021). In particular, studies of carpal morphology have played an important role in reconstructing primate behavior in the past (Ciochon, 1993b; Frost et al., 2015; Kivell, 2016b; Lovejoy et al., 2009; Marzke, 1983; O'Connor, 1975; Orr, 2018; Tocheri et al., 2005). Here we describe for the first time the functional morphology of associated cercopithecoid carpal bones (KB 5378) from Kromdraai B, South Africa that were originally discovered during Elisabeth Vrba's excavations in 1977-1980. These carpal fossils include a partial scaphoid, and complete os centrale, lunate, hamate, capitate, trapezoid, and trapezium, all from the left side (Figure 1,3). They articulate well together and are considered to be from a single individual. Below I qualitatively and quantitatively describe the morphology of each carpal within a comparative context of extant cercopithecoids and hominoids from a diverse array of arboreal and terrestrial locomotor modes. The aim of this study is to determine

the likely taxonomic attribution and locomotor behavior of the primate that possessed these carpal bones.

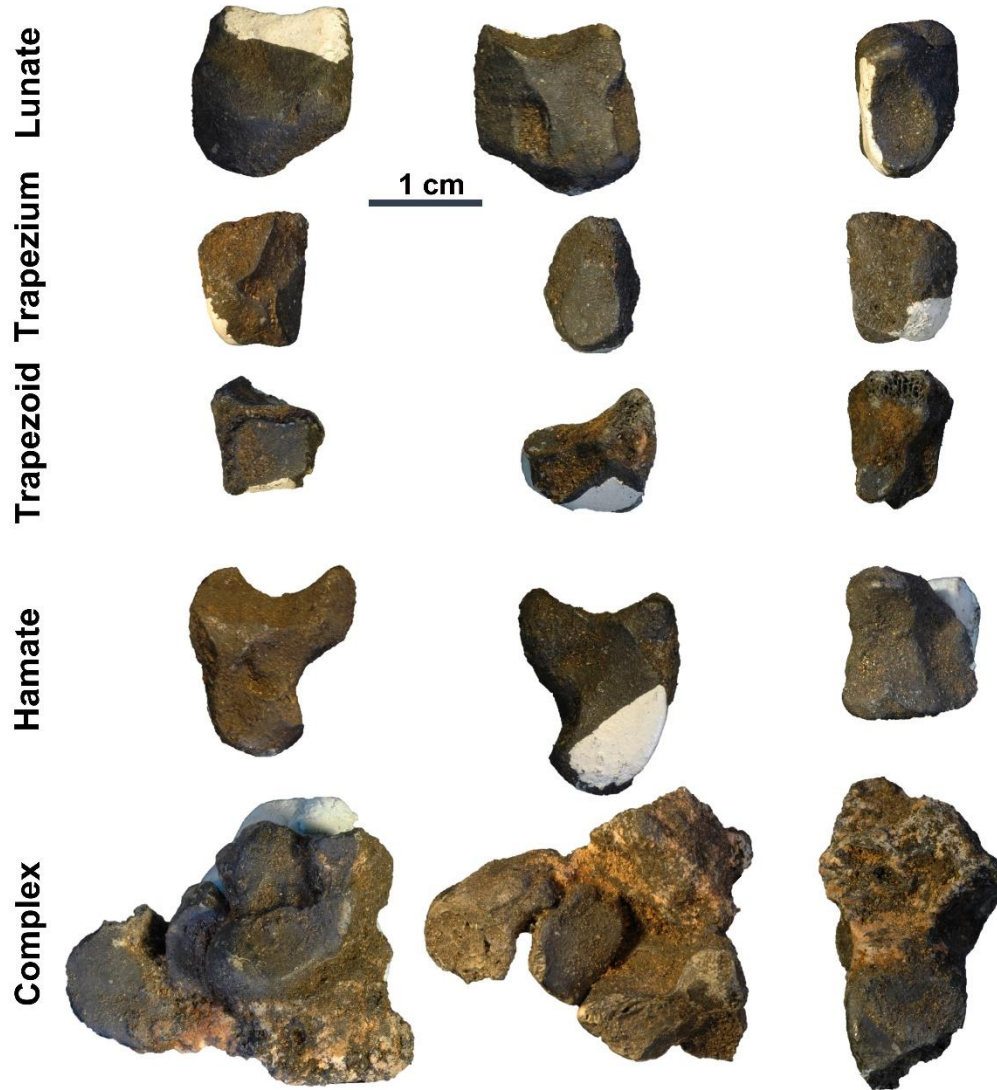


**Figure 1.** The KB 5378 carpal bones. Each bone is displayed in order to show the most informative morphology. From left to right, the lunate, trapezoid and hamate are shown in radial, ulnar and distal views and the trapezium is shown in palmar, ulnar and dorsal views. The complex still emdedded in stone (breccia) includes the capitate, os centrale and scaphoid fragment and is shown first to display the hamate facet of the capitate, ulnar view of the os centrale and partial lunate facet of the scaphoid fragment, then to show the distal facets of the capitate, the trapezium/trapezoid facet of the os centrale, and an oblique view of the scaphoid radial facet and the area of fragmentation, and lastly the proximal view of the radial facet of the scaphoid fragment. Each bone is scaled to the 1 cm

### KB 5378 carpal fossils

The KB 5378 carpal fossils in this study consist of several carpal bones that comprise a nearly complete left carpus. The capitate, os centrale and a large fragment of scaphoid form a complex held together by breccia, while the hamate, lunate, trapezoid, and trapezium are isolated (see figure 1, 2). Each carpal is well preserved, with the exception of the partial scaphoid that is missing its distal half and articulate well with each other.

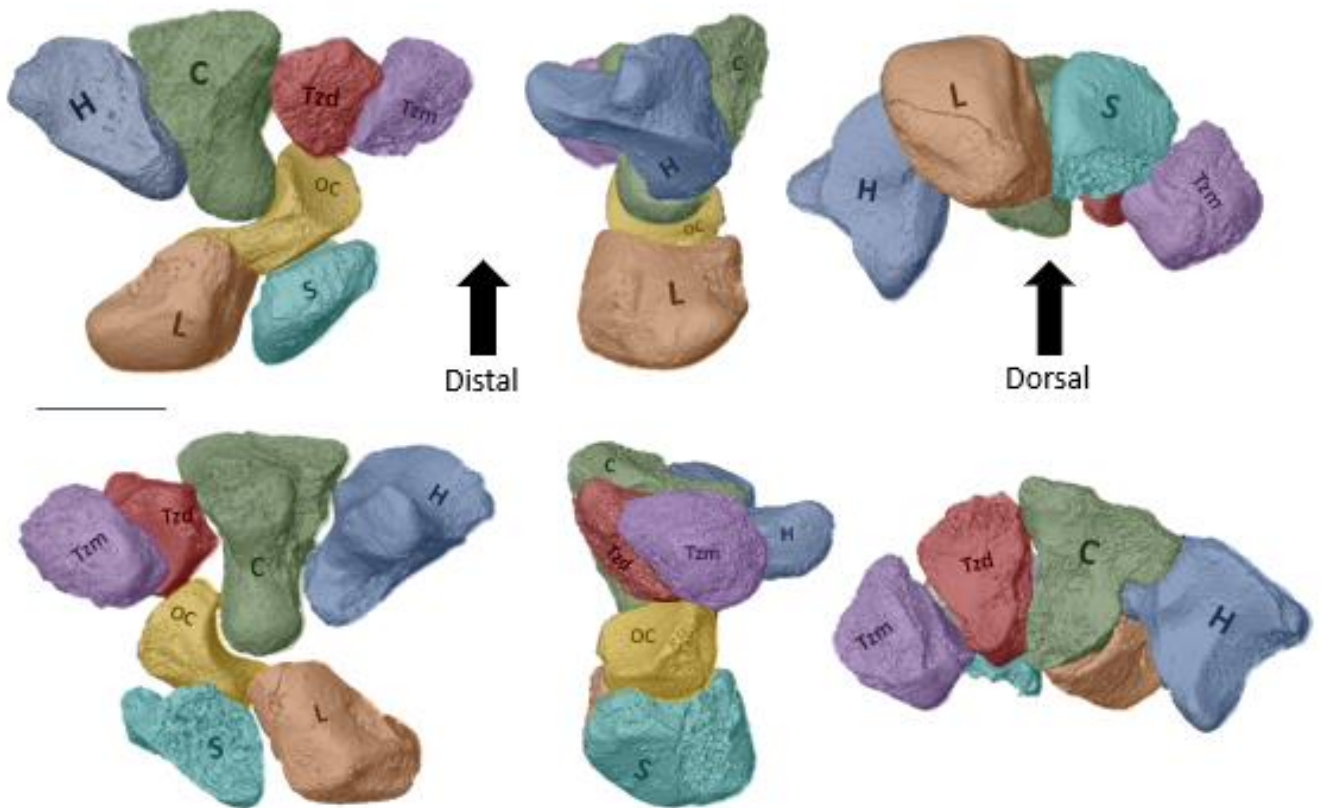


**Figure 2.** Surface models of the KB 5378 carpal bones shown in approximate articulation. H, hamate; C, capitate; Tzd, trapezoid; Tzm, trapezium; OC, os centrale; L, lunate; S, scaphoid.

The KB 5378 carpals are found within the context of several other fossils excavated from the surrounding breccia. The KB 5378 carpals were excavated directly adjacent to several other fossils in the surrounding breccia, including associated juvenile metacarpals and proximal phalanges, as well as a left hamate that are also assigned KB 5378 (Figure 3), a juvenile mandible with dentition of a large baboon (KB 5227), and a partial hominin dentition (KB 5223) (Vrba 1981, pers. comm Braga). The KB 5378

metacarpals and phalanges sample includes all five metacarpals and four proximal phalanges of the left hand and were initially reported as being from a large, juvenile baboon (Vrba 1981) but a full description of these hand bones has yet been completed. KB 5227 is a partial juvenile mandible preserving fully erupted second molars and premolars as well as unerupted third molars and a canine (Vrba 1981). Due to size, and in the case of KB 5227 similarities in third premolar lengths with additional *G. major* premolars from Kromdraai A (KA 150), both KB 5227 and KB 5378 wrist and hand bones have been suggested to belong to a juvenile *G. major* (Vrba 1981). Moreover, the KB 5378 carpals articulate well with the proximal metacarpals and display a similar color of preservation (Braga pers. comm.). Therefore, the carpals and hand bones of KB 5378 have been potentially attributed to the same individual (Vrba 1981, Braga pers. comm.)

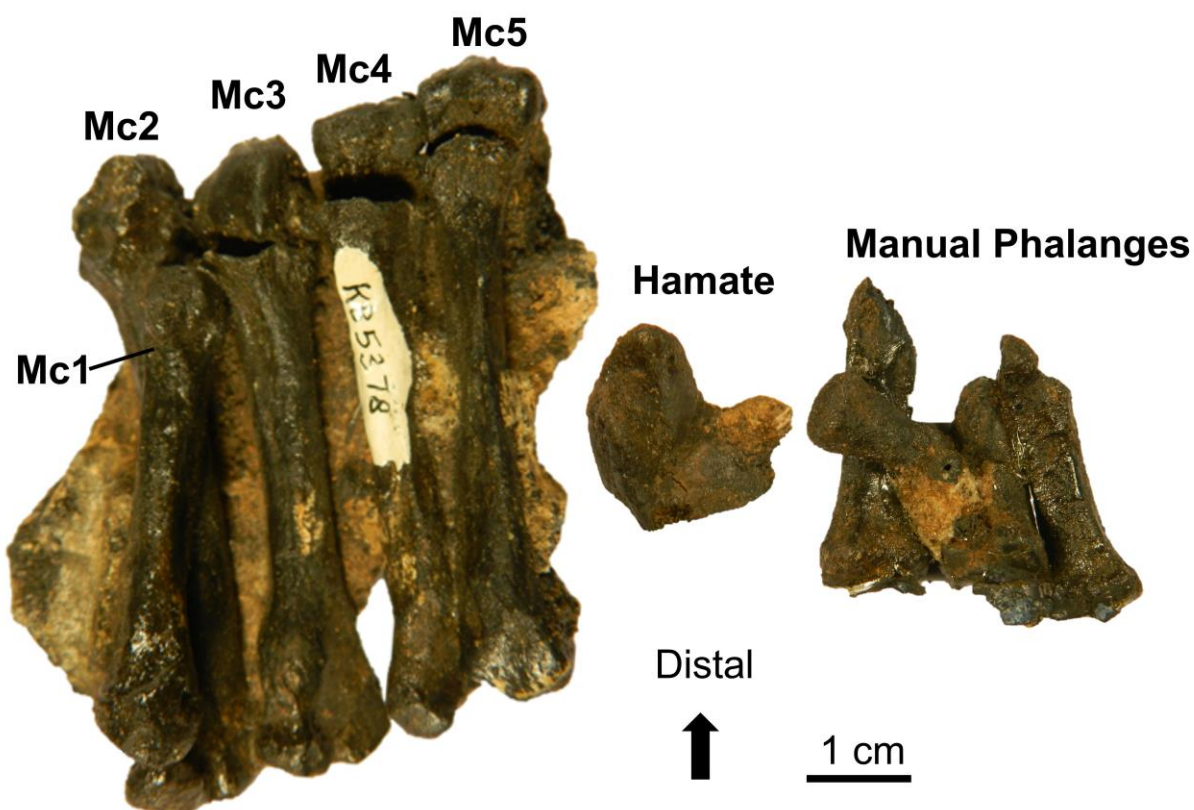


**Figure 3:** The KB 5378 associated metacarpals (left) hamate (center) and manual phalanges (right) associated with KB 5378. Phalanges are shown in palmar view. Photo credit: Mirriam Tawane.

Kromdraai is a hominin fossil-bearing site located within the Cradle of Humankind in the Gauteng province of South Africa approximately 2 km east of the Sterkfontein caves. Kromdraai is a roofless dolomitic cave that is delineated into three subareas: Kromdraai A (KA), Kromdraai B (KB) and Kromdraai C (KC) (Fig. 4) (Vrba 1981; Braga, et al. 2016). The KB 5378 carpal bones were uncovered in Kromdraai B, which is a rectangular, unroofed cave spanning approximately 3 m wide at its extreme ends and 40 m long at its surface (Bruxelles et al., 2016). Kromdraai B sedimentary deposits fill an east-west fissure approximately 46 m in length split on the western end by a pronounced dolomite bridge in a north-south direction (Bruxelles et al., 2016). Elizabeth Vrba further delineated KB broadly into KB East and KB West using this dolomite bridge (Vrba 1981). This site is described using a grid system established by Vrba (1981)), who led excavations of the site from 1977 through 1980. Using this grid, the KB 5378 fossils derive from breccia block 74, originally excavated at approximately 27.29 m east, 3 m north and 1.75 m below Vrba's datum point (see Fig. 4).

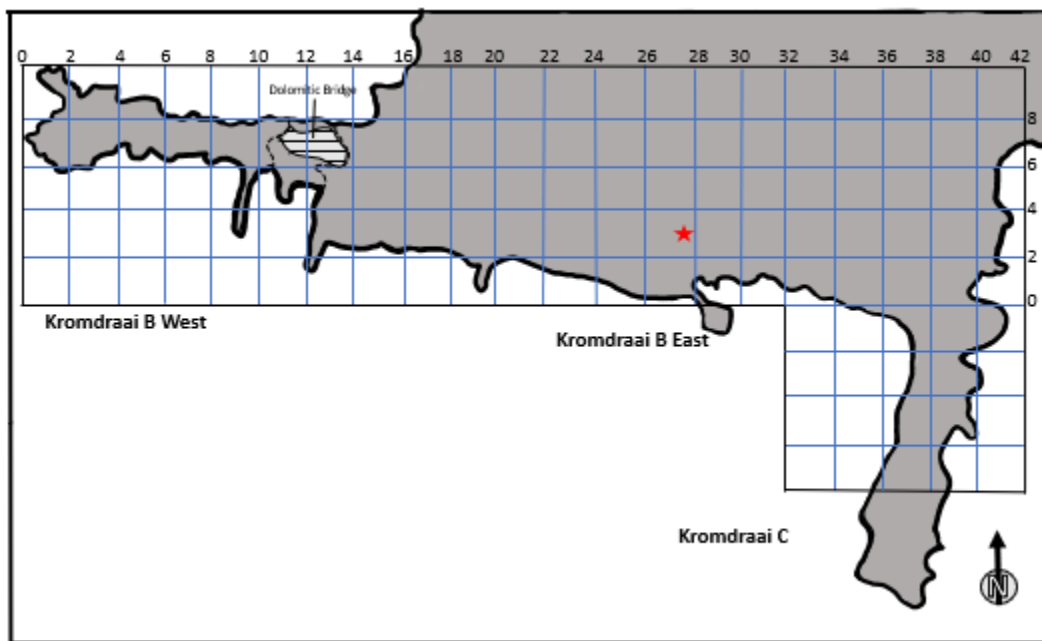


**Figure 4:** A map of Kromdraai B, the adjacent extension site and attached site Kromdraai C (adapted from Bruxelles 2016). Note that Kromdraai B is separated into West and East portions by the marked dolomitic bridge. Each square represents a 2x2m section. A red star indicates the location of the KB 5378 carpals in situ, at approximately 27.29m east, and 3m north. Not shown is the depth below datum that the fossils were excavated from, which was 1.75m below datum.

Using a combination of faunal reconstruction and paleomagnetic data, deposits within Kromdraai B have been tentatively dated between 1.5 and 2.0 million years old (Ma) (Thackeray 2002, Vrba 1981, Braga 2016, Fouvrel 2016). More specific studies of

the individual stratigraphic layers (members) within Kromdraai B are limited and have focused on using paleomagnetic reversals with reference to the Olduvai Event, an interval of time from 1.95 to 1.77 Ma during which normal magnetic polarity pervaded in the sediments of Africa (Tamrat 1994). Using the Olduvai event as a reference point in combination with faunal reconstruction, the age of the earliest members (1 and 2) of Kromdraai B is estimated to be c.1.9 Ma, just before the Olduvai Event took place (Thackeray 2002).

However, further complicating the dating process of individual specimens from Kromdraai is the fact that until 2014, most fossil discoveries at Kromdraai were made in *ex situ* breccia removed over the previous decades of excavation starting with those of Broom in 1938 (Broom (1940)); Brain (1975)); but see review in Thackeray (2017)). This method of excavation, in addition to the lack of comprehensive paleomagnetic and faunal assemblage studies, have resulted in a lack of consensus on the chronology of any Kromdraai fossils (Braga et al., 2016; Braga et al., 2017).

The reconstruction of the paleoecology of Kromdraai has yielded mixed results (see Thackeray (2017)) for review). Carbon isotope values from both soil carbonates and deep sea sediments indicate that woodland environments were replaced by grasslands in sub-Saharan Africa between 3.0 and 2.0 Ma (Braga et al., 2016). Therefore, at c. 1.9 Ma, Kromdraai B would fall at the end of the environmental shift to more open grasslands. Additionally, analyses of carbon-13 isotopes in attached breccia and calcite inclusion as well as fossil enamel of South African plio-pleistocene fossils have been interpreted as reflecting an increase of habitual feeding on grasses at this time (Braga et al., 2016; (Lee-Thorp et al., 2007)). However, paleoenvironmental reconstructions based on faunal remains, including the presence of leaf-eating monkeys throughout Kromdraai B, suggest it may have been more wooded than grassland (Braga et al., 2016; Fourvel et al., 2016). Regardless of the degree of closed wooded to open grasslands present at Kromdraai B, there are numerous indicators in the available fossil record that together suggest a largely terrestrial lifestyle present in the cercopithecoid primates (see below) that have been uncovered from the site (Benefit 1999; Benefit 1987; Ciochon 1993b; Delson, et al. 2000; Leakey 1982; McCrossin, et al. 1998). These adaptations include large body mass, large entheses on the forelimb bones for musculature required for terrestrial locomotion, flattened, and expanded joint surfaces of the long bones (relative to more arboreal primates) to increase stability, and foot bones (calcaneus) with facet morphology indicative of terrestrial locomotion (McCrossin, et al. 1998; Ciochon 1993b; Leakey 1982; Delson, et al. 2000). Furthermore, analyses of dental morphology indicate a diet containing a large proportion of ground level foliage (Benefit 1999; Benefit 1987; Delson, et al. 2000; Leakey 1982).

#### Fossil cercopithecoids from Kromdraai

In addition to being a well-known, hominin-rich site, Kromdraai B has produced an array of fossil cercopithecoids from at least five genera and multiple proposed species therein (Benefit, 1999; Broom, 1940; Broom and Robinson, 1949; Freedman, 1957; Vrba, 1981). Currently, the record of cercopithecine taxa from both Kromdraai A and B include the following taxa: *Parapapio jonesi* (Broom, 1940), *Papio robinsoni* (Freedman, 1957) *Papio angusticeps* (Broom, 1940; Freedman, 1957), *Papio izodi* (Gear, 1926), *Gorgopithecus major* (Broom and Robinson, 1949; Vrba, 1981), and *Theropithecus oswaldi* (Benefit, 1999; Broom, 1940; Broom and Robinson, 1949; Freedman, 1957; Hartwig, 2002; Vrba, 1981). Additionally, one colobine taxon, *Cercopithecoides williamsi* (van der Spuy Mollett, 1947), is also present at Kromdraai B. Each of these taxa is described in more detail below.

*Parapapio jonesi* is best represented at Sterkfontein with over 20 cranial and postcranial remains of both sexes deriving from its members, but is also found at Kromdraai B, Swartkrans, Taung and Makapansgat, as well as in East Africa (Hartwig 2002). Based on body mass (BM) reconstructions using both postcranial and craniodental remains, *Pa. jonesi* was likely a medium-sized (BM male mean 17 kg and female mean 13 kg; Delson et al. (2000); (Benefit, 1999; Frost and Delson, 2002) macaque-like cercopithecoid. Studies of postcranial remains (associated with crania) from Hadar, Ethiopia indicate humerus morphology similar to extant arboreally-adapted primates such as *Lophocebus* or *Cercopithecus mitis* in having a long, large and medially-projecting medial epicondyle and a short trochlear flange which permit mobility at the elbow joint in arboreal primates (Frost and Delson, 2002; Schmitt, 2003). However, the same study found morphological features of the femoral proximal and distal epiphyses that overlap with both arboreal and terrestrial taxa (Frost and Delson, 2002). Therefore, *Pa. jonesi* may have employed a mixture of terrestrial and arboreal behaviors (Frost and Delson 2002).

Three species from the genus *Papio* are found at Kromdraai A and/or B including *P. robinsoni* (mean BM for males 29kg and females 18kg; Delson et al. (2000); (Freedman, 1957), *P. angusticeps* (BM male mean 21 kg and female mean 16.5 kg; Bettridge and Dunbar 2012; Broom 1940; Freedman 1957) and *P. izodi* (BM male mean 20 kg, female mean 15 kg; Delson, et al. 2000; Gear 1926; Hartwig 2002). All *Papio* species are estimated to be larger in body mass than *Parapapio* based on body mass reconstructions using craniodental remains and exhibit a high degree of dental and body size sexual dimorphism (Gear 1926, Benefit 1999, Bettridge and Dunbar 2012, Delson 2000, Freedman 1957, Hartwig 2002, Ciochon 1993). Each of these taxa can also be found across fossil bearing sites in South and East Africa, including, among others, Kromdraai A and B, Swartkrans, Gladysvale, Sterkfontein, and the Omo Valley (Gear 1926, Benefit 1999, Bettridge and Dunbar 2012, Delson 2000, Freedman 1957, Hartwig 2002, Ciochon 1993). Additionally, though studies of the postcranial remains of *Papio* species are limited, most researchers agree that fossil *Papio* engaged primarily in

terrestrial locomotion much like extant *Papio* (Benefit, 1999; Bettridge and Dunbar, 2012; Ciochon, 1993b; Delson et al., 2000; Hartwig, 2002).

*Cercopithecoides williamsi* was a large (BM male mean 21 kg, female mean 15 kg; Delson et al. (2000)), terrestrial colobine known from fossil bearing sites across South and East Africa, including Kromdraai A and B, Sterkfontein, Bolts Farm, Makapansgat and Lake Turkana (Hartwig 2002). *C. williamsi* has teeth highly derived for folivory (Benefit 1999; Williams and Geissler 2014). Carbon isotopic analyses reveal that up to 60% of the diet of *C. williamsi* was likely comprised of grasses, suggesting not only a large proportion of foliage, but specifically a large proportion of ground level foliage being consumed (Williams and Geissler 2014). Moreover, a humerus of *C. williamsi* from Kenya (KNM-ER 4420) shows adaptations for quadrupedal terrestrial locomotion including a prominent greater tubercle, an extended medial flange and trochlea to stabilize the elbow joint, and a large olecranon process reflecting a strong triceps brachii (Williams and Geissler 2014). This diet and postcranial anatomy, in addition to the large body mass of *C. williamsi*, supports the likelihood of a primarily terrestrial lifestyle (Benefit, 1999; Leakey, 1982; Williams and Geissler, 2014). This species also exhibits the earliest known evidence of thumb reduction in colobine fossils, showing reduction of its first metacarpal to an equal degree of modern African colobine primates (Frost et al., 2015).

*Theropithecus oswaldi* is the largest cercopithecoid found at numerous sites throughout both South and East Africa, with a body mass estimate of between 42 and 72 kg for males and 24 kg for females (Delson et al., 2000). Based on a mix of molar morphology, and wear and striation patterns in the dentition of *T. oswaldi*, it is thought to have likely consumed ground level foliage that included a large amount of grit including grass blades, seeds and tubers (Benefit, 1999; Fleagle, 1998; Hartwig, 2002; Williams and Geissler, 2014). *T. oswaldi* has many postcranial adaptations, in addition to its large body mass, that suggest terrestrial locomotion. From the forelimb alone, *T. oswaldi* exhibits lengthened radial and ulnar styloid processes, an oblong, angled radial head, a posteriorly- projecting medial epicondyle, and expanded joint surfaces, all features considered advantageous for stabilizing the elbow and carpus in highly terrestrial cercopithecoids (Krentz 1993). However, *T. oswaldi* also had features associated with increased mobility of the shoulder joint, including a globular humeral head and narrow bicipital groove, as well as well-developed attachment on the proximal ulna for the main abductor of the thumb (m. abductor pollicis longus), suggesting it may have still been engaging in some arboreal behaviors (Krentz 1993). In addition, proximal ulna morphology associated with well-developed digital flexor muscles, combined with thumb musculature, may also indicate a high degree of manual dexterity for a diet of fine grasses, seeds and tubers (Williams and Geissler, Krentz 1993). Altogether, *T. oswaldi* is considered to be a primarily terrestrial cercopithecoid with a diet similar to that of the extant species *Theropithecus gelada* (Krentz 1993, Delson 2000, Benefit 1999, Fleagle 1998, Hartwig 2002, Williams and Geissler 2014).

Finally, *Gorgopithecus major* (Broom, 1940) was a large terrestrial cercopithecoid found in South Africa at Kromdraai A and B, and Coopers Cave (BM male mean 37 kg and female mean 30kg; Delson, et al. 2000). *G. major* has dental morphology and microwear indicative of a diet largely comprising grasses and some fruits (El-Zaatari et al., 2005; Fleagle, 1998; Hartwig, 2002). Though no postcranial remains from *G. major* have been reported, terrestriality is often assumed to be the primary mode of locomotion for this species due to both its large body size and inferred diet of ground-level foliage (Benefit, 1999; Bettridge and Dunbar, 2012; Fleagle, 1998).

### Primate Carpal Morphology and Organization

The carpals of cercopithecoids and platyrrhines -referred to collectively as monkeys from here on out- have long been described as generally similar to the basic mammalian quadrupedal wrist described below (Lewis 1989). However, the locomotor and habitat diversity within primates has led to changes in the carpal morphology to better accommodate distinct habitual activities. Most non-hominoid primate wrists are comprised of nine carpals, which can be further subdivided into two functional rows and three main sets of joints: the antebrachio-carpal joint of non-hominoid primates comprises the joint between both the radius and ulna and the proximal row of the carpus; the midcarpal joint refers to the articulations between the proximal and distal carpal rows; and the carpometacarpal joint refers to the articulations between the distal carpal row and proximal metacarpals of the palm (figure 5).

Generally, quadrupedal monkeys tend to have carpal morphology advantageous for stabilizing the wrist during compression in an extended, pronated posture, which is the posture most frequently used during quadrupedal locomotion both arboreally and terrestrially in these taxa (Kivell 2016a; Hamrick 2007; O'Connor 1975; Patel 2010a; Patel 2010b). In the antebrachio-carpal joint these features include a flattened radiocarpal articulation and a robust pisiform that projects proximally and contacts the constricted neck of the ulnar styloid process (Lewis 1989, Kivell 2016a). Additionally, the entire carpus of quadrupedal monkeys reaches maximum congruency —the most stable position of the carpus— during an extended, pronated, and ulnarly deviated posture which prevents excessive radioulnar deviation during the support phase of quadrupedal locomotion (O'Connor 1975; Patel 2010a; Patel 2010b; Kivell 2016a).

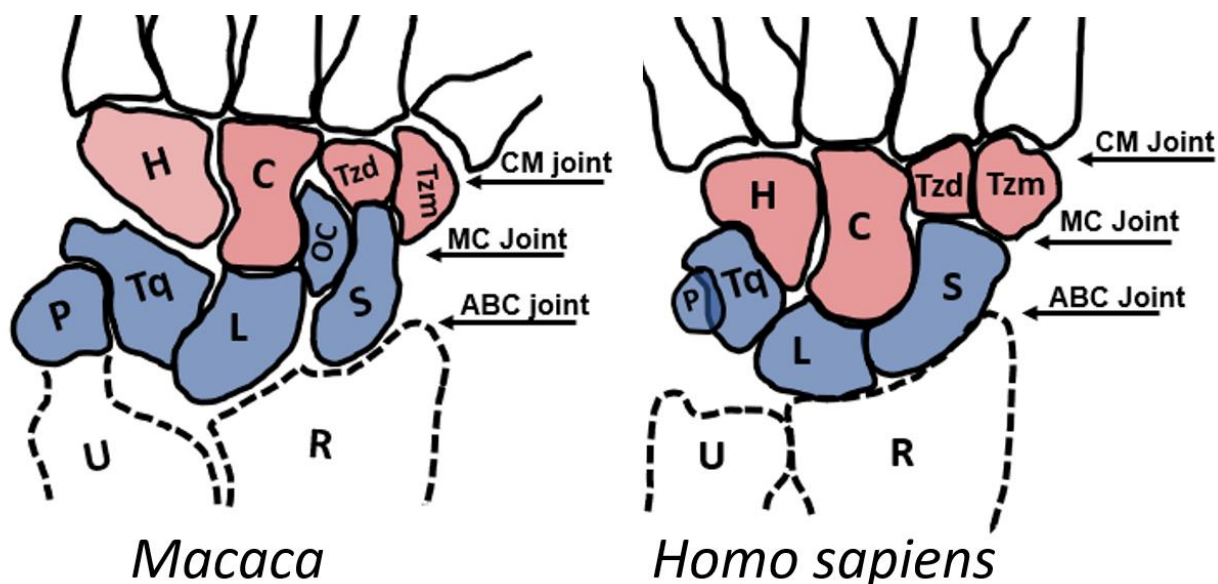


**Figure 5.** A diagram of the primate wrist in *Macaca* and *Homo sapiens*. Bones are labelled as follows: S, scaphoid; OC, os centrale (*Macaca* only); L, lunate; Tq, triquetrum; P, pisiform; Tzm, trapezium; Tzd, trapezoid; C, capitate; H, hamate. Bones in red represent the distal row of the carpus, and those in blue represent the proximal row. Each joint of the wrist is labelled as follows: CM, carpometacarpal joint; MC, midcarpal joint; ABC, antebrachiocarpal joint. Adapted from Kivell 2016a.

Arboreal quadrupedal monkeys do not tend to deviate from the generalized quadrupedal monkey wrist condition (Lewis 1989; Daver 2012; Hamrick 2007). Some taxa show subtle alterations to the antebrachiocarpal and midcarpal joint that facilitate increased mobility, such as increased mobility between the scaphoid and os centrale (Daver 2012) or loss of contact between the pisiform and ulna (Kivell, 2016a), that would be advantageous for navigating environments with variable support diameters.

Conversely, monkeys that habitually use digitigrade, predominantly terrestrial locomotion (e.g. *Papio*, *Mandrillus*, and *Theropithecus*) exhibit distinct features in their carpal morphology to accommodate the distinct forces produced during digitigrade terrestrial locomotion (Lewis, 1989; O'Connor, 1975). These features maximize stability of the carpus during dorsiflexion, the posture most often employed during digitigrade locomotion (O'Connor, 1975; Patel, 2010a, b; Vanhoof et al., 2021). Some of the morphological features found in wrist of digitigrade, terrestrial monkeys include a radioulnarly broad ulnar styloid process that works in conjunction with the triquetrum and rod-like pisiform to form a tight cup, which prevents ulnar and radial deviation about the antebrachial joint during maximum dorsiflexion (Lewis, 1989; O'Connor, 1975). These taxa often have a projecting dorsal process of the radius articulates with the scaphoid via a meniscus that limits extension of the proximal carpal row (Daver et al., 2012; Lewis, 1989). Additionally, the terrestrial, digitigrade monkeys the radius' lunate facet has a significantly denser subchondral cortical plate than that of non-digitigrade monkeys,

possibly due to the frequent use of a position of maximum congruence of the radial-lunate joint during extension (Carlson and Patel, 2006; Daver et al., 2012). Finally, digitigrade baboons have a short hamate hamulus which limits space in the carpal tunnel for large antebrachial flexor tendons, indicating reduced digit flexion and, consequently, reduced climbing behaviors (Kivell 2016a). Together these features act to stabilize the carpus and allow it to better resist the high magnitude, and highly variable forces placed on the carpus during terrestrial locomotion (Daver et al., 2012; Kivell, 2016a; Lewis, 1989; O'Connor, 1975; Schmitt, 2003).

Meanwhile, primates that more regularly engage in or suspensory behaviors have a carpus more advantageous for the vertical hand postures involved in their locomotion. Adaptations of the antebrachiocarpal joint in these primates include an overall curved joint configuration, and often (e.g. *Ateles*) a loss of contact between the pisiform and ulna (Lewis 1989, Kivell 2016a). At the midcarpal joint suspensory primates (e.g. *Hylobates*, *Ateles*) have a carpal configuration that forms a pseudo-ball and socket joint to maximize the degree of supination allowed at that joint (Lewis 1989, Kivell 2016a). These adaptations facilitate mobility and rotation, rather than the stability and lack of radioulnar deviation created by the quadrupedal carpus.

Here I provide the first morphological description and functional interpretation of the fossil cercopithecoid carpus KB 5378 within a comparative context of diverse sample of extant primates. I aim to understand its potential taxonomic affiliation and its locomotor behavior. I test the following predictions based on the reported suggestion that the KB 5378 carpal (and hand) fossils are attributed to *G. major* (Vrba, 1981):

1. If the KB 5378 carpals are attributed to *G. major*, I expect the carpals to be within the size range of extant *Pan* specimens, a taxon that is of the same body size (c. 31-39 kg for *Pan paniscus* and 32-37 kg for female, 40-60 kg for male *Pan troglodytes*) estimated for *Gorgopithecus* (c. 30-37 kg).
2. If the KB 5378 carpals are attributed to *G. major*, I expect the external carpal morphology to be more similar to that of extant large-bodied terrestrial quadrupedal monkeys than that of arboreal quadrupedal monkeys in our study sample.
3. If the KB 5378 carpals are attributed to *G. major*, I expect the carpals and metacarpals to be similar in size and preservation indicating they are likely to belong to the same individual.

## **Materials and Methods**

### Sample

The KB 5378 carpals are curated at the Ditsong National Museum of Natural History, Pretoria, South Africa. These carpals were compared quantitatively and qualitatively to a diverse sample of extant hominoids, cercopithecoids, and platyrrhines (Table 1),. The comparative sample was chosen to encompass all major locomotor

groups to allow a more robust understanding of how KB 5378 may fit into those groups. Comparative extant samples are curated at the following institutions: University of Toronto Biological Anthropology collections (BAA), University of Toronto at Scarborough (UTSC), and Royal Ontario Museum (ROM) in Canada; the Museum of Comparative Zoology, Harvard (MCZ), State University New York (SUNY), Cleveland Museum of Natural History (CMNH), American Museum of Natural History (AMNH) and Smithsonian National Museum of Natural History (NMNH) in the USA; Royal Museum for Central Africa (MRAC), Belgium; Museum für Naturkunde, Berlin (ZMB) and Max Planck Institute for Evolutionary Anthropology Tai Chimpanzee collection (MPI-EVA), Senckenberg Museum Frankfurt (SMF) in Germany; and Powell Cotton Museum (PCM), UK. Additionally, to assess the association of the KB 5378 carpus and hand bones, linear measurements of the KB 5378 metacarpals were taken from digital images.

Genus	Species	Body Mass (kg)	Element	N	♀	♂	?
<i>Alouatta</i>	<i>palliata</i>	♂ 4.5-9.8 <sup>1</sup>	Lunate, Capitate,	9	6	3	-
		♀ 3.1-7.6 <sup>1</sup>	Hamate				
	<i>caraya</i>	♂ 5-8.2 <sup>1</sup>	Lunate, Capitate,	2	1	1	-
		♀ 3.8-5.4 <sup>1</sup>	Hamate				
	<i>fusca</i>	♂ 5.3-7.1 <sup>1</sup>	Lunate, Capitate,	1	1	-	-
♀ 4.1-5.0 <sup>1</sup>		Hamate					
<i>sp.</i>		Lunate, Capitate,	4	3	-	1	
			<b>TOTAL</b>	<b>16</b>	<b>11</b>	<b>4</b>	<b>1</b>
<i>Ateles</i>	<i>paniscus</i>	♂ 5.5-9.2 <sup>1</sup>	Lunate, Hamate	1	-	1	-
		♀ 6.5-11 <sup>1</sup>					
	<i>geoffroyi</i>	♂ 7.4-9.0 <sup>1</sup>	Lunate, Capitate,	2	1	-	1
		♀ 6-8.9 <sup>1</sup>	Hamate				
	<i>fusciceps</i>	♂ 8.9 <sup>1</sup>	Lunate, Hamate	2	-	2	-
♀ 8.8 <sup>1</sup>		Capitate					
<i>sp.</i>		Lunate, Capitate,	1	1	-	-	
			<b>TOTAL</b>	<b>6</b>	<b>2</b>	<b>3</b>	<b>1</b>
<i>Cercocebus</i>	<i>torquatus</i>	♂ 10.7 <sup>1</sup>	Lunate, Trapezium,	7	2	5	-
		♀ 5.5 <sup>2</sup>	Trapezoid, Capitate, Hamate, OC				
			<b>TOTAL</b>	<b>7</b>	<b>2</b>	<b>5</b>	<b>0</b>
<i>Cercopithecus</i>	<i>neglectus</i>	♂ 7.0-8.0 <sup>1</sup>	Lunate,	1	-	1	-
		♀ 4.5 <sup>1</sup>					
	<i>nictitans</i>	♂ 6.3 <sup>1</sup>	Lunate, Trapezium,	6	3	4	-
	♀ 4.1 <sup>1</sup>	Trapezoid,					

			Capitate, Hamate, OC				
	<i>ascanius</i>	♂4.2 <sup>1</sup> ♀3.3 <sup>1</sup>	Lunate, Hamate, OC	1	-	1	-
	<i>mitis</i>	♂7.4 <sup>1</sup> ♀4.2 <sup>1</sup>	Lunate, Capitate, Hamate	11	5	6	-
			<b>TOTAL</b>	<b>19</b>	<b>8</b>	<b>11</b>	<b>0</b>
<i>Chlorocebus</i>	<i>aethiops</i>	♂4.6 <sup>1</sup> ♀3.3 <sup>1</sup>	Lunate, Capitate, Hamate, OC	12	2	8	2
			<b>TOTAL</b>	<b>12</b>	<b>2</b>	<b>8</b>	<b>2</b>
<i>Colobus</i>	<i>guereza</i>	♂13.5 <sup>1</sup> ♀7.9-9.2 <sup>1</sup>	Lunate, Trapezium, Trapezoid, Capitate, Hamate, OC	7	2	5	-
	<i>badius</i>	♂8.3 <sup>1</sup> ♀8.2 <sup>1</sup>	Lunate, Trapezium, Trapezoid, Capitate, Hamate, OC	1	-	1	-
			<b>TOTAL</b>	<b>8</b>	<b>2</b>	<b>6</b>	<b>0</b>
<i>Erythrocebus</i>	<i>patas</i>	♂7.0-13.0 <sup>1</sup> ♀4.0-7.0 <sup>1</sup>	Capitate, Hamate, OC	6	2	3	1
			<b>TOTAL</b>	<b>6</b>	<b>2</b>	<b>3</b>	<b>1</b>
<i>Gorilla</i>	<i>gorilla</i>	♂169.5 <sup>1</sup> ♀71.5 <sup>1</sup>	Lunate, Trapezium, Trapezoid, Capitate, Hamate	23	12	10	1
	<i>beringei</i>	♂159.2 <sup>1</sup> ♀97.7 <sup>1</sup>	Lunate, Trapezium, Trapezoid, Capitate, Hamate	12	6	6	-
			<b>TOTAL</b>	<b>35</b>	<b>18</b>	<b>16</b>	<b>1</b>
<i>Hylobates</i>	<i>lar</i>	♂4.9-7.6 <sup>1</sup> ♀4.4-6.8 <sup>1</sup>	Lunate, Capitate, Hamate, OC	29	13	14	2
	<i>moloch</i>	♂/♀ 5.7 <sup>1</sup>	OC	2	-	2	-
	<i>muelleri</i>	♂/♀ 5.0- 6.4 <sup>1</sup>	OC	2	2	-	-
	<i>pileatus</i>	♂7.9-10.4 <sup>1</sup> ♀6.3-8.6 <sup>1</sup>	OC	1	-	1	-
	<i>concolor</i>	♂/♀ 4.5- 9.0 <sup>1</sup>	OC	1	-	1	-
	<i>agilis</i>	♂5.88 <sup>2</sup> ♀5.5-6.4 <sup>1</sup>	OC	1	-	1	-
	<i>klossi</i>	♂/♀ 5.8 <sup>1</sup>	OC	1	1	-	-
	<i>sp.</i>		OC	2	1	1	-
			<b>TOTAL</b>	<b>39</b>	<b>17</b>	<b>20</b>	<b>2</b>

<i>Lagothrix</i>	<i>lagrothricha</i>	♂3.6-10.0 <sup>1</sup> ♀3.5-6.5 <sup>1</sup>	Lunate, Capitate, 6 Hamate 3	3	3	-
	<i>sp.</i>		Lunate, Capitate, 1 Hamate	-	1	-
			<b>TOTAL</b>	<b>7</b>	<b>3</b>	<b>4</b>
<i>Lophocebus</i>	<i>albigena</i>	♂6.8-7.7 <sup>1</sup> ♀5.7 <sup>1</sup>	Lunate, Trapezium, 6 Trapezoid, Capitate, Hamate, OC, MC1-5	2	4	-
			<b>TOTAL</b>	<b>6</b>	<b>2</b>	<b>4</b>
<i>Macaca</i>	<i>fascicularis</i>	♂4.7-8.3 <sup>1</sup> ♀2.5-5.7 <sup>1</sup>	Lunate, Capitate, 35 Hamate, OC	18	17	-
	<i>mulatta</i>	♂5.6-10.9 <sup>1</sup> ♀4.4-10.9 <sup>1</sup>	Lunate, Capitate, 33 Hamate, OC	15	13	5
			<b>TOTAL</b>	<b>68</b>	<b>33</b>	<b>30</b>
<i>Mandrillus</i>	<i>leucophaeus</i>	♂17.0 <sup>1</sup> ♀10.0 <sup>1</sup>	Lunate, Trapezium, 2 Trapezoid, Capitate, Hamate, OC, MC1-5	1	1	-
	<i>sphinx</i>	♂26.9 <sup>1</sup> ♀11.5 <sup>1</sup>	Lunate, Trapezium, 1 Trapezoid, Capitate, Hamate, OC, MC1-5	-	1	-
			<b>TOTAL</b>	<b>3</b>	<b>1</b>	<b>2</b>
<i>Pan</i>	<i>paniscus</i>	♂39.0 <sup>1</sup> ♀31.0 <sup>1</sup>	Lunate, Trapezium, 12 Trapezoid, Capitate, Hamate, MC1-5	5	7	-
	<i>trogodytes</i>	♂40-60 <sup>1</sup> ♀32-47 <sup>1</sup>	Lunate, Trapezium, 26 Trapezoid, Capitate, Hamate, MC1-5	13	10	3
			<b>TOTAL</b>	<b>38</b>	<b>18</b>	<b>17</b>
<i>Papio</i>	<i>anubis</i>	♂22-37.2 <sup>1</sup> ♀14.5- 14.9 <sup>1</sup>	Lunate, Trapezium, 13 Trapezoid, Capitate, Hamate, OC, MC1-5	5	8	-
	<i>hamadryas</i>	♂21.3 <sup>1</sup> ♀12 <sup>1</sup>	Lunate, Trapezium, 3 Trapezoid, Capitate, Hamate, OC	1	2	-
	<i>cynocephalus</i>	♂22.8- 28.3 <sup>1</sup> ♀12.3 <sup>1</sup>	OC	1	1	-

	<i>papio</i>	♂/♀ 17.6 <sup>1</sup>	Lunate, OC, MC1-5	Hamate	1	1	-	-
	<i>doguera</i>	♂22-37.2 <sup>1</sup> ♀14.5-14.9 <sup>1</sup>	Lunate, OC	Hamate	2	-	2	-
	<i>sp.</i>		Lunate, OC,	Hamate	2	-	1	1
			<b>TOTAL</b>		<b>22</b>	<b>8</b>	<b>13</b>	<b>1</b>
<i>Presbytis</i>	<i>potenziani</i>	♂6.5 <sup>1</sup> ♀6.4 <sup>1</sup>	Lunate, Hamate	Capitate,	1	-	1	-
	<i>frontatus</i>	♂5.6 <sup>1</sup> ♀5.7 <sup>1</sup>	Capitate,	Hamate	1	1	-	-
	<i>sp.</i>		Lunate, Hamate	Capitate,	1	-	1	-
			<b>TOTAL</b>		<b>3</b>	<b>1</b>	<b>2</b>	<b>0</b>
<i>Theropithecus</i>	<i>gelada</i>	♂20.0 <sup>1</sup> ♀11.7 <sup>1</sup>	Capitate,	Hamate	4	1	3	-
			<b>TOTAL</b>		<b>4</b>	<b>1</b>	<b>3</b>	<b>0</b>
			<b>FULL SAMPLE</b>		<b>29</b>	<b>131</b>	<b>151</b>	<b>17</b>

Table 1. Maximum comparative sample of extant taxa. Sample varies per bone, so the elements present per species is listed. Individuals of an unknown sex are listed in the column labeled “n?”. Body masses taken from literature including Rowe et. al 1996 (1) and Smith & Jungers 1996 (2).

Extant taxa were categorized by locomotor behavior based on their degree of terrestriality vs. arboreality, recognizing that species within each category engage in a variety of different locomotor behaviors and at different frequencies (see table 2): knuckle-walkers (*Pan*, *Gorilla*), terrestrial quadrupeds (*Papio*, *Theropithecus*, *Mandrillus*, *Macaca mulatta*, *Erythrocebus*), arboreal quadrupeds (*Alouatta*, *Cercocebus*, *Cercopithecus*, *Chlorocebus*, *Colobus*, *Lagothrix*, *Lophocebus*, *Macaca fascicularis*, *Presbytis*) and suspensory (*Hylobates*, *Ateles*). Typically, the sample was separated by genus. However, *M. mulatta* and *M. fascicularis* were distinguished at the species level due to the high degree of terrestriality in *M. mulatta* compared to the more arboreal *M. fascicularis* (Fleagle, 1998; Patel, 2010a, b; Rodman, 1979; Tuttle, 1969). A full list of taxa and associated literature used to define the functional categories of each taxon are listed in Table 2.

Functional Locomotor Group	Taxa	Description	Literature Source
Suspensory	<i>Ateles</i>	26-38.6% of locomotion tail/arm suspension, while 22-25.4% arboreal quadrupedalism	(Cant, 1986; Mittermeier, 1978)
	<i>Hylobates</i>	51% of travel and 23% feeding used brachiation involving suspension by the forelimbs.	(Fleagle, 1976; Hunt, 1991)
Arboreal quadrupeds	<i>Alouatta</i>	96% of locomotion arboreal quadrupedal	(Cant, 1986)
	<i>Cercopithecus mitis, nictitans, ascanius</i>	<i>C. Mitis</i> and <i>C. ascanius</i> spend 54% and 42% of time using arboreal quadrupedalism in the upper and middle canopy. <i>C. ascanius</i> uses arboreal quadrupedalism 39% of its travel and feeding and prefers mid-canopy.	(Gebo and Chapman, 1995; Gebo and Sargis, 1994; Nakatsukasa, 1994; Rose, 1973)
	<i>Colobus guereza</i>	Arboreal quadrupedalism 41% of travel time, prefers upper canopy.	(Gebo and Chapman, 1995; Morbeck, 1977)
	<i>Lagothrix lagotricha</i>	41.8% of its travel time, and 42.8% of feeding time spent using arboreal quadrupedalism	(Defler, 2000)
	<i>Lophocebus albigena</i>	Arboreal quadrupedalism 47% of travel time in mid canopy.	(Gebo and Chapman, 1995)
	<i>Macaca fascicularis</i>	"An arboreal species that normally feeds and travels in the trees." (Fleagle 1998 pg. 190)	(Cant, 1988; Fleagle, 1998; Rodman, 1979)
	<i>Presbytis</i>	Arboreal quadrupeds that additionally utilize leaping and arm suspension.	(Fleagle, 1978; Fleagle, 1998; Patel, 2010a)
	<i>Cercocebus torquatus</i>	"Spends considerable time on ground and lower stratum, arboreal for eating and sleeping (Nakatsukasa 1994 pg.5, table 1"	(Nakatsukasa, 1994; Patel, 2010a)

	<i>Chlorocebus aethiops</i>	Travels and feeds on ground, keeping arboreal abilities for escape.	(Gebo and Sargis, 1994; McGraw, 2004; Patel, 2010a)
Terrestrial quadruped	<i>Erythrocebus patas</i>	Spends 59.6% of time on ground, and 90.5% of feeding on ground.	(Gebo and Sargis, 1994; Patel, 2010b)
	<i>Papio anubis, hamadryas, cynocephalus, doguera,</i>	Terrestrial but partly arboreal for sleeping and escape.	(Dunbar and Dunbar, 1974; Patel, 2010b; Rose, 1973; Tuttle, 1969)
	<i>Macaca mulatta</i>	Equally terrestrial and arboreal	(Fleagle, 1998; Patel, 2010b; Tuttle, 1969)
	<i>Mandrillus</i>	Primarily terrestrial, with males being more terrestrial than females and young.	(Rowe 1996)
	<i>Theropithecus gelada</i>	Only 1.6% of individuals observed were in trees, known to be “the most terrestrial of non-human primates” (Fleagle 1998 pg.198)	(Dunbar and Dunbar, 1974; Fleagle, 1998)
Knuckle-walkers	<i>Pan troglodytes, paniscus</i>	“The knuckle-walking postures of chimpanzees and gorillas in unique among primates and allows these apes to utilize the opportunities of terrestrial locomotion....” (Tuttle 1967 pg. 171)	(Hunt, 1991; Tuttle, 1967)
	<i>Gorilla gorilla, beringei</i>		(Hunt, 1991; Tuttle, 1967)

Table 2. Description of categorization of comparative sample into locomotor groups. Column 3 contains a brief description, or direct quote, from the literature sources listed in column 4. The arboreal quadrupedal category is organized, from top to bottom, on a scale of most arboreal, to least arboreal to further organize the diverse group of taxa therein.

### External morphological analysis

The external morphology of each carpal was assessed through qualitative comparisons and quantitative linear measurements. The morphometric variables used to quantify each carpal are listed and defined in Table 3 (for images of measurements, see Kivell and Begun, 2009; Kivell et al., 2013; Kivell et al., 2018). All linear measurements of the extant samples were taken manually using digital calipers (Wiha digimax or Mitutoyo digital calipers) on original specimens by MRS or TLK. Linear measurements of the KB

5378 carpals were taken directly from the fossils, apart from specific measurements that were inaccessible due their preservation within the breccia. In these cases, measurements were measured digitally from surface models rendered from high-resolution microCT scans in Avizo 9.0 lite (Thermo Fisher Scientific 2019).

To test the influence of intraobserver error each carpal was measured twice, and cross-validated on a randomized subset of bones (to 0.1 mm of accuracy) over the course of several weeks. KB 5378 carpals were also measured by hand (or digitally for specific variables) three times over the course of several weeks. Measurements of the associated KB 5378 metacarpals were taken from photographs using ImageJ (version 1.53r) and repeated three times each.

All of the KB 5378 carpals were scanned using a Diondo 1 microCT scanner housed at the Imaging Centre for Life Sciences, University of Kent (Canterbury, UK) at 140 kV, 140 Ma, and a resolution of 24.035 microns. The three carpals articulated within the breccia were segmented manually in Avizo 9.0 lite (Thermo Fisher Scientific 2019). A 3D surface model of each carpal was generated and measured using the 3D measure tool in Avizo 9.0 lite (Thermo Fisher Scientific 2019).

To account for variation in body (carpal) size across the comparative sample, a geometric mean of a custom set of measurements for each bone was calculated (Jungers et al., 1995; Table 4) and used in all comparative analyses excluding those of absolute size. Each morphometric variable was divided by the geometric mean of the respective carpal to create 'size adjusted' variables (Jungers et al., 1995), in addition to the raw variables. For analyses of absolute size, unadjusted, raw data was used.

### Statistical analyses

All data was analyzed in R Studio (version 4.1.2 packages Dplyr, Ggally and ggplot2) and PAST (version 4.03). Normality of the data was assessed using a Shapiro Wilks test for all variables, and each taxon. Covariance between variables was assessed using Pearson's correlation coefficients to exclude any variables that were highly ( $r > 0.9$ ) correlated. Variation in individual measured variables between taxa was investigated using box-and-whiskers plots. Further, to assess variation in shape ratios, within-group, covariance-variance principal component analyses (PCA) were performed in PAST. Covariance-variance matrix based, within-group PCA was favored for this study because all variables within this study are measured in the same units, and because differences in the variance between variables are the main factor being identified (Queen et al., 2002). Due to the irregular and often small ( $n < 10$ ) number of individuals per taxa in this study, between group PCA tests were deemed inappropriate (Bookstein, 2019). Finally, bivariate plots comparing the length of the capitate body to the lengths of each metacarpal were performed to assess how likely the KB 5378 carpus and metacarpals are associated to the same individual. In this study, the length of the capitate body is used as a proxy to

general carpus size due to the central location of the capitate in the carpus as well as the ease of measurement of this metric.

Variable	Description
<b>Os Centrale</b>	
OCH	Maximum dorsopalmar measure of os centrale body
OCB	Maximum radioulnar measure of os centrale body
OCL	Maximum proximodistal measure of os centrale body
OCDFH	Maximum dorsopalmar measure of distal facet of os centrale
OCDFL	Maximum proximodistal measure of distal facet of os centrale
<b>Lunate</b>	
HLB	Maximum dorsopalmar measure of lunate body
LLB	Maximum proximodistal measure of lunate body
LLSF	Maximum proximodistal measure of lunate scaphoid facet
HLSF	Maximum dorsopalmar measure of lunate scaphoid facet
LLTF	Maximum proximodistal measure of lunate triquetrum facet
HLTF	Maximum dorsopalmar measure of lunate triquetrum facet
HLDF	Maximum dorsopalmar measure of lunate distal facet
BLDF	Maximum radioulnar measure of lunate distal facet
BLB	Maximum radioulnar measure of lunate base in palmar view
BLRF	Maximum radioulnar measure of lunate radial facet
HLRF	Maximum dorsopalmar measure of lunate radial facet
<b>Trapezium</b>	
LTMB	Maximum proximodistal measure of trapezium body

HTMB	Maximum dorsopalmar measure of trapezium
LMC1F*	In hominoids: Maximum proximodistal measure of the trapezium Mc1 facet In non-hominoids: Maximum measure across proximal most edge of trapezium Mc1 facet
BMC1F*	In hominoids: Maximum radioulnar measure of the trapezium Mc1 facet In non-hominoids: Maximum measure perpendicular to LMC1F of the trapezium Mc1 facet.
LTDF	Maximum proximodistal measure of the trapezium trapezoid facet
HTDF	Maximum dorsopalmar measure of the trapezium trapezoid facet
BTPF	Maximum radioulnar measure of trapezium proximal facet, encompassing scaphoid facet (hominoids) and os centrale facet (non-hominoids) if present.
LTPF	Maximum proximodistal measure of trapezium proximal facet, encompassing both scaphoid facet (hominoid) and os centrale facet (non-hominoid) if present.
LTDSF	Total maximum measure from extreme distal edge of trapezoid facet to extreme proximal, or opposite edge of proximal facet encompassing the entire trapezoid, scaphoid and os centrale facets.
<b>Trapezoid</b>	
HTDB	Maximum dorsopalmar measure of trapezoid body
LTDPS	Maximum proximodistal measure of trapezoid palmar surface
BTDDS	Maximum radioulnar measure of trapezoid distal surface
LDDS	Maximum proximodistal measure of trapezoid distal surface
HTDMC2	Maximum dorsopalmar measure of trapezoid Mc2 facet
BTDMC2	Maximum radioulnar measure of trapezoid Mc2 facet
HTDTMF	Maximum measure from border of trapezoid Mc2 facet to opposite, typically palmar, extreme of trapezoid trapezium facet.
LTDTMF	Maximum proximodistal measure of trapezoid trapezium facet
<b>Capitate</b>	
LCB	Maximum proximodistal measure of capitate body
HCB	Maximum dorsopalmar measure of capitate body
BCB	Maximum radioulnar measure of capitate body

LCHF	Maximum proximodistal measure of capitate hamate facet
HCHF	Maximum dorsopalmar measure of capitate hamate facet
HCTF	Maximum dorsopalmar measure of capitate trapezoid facet
LCTF	Maximum proximodistal measure of capitate trapezoid facet
HMC2	Maximum dorsopalmar measure of the total capitate Mc2 facet (if facet presented discontinuously, individual heights were summed and totaled to equal this variable).
LMC2	Maximum proximodistal measure of the total capitate Mc2 facet
DBMC3	Maximum radioulnar measure of the dorsal extreme of capitate Mc3 facet
PBMC3	Maximum radioulnar measure of the proximal extreme of capitate Mc3 facet
HMC3	Maximum dorsopalmar measure of capitate Mc3 facet
BCN	Minimum radioulnar measure of thinnest portion of capitate neck
HCPF	Maximum dorsopalmar measure of capitate proximal facet
BCPF	Maximum radioulnar measure of capitate proximal facet
<b>Hamate</b>	
HHB	Maximum dorsopalmar measure of hamate, including hamulus
HHB-H	Maximum dorsopalmar measure of hamate, excluding hamulus
HHH	Maximum dorsopalmar measure of hamate hamulus, typically obtained from subtraction of HHB-H from HHB
LHB	Maximum proximodistal measure of hamate, including hamulus
LHB-H	Maximum proximodistal measure of hamate, excluding hamulus
LHH	Maximum proximodistal measure of hamulus, typically obtained from subtraction of LHB-H from LHB.
HHCF	Maximum dorsopalmar measure of hamate capitate facet
LCHF	Maximum proximodistal measure of hamate capitate facet
HHTF	Maximum dorsopalmar measure of hamate triquetrum facet
LHTF	Maximum proximodistal measure of hamate triquetrum facet
BHB	Maximum radioulnar measure of hamate from dorsal view

BHDF	Maximum radioulnar measure of hamate distal facet, encompassing all metacarpal facets
HHDF	Maximum dorsopalmar measure of hamate distal facet, encompassing all metacarpal facets
BMC4	Maximum radioulnar measure of hamate Mc4 facet
HMC4	Maximum dorsopalmar measure of hamate Mc4 facet
BMC5	Maximum radioulnar measure of hamate Mc5 facet
HMC5	Maximum dorsopalmar measure of hamate Mc5 facet
<b>Metacarpals</b>	
LMC1	Maximum proximodistal length of the first metacarpal
LMC2	Maximum proximodistal length of the second metacarpal
LMC3	Maximum proximodistal length of the third metacarpal
LMC4	Maximum proximodistal length of the fourth metacarpal
LMC5	Maximum proximodistal length of the fifth metacarpal

Table 3: Description of each linear variable used to quantify external morphology of each carpal.

Bone	Variable
Os centrale	OCH, OCL, OCB, OCDFH, OCDFL
Lunate	LLB, HLB, BLB, HLSF, LLSF, HLDF, BLDF, HLRF, BLRF, HLTF, LLTF
Trapezium	LTMB, HTMB, LTDF, HTDF, BTPF, LTPF, LMC1, BMC1, LTDSF
Trapezoid	HTDB, LTDPS, LTDDS, BTDDS, HTDTMF, LTDTMF, HTDMC2, BTDMC2
Capitate	LCB, HCB, BCB, LCHF, BCPF, HCPF
Hamate	LHB, LHB-H, HHB, HHB-H, BHB, HHCF, LHCF, HHTF, LHTF
Metacarpals	LMC1, LMC2, LMC3, LMC4, LMC5

Table 4: Variables included in geometric mean.

## Results

### Anatomical Description of KB 5378 Carpals

#### Left Scaphoid Fragment:

**Preservation:** The scaphoid of KB 5378 preserves only the proximal half, including only partial radial, os centrale and lunate facets. It remains embedded within matrix with the capitate and os centrale. A surface model reveals that the cortex is well preserved, outside of the area of breakage.

**Morphology** (Figure 6): The fragment measures 13.1 mm in dorsopalmar (DP) height, 10.8 mm in proximodistal (PD) length, and 5.4 mm in radioulnar (RU) breadth. No complete facets are preserved. The partial radial facet is radioulnarly and dorsopalmarly flat and measures 11.1 mm in DP height and 12.9 mm in PD length. The fragment contains a nearly complete lunate facet, missing only its palmar-most edge, measuring 10.8 mm in PD length, and 6.2 mm in DP height. The lunate facet is slightly convex and is oriented ulnarly. The partial capitate (ulnar) facet is missing its palmar edge, is concave and measures 9.1 mm PD and 8.9 mm DP.

#### Left Os Centrale

**Preservation:** The KB 5378 os centrale is complete and all facets are well preserved. However, it remains embedded within matrix roughly in anatomical position with the capitate and the partial scaphoid. Thus, the morphology described below is based on digital reconstruction from high-resolution microCT scans.

**Morphology** (Figure 7): The os centrale measures 9.2 mm in DP height, 11.7 mm in PD length and 5.9 mm in RU breadth. The distal facet for the capitate is concave and circular in shape, measuring 9.3 mm DP and 8.8 mm PD. Additionally, there is a small facet present on the proximoulnar corner measuring 5.6 mm PD and 2.7 mm RU that contacts the distal most edge of the radial facet of the lunate. The scaphoid facet of the os centrale is convex measuring 7.1 mm in DP height and 7.2 mm in PD length. Finally, the trapezoid-trapezium facet is round, concave and expands across the entire radial side of the os centrale. It measures 9.7 mm in RU breadth, and 7.9 mm in DP height. The angle between the scaphoid and trapezium facet, taken at the approximate midpoint of each facet, is 88.1 degrees.

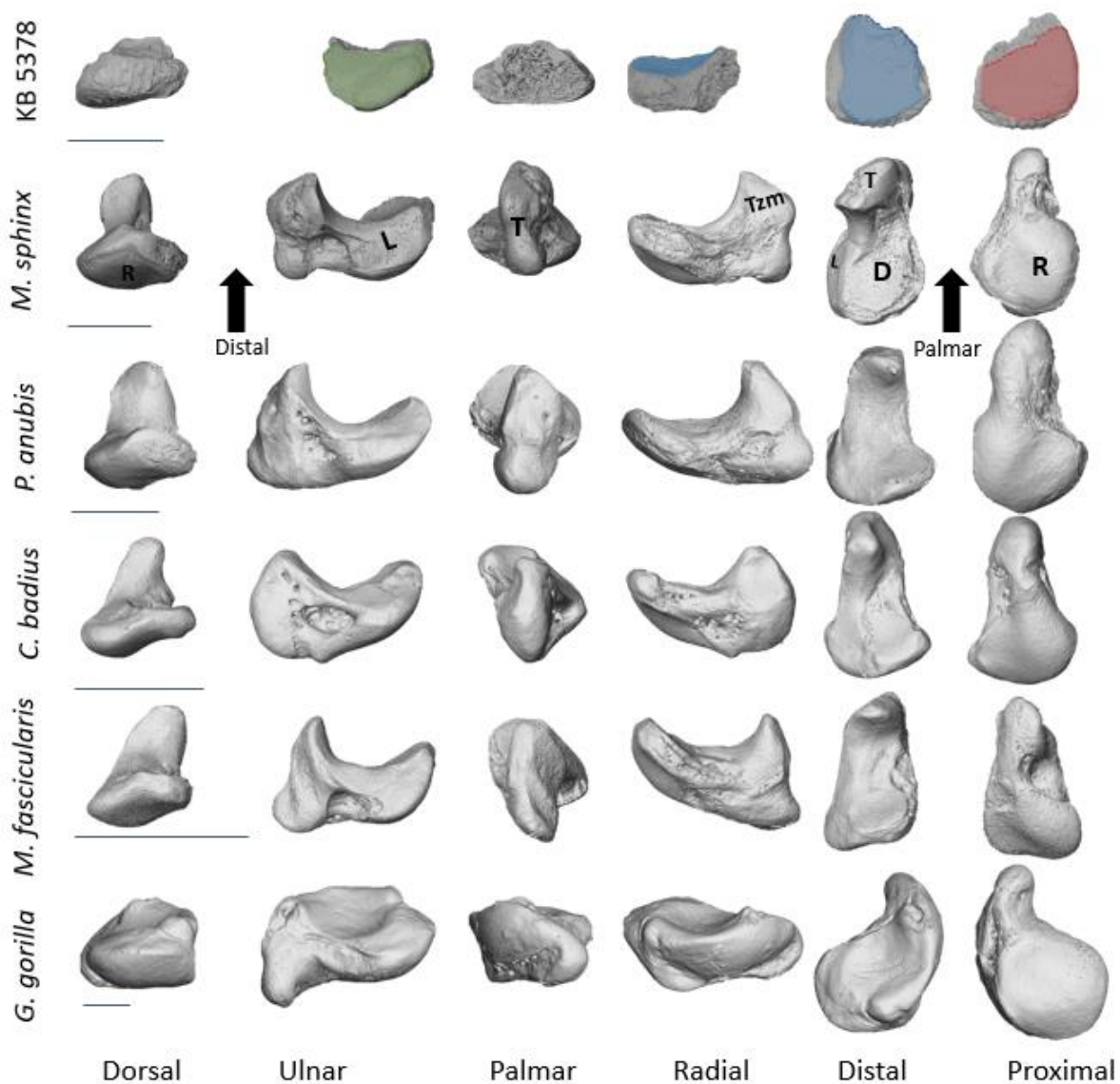


Figure 6. Anatomical views of the KB 5378 scaphoid in comparison to, from top to bottom, *M. sphinx*, *P. Anubis*, *C. badius*, *M. fascicularis*, and *G. gorilla*. All bones are oriented to represent the left side and are scaled to the same size, with the bar beneath each taxon representing 1cm. The articular facets are labelled in *M. sphinx* as follows: R, radial facet; L, lunate; T, tubercle; Tzm, trapezium and/or trapezoid shared facet; D, distal facet. Note that the broken areas of the KB 5378 fragment are clearest in the palmar and radial view.

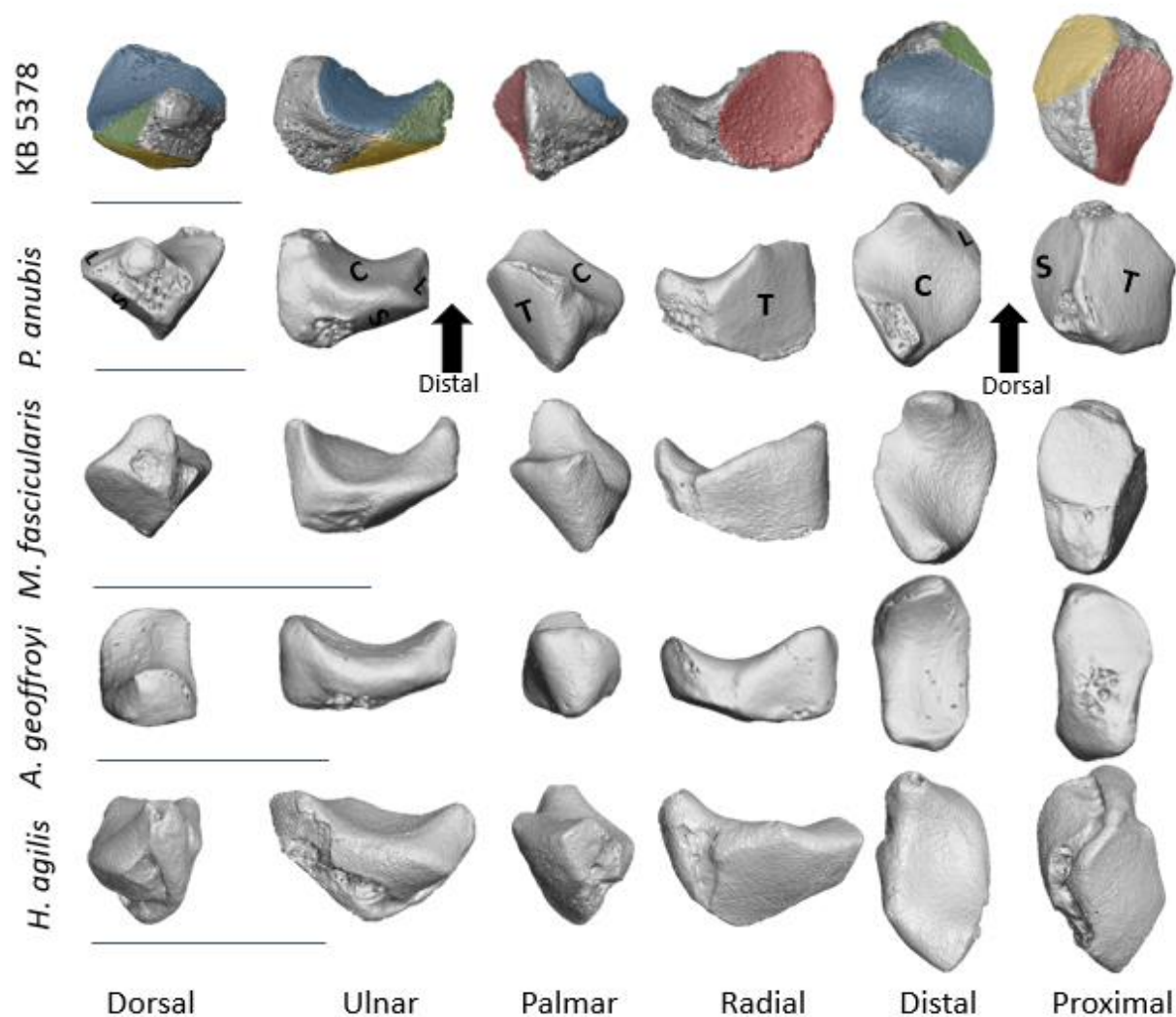


Figure 7: Anatomical views of the KB 5378 os centrale in comparison to, from top to bottom, *P. anubis*, *M. fascicularis*, *A. geoffroyi*, and *H. agilis*. All bones are oriented to represent the left side and are scaled to the same size, with a bar placed beneath each taxa representing 1cm. The articular facets are labelled in *P. anubis* as follows: D, non-articular dorsal surface; S, scaphoid; C, capitate; L, lunate; T, trapezoid/trapezium shared facet.

#### Left Lunate:

**Preservation:** The lunate is complete and well preserved. All facets are clearly distinguishable and well defined. There is a crack in the cortex that obliquely crosses the triquetrum facet from the radial facet to the distal facet and continues dorsopalmarly

across the distal facet to its dorsal extreme. This crack does not significantly alter the facet morphology.

**Morphology** (Figure 8): The lunate body of KB 5378 is proximodistally longer than it is dorsopalmarly tall, and approximately twice as long as it is broad. It becomes significantly RU broader proximally towards the radial facet. The overall size is 14.7 mm in PD length, 13.7 mm in DP height and 8.7 mm in RU breadth. The scaphoid facet is flat and extends DP along the entire edge of the distal facet. The scaphoid facet measures a maximum of 5.9 mm PD length and 11.0 mm DP height, and its palmar half is PD longer than the dorsal half. The distal articulation is concave and shows only an articulation for the capitate (a hamate facet is not present), measuring 10.4 mm in DP height and 6.2 mm in RU breadth. The triquetrum facet is flat and rectangular, expanding across nearly the full PD length of the ulnar side of the lunate, and measures 9.6 mm in DP height and 10.9 mm in PD length. The radial facet is large, proximodistally convex, and dominates the proximal view of the lunate measuring 13.2 mm in DP height and 9.7 mm in RU breadth.

#### Left Trapezium:

**Preservation:** The cortex of the trapezium shows small areas of cortex wear on the Mc1 facet rendering that facet rough in texture. Otherwise, the bone is complete, and all facets are clearly distinguishable.

**Morphology** (Figure 9): The trapezium of KB 5378 is rectangular in shape and does not have a pronounced tubercle. The overall size is 12.7 mm in PD length, 8.4 mm in DP height, and 8.0 mm in RU breadth. The Mc1 facet is oval-shaped, slightly convex, and spans the entire distal length of the bone, measuring 8.5 mm in RU breadth and 7.3 mm in PD length. The trapezoid facet is also oval in shape, slightly convex radioulnarly and covers approximately half of the ulnar side of the bone. It is 7.4 mm in PD length and 5.7 mm in DP height and slightly convex. The proximal facet, which articulates with the scaphoid and, in monkeys, the os centrale, is small, oblong and measures 5.5 mm in RU breadth and 6.0 mm in PD length. It is positioned parallel to the Mc1 facet's distal-most edge

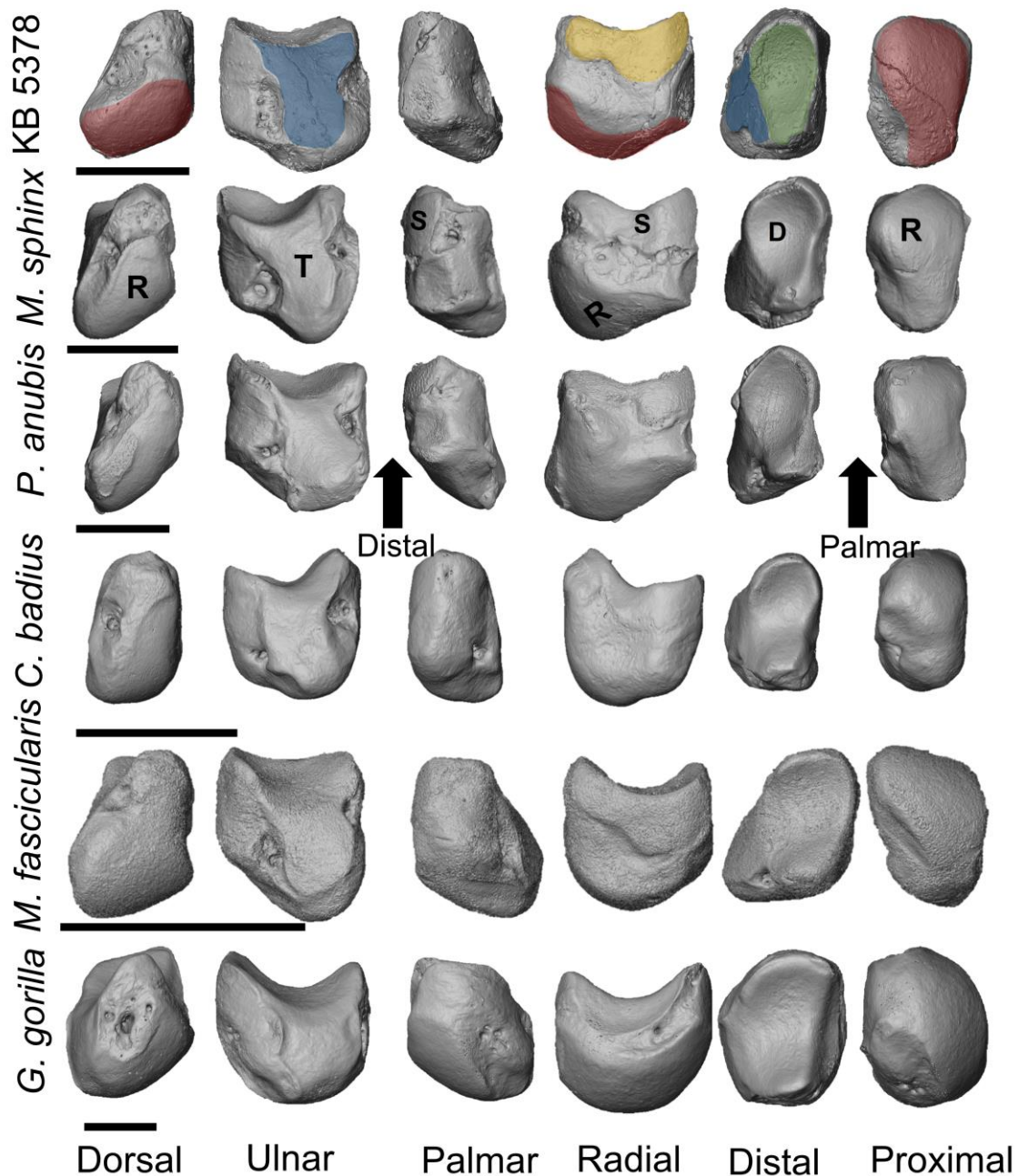


Figure 8: Anatomical views of the KB 5378 lunate in comparison to, from top to bottom, *M. sphinx*, *P. anubis*, *C. badius*, *M. fascicularis*, and *G. gorilla*. All bones are oriented to represent the left side and are scaled to the same size, with a bar beneath each taxon representing 1 cm. The articular facets are labelled in *M. sphinx* as follows: R, radial; T, triquetrum; S, scaphoid; D, distal facet.

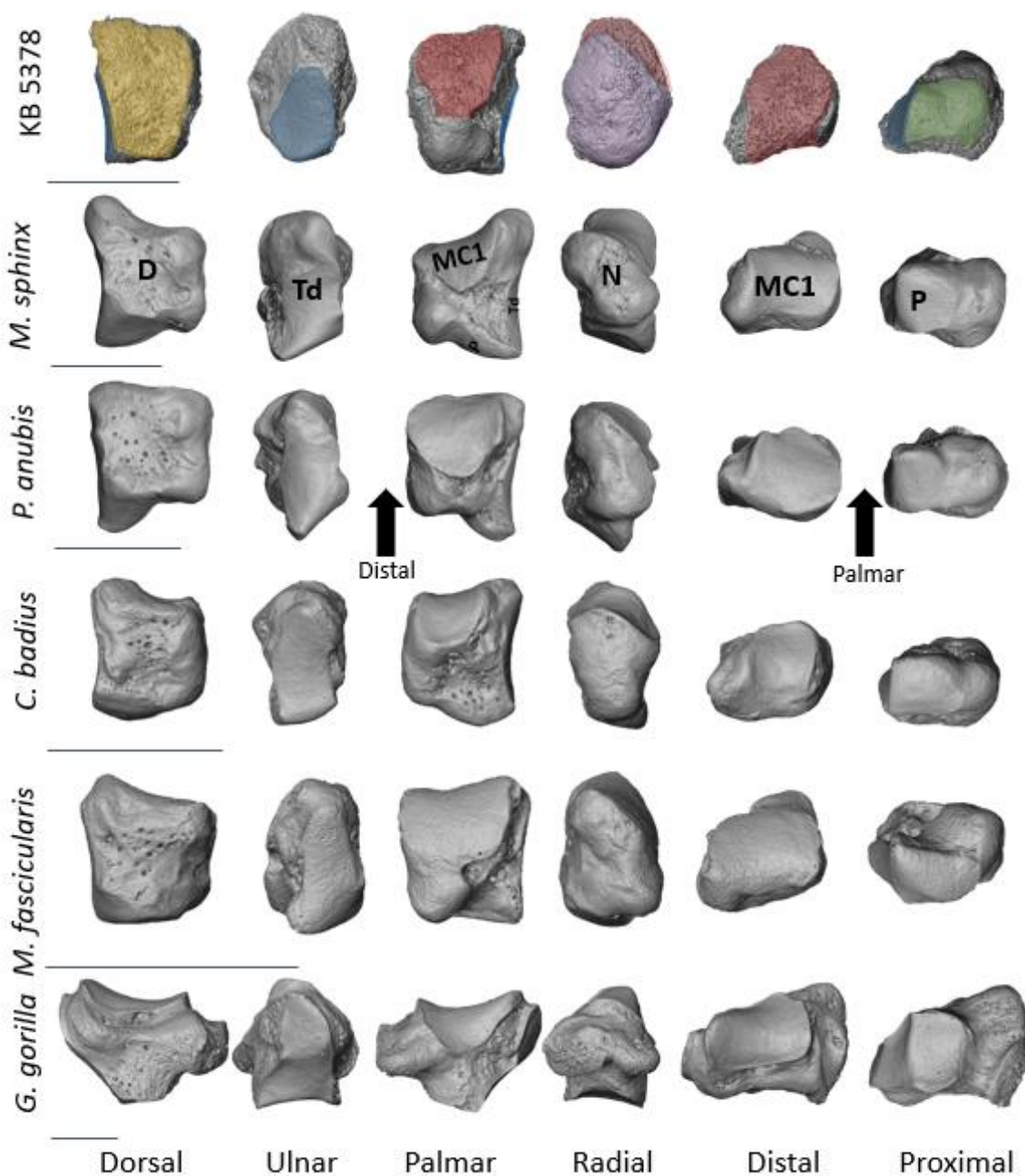


Fig 9: Anatomical views of the KB 5378 trapezium in comparison to, from top to bottom, *M. sphinx*, *P. Anubis*, *C. badius*, *M. fascicularis*, and *G. gorilla*. All bones are oriented to represent the left side bone and scaled to the same size, with a bar placed beneath each taxa representing 1cm for scale. The articular facets are labelled in *M. sphinx* as follows: D, non-articular dorsal surface; Td, trapezoid; Mc1, metacarpal 1; N, radial non articular surface; P, proximal facet encompassing the scaphoid facet (hominoids) and os centrale facet (non-hominoids) if present.

Left Trapezoid:

**Preservation:** The trapezoid is complete and well preserved apart from a small area of cortical wear at the dorsal-most edge of the Mc2 articular surface that exposes trabecular bone.

**Morphology** (Figure 10): The trapezoid is triangular in shape. Overall, its body measures 12.5 mm in PD length, 12.3 mm in DP height and 9.1 mm in RU breadth. The Mc2 articulation of the trapezoid is slightly concave and measures 11.9 mm DP and 8.9 mm RU. The trapezoid is keeled distally, but the ridge on the dorsal-most edge that creates a keeled appearance does not extend palmarly onto the Mc2 facet. The capitate facet is smooth and convex, measuring 9.3 mm DP and 5.8 mm PD and covers most of the ulnar side of the bone. A sulcus measuring 3.2 mm in PD length and 8.8 mm in DP height for the capito-trapezoid interosseous ligament separates the capitate and Mc2 facets. The trapezium facet is rectangular in shape, flat and measures 5.9 mm in PD length and 7.3 mm in DP height.

Left Capitate:

**Preservation:** The capitate of KB 5378 is complete, and still partially embedded in the matrix also containing the os centrale, and partial scaphoid fragment. The cortex is eroded in some areas of the distal metacarpal facets to expose trabecular bone. The descriptions below were taken from both the physical bone and 3D surface models.

**Morphology** (Figure 11): The capitate of KB 5378 measures 17.2 mm in PD length, 14.7 mm in DP height and 13.3 mm in RU breadth. It exhibits clear constriction at the neck of the capitate, which measures 5.9 mm in RU breadth. The proximal facet is round and measures 6.1 mm in RU breadth and 7.0 mm in DP height and does not show a clear distinction between scaphoid and lunate articulations. The trapezoid facet is triangular and bordered palmarly by the sulcus for the capitate-trapezoid interosseous ligament. It measures 3.3 mm in DP height and 6.6 mm in PD length. The Mc3 facet dominates the entire distal facet of the capitate measuring 14.0 mm in DP height. It is RU broader dorsally (13.3 mm) than it is palmarly (4.4 mm), such that it tapers to a point towards its palmar end. The Mc3 facet surface is dorsally concave but flattens palmarly. The Mc2 facet is split into two thin, radially-facing facets by the same non-articular sulcus dividing the trapezoid facet. Its dorsal portion is rectangular, measuring 2.8mm in PD length and 4.5 mm in DP height, while its palmar portion is 0.5 mm in PD length and 3.1 mm in DP. Together, including the distance across the sulcus, the Mc2 facets measures 13.8 mm DP and 2.8 mm PD. Finally, the hamate facet measures 10.8 mm DP height and 12.2 mm PD length and follows the entire dorsal edge of the ulnar side of the capitate. It is slightly concave at its PD midpoint as it follows the taper of the capitate neck. The hamate facet's proximal end is round and RU concave while the distal end is DP narrow, flat and ends at the edge of the Mc3 facet.

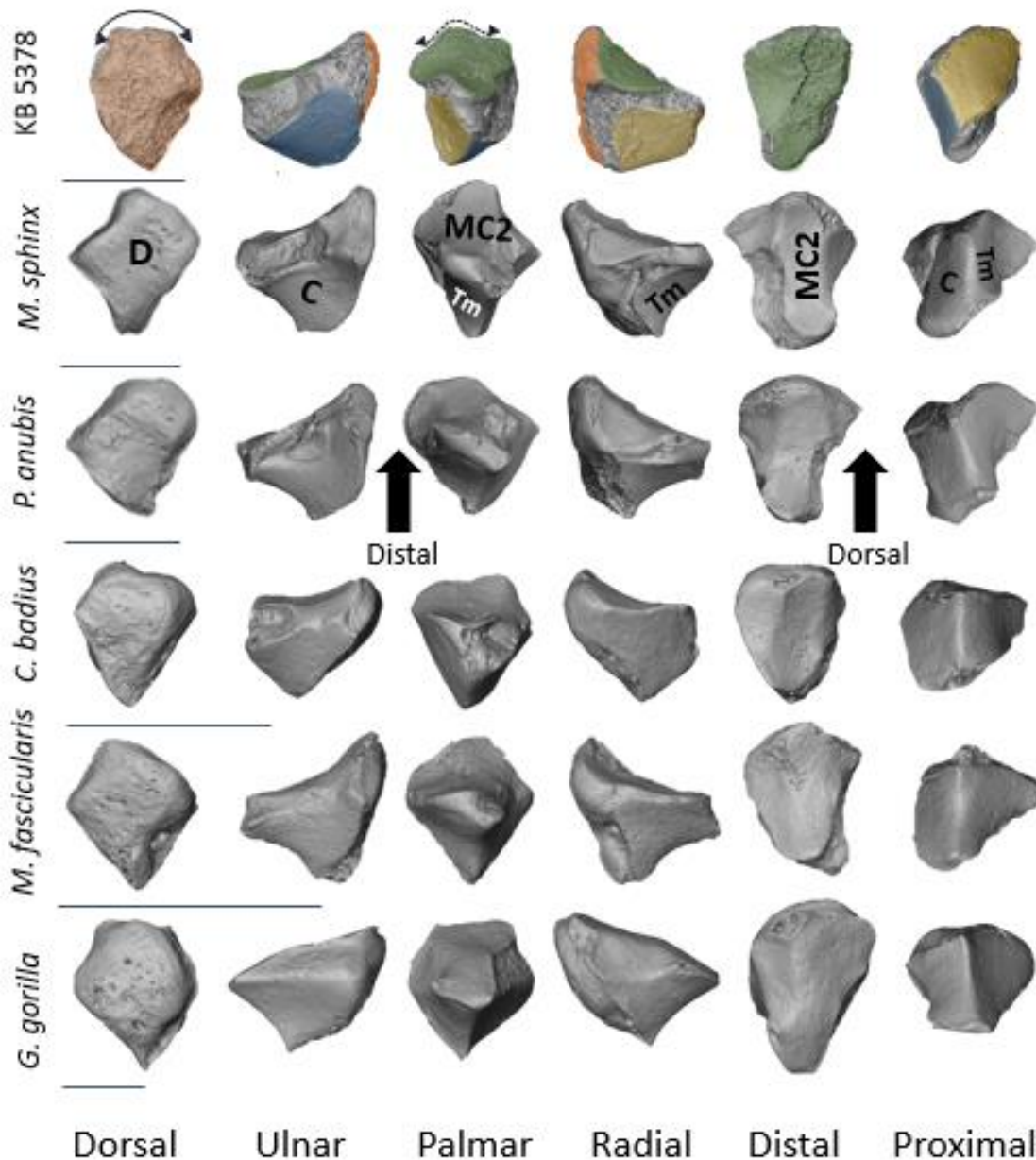


Fig 10: Anatomical views of the KB 5378 trapezoid bone in comparison to, from top to bottom, *M. sphinx*, *P. Anubis*, *C. badius*, *M. fascicularis*, and *G. gorilla*. All bones are oriented to represent the left side and scaled to the same size, with a bar placed beneath each taxa representing 1cm for scale. The articular facets are labelled in *M. sphinx* as follows: D, non-articular dorsal surface; C, capitate; Tm, trapezium facet; Mc2, metacarpal 2.

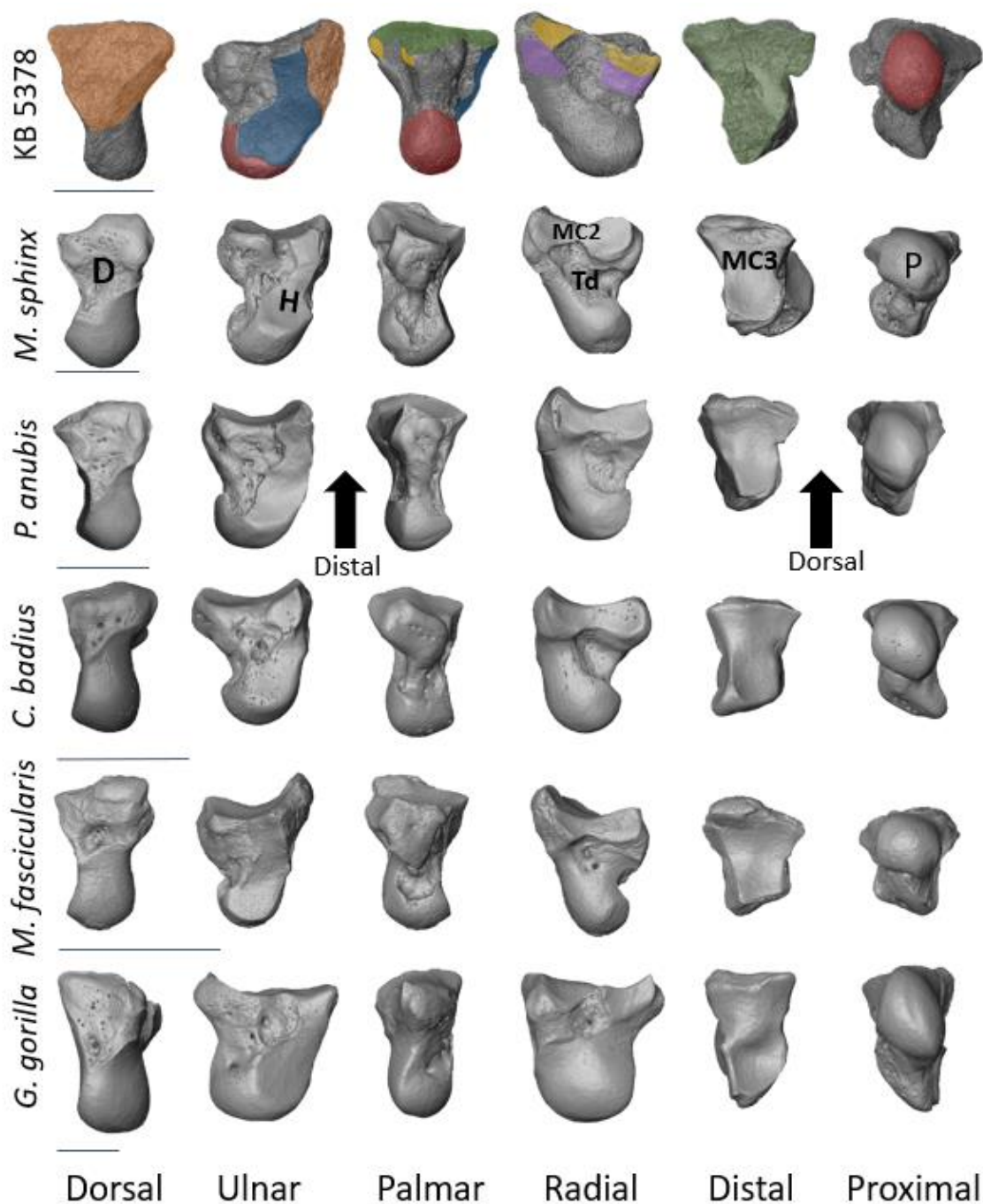


Fig 11: Anatomical views of the KB 5378 capitate bone in comparison to, from top to bottom, *M. sphinx*, *P. anubis*, *C. badius*, *M. fascicularis*, and *G. gorilla*. All bones are oriented to represent the left sided bone and scaled to the same size, with a bar placed beneath each taxa representing 1cm for scale. Articular facets are labelled in *M. sphinx* as follows: D, dorsal non articular surface; H, hamate; MC2, metacarpal 2; Td, trapezoid; Mc3, metacarpal 3; P, proximal facet/ "head" of the capitate.

Left Hamate:

**Preservation:** The hamate is complete and well preserved; all facets are clearly distinguishable.

**Morphology** (Figure 12): The hamate of KB 5378 is 17.1 mm in PD length, 11.1 mm in RU breadth and 13.2 mm in DP height, giving it an overall narrow appearance. Its hamulus is small, RU broad, and rounded, extending only slightly DP beyond the distal Mc articular surfaces. The hamulus extends distally and does not curve ulnar or radially. The capitate facet takes up most of the radial side of the hamate measuring 8.1 mm DP and 11.5 mm PD. This facet is expanded at its distal and proximal ends but is constricted at approximately half of its length giving it a curved “hourglass” shape. It is flat distally but follows the overall curve of the proximal end of the hamate to become convex at its proximal extreme. The triquetrum facet is large and smooth, measuring 7.2 mm DP and 13.6 mm PD, covering the entire ulnar side of the hamate. It is flat proximally but becomes radioulnarly concave distally, and the entire facet is proximally oriented when in articulation. The Mc4 facet measures 10.8 mm in DP height and 6.4 mm in RU breadth, with its palmar border at the start of the hamulus. It is angled radially at approximately 45 degrees relative to the distally-facing Mc5 facet. The Mc5 facet is rectangular and concave, measuring 11.0 mm in DP height and 7.7 mm in RU breadth. The angled morphology of the Mc4 and Mc5 facets produce a sharply angled distal edge of the dorsal surface of the hamate.

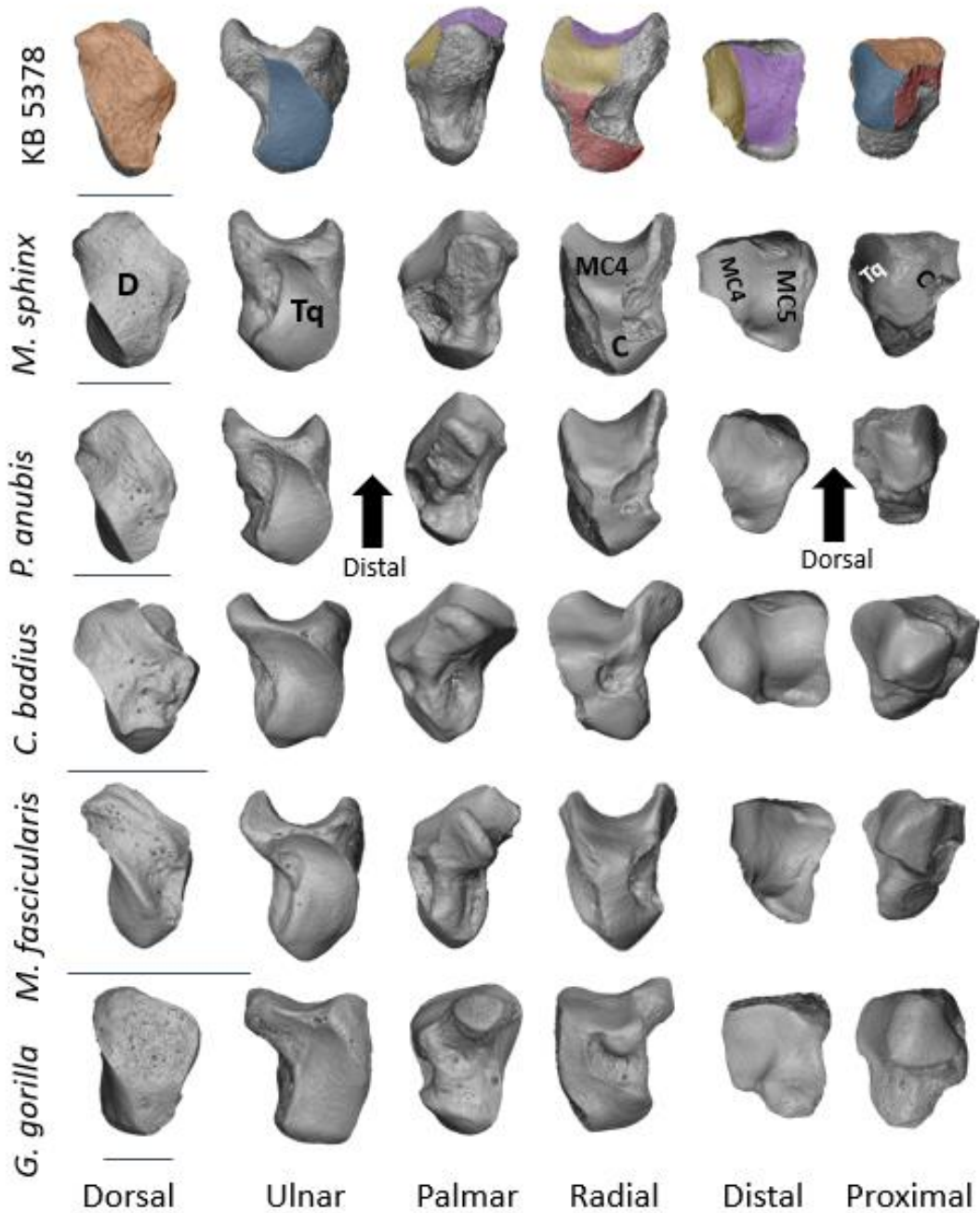


Figure 12: Anatomical views of the KB 5378 hamate in comparison to, from top to bottom, *M. sphinx*, *P. anubis*, *C. badius*, *M. fascicularis*, and *G. gorilla*. All bones are oriented to represent the left sided and scaled to the same size, with a bar placed beneath each taxa representing 1cm for scale. Articular facets are labelled in *M. sphinx* as follows: D, non-articular dorsal surface; Tq, triquetrum; Mc4, metacarpal 4; C, capitate; Mc5, metacarpal 5.

### Comparative morphology

This section details the morphology of each KB 5378 carpal in the context of the comparative sample. All measurements discussed below have been divided by a geometric mean to adjust for differences in carpal size. Latter sections on absolute size comparisons are based on raw data.

### Scaphoid:

The scaphoid of KB 5378 preserves only limited informative morphology. The most functionally (and taxonomically) diagnostic features of the scaphoid, such as the size and orientation of the tubercle, are not preserved and none of the facets are complete (Fig. 6). The lunate facet is the most complete and is similar in morphology to *Mandrillus* and, to a lesser degree, *M. fascicularis* in being DP broad, flat, and oriented distoulnarly. The partial radial facet is flat, most similar to other cercopithecoids in our sample. The partial os centrale facet is shallowly concave like *Mandrillus* and other cercopithecoids in our sample and dissimilar to the more deeply concave os centrale facet of the arboreal *Colobus*.

### Os centrale:

KB 5378 has an os centrale characterized by a RU narrow and DP tall body when compared to all extant taxa, although there is substantial overlap with both arboreal and terrestrial quadrupedal taxa (fig. 13). Its distal facet for the capitata is distinct among the comparative sample in being particularly DP tall but PD short. In DP height, it falls outside the range of variation for all taxa and is only similar to the outliers of *M. fascicularis* but in PD length is most similar to *Colobus* and the terrestrial quadrupeds. In general, the os centrale morphology of KB 5378 does not align with any particular functional group.

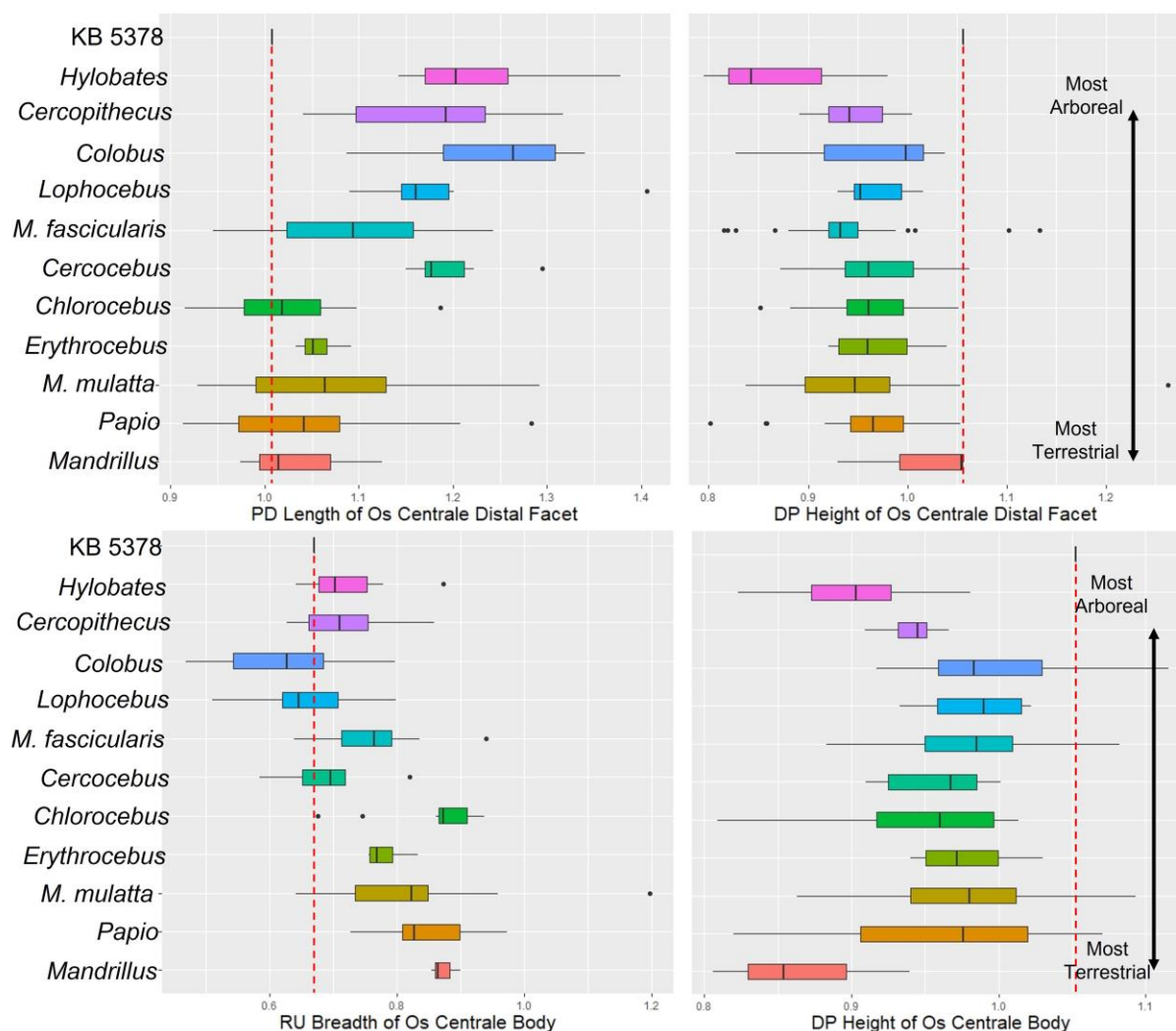


Fig 13. Box-and-whisker plots of the os centrale body and distal facet. All values are adjusted by geometric mean.

The PCA analyses support the findings of the univariate analyses of the os centrale. PC1 describes 60.0% of variation and is driven by PD length of the distal facet, PD length of the body, and RU breadth of the body but does not separate any functional group from another. KB 5378 os centrale falls on the midline of PC1, indicating that it has intermediate in PD length of distal facet, and PD length and RU breadth of the os centrale body (Fig. 14). Along PC1 KB 5378 falls within both the arboreal and terrestrial quadrupedal functional groups, but outside of the suspensory group.

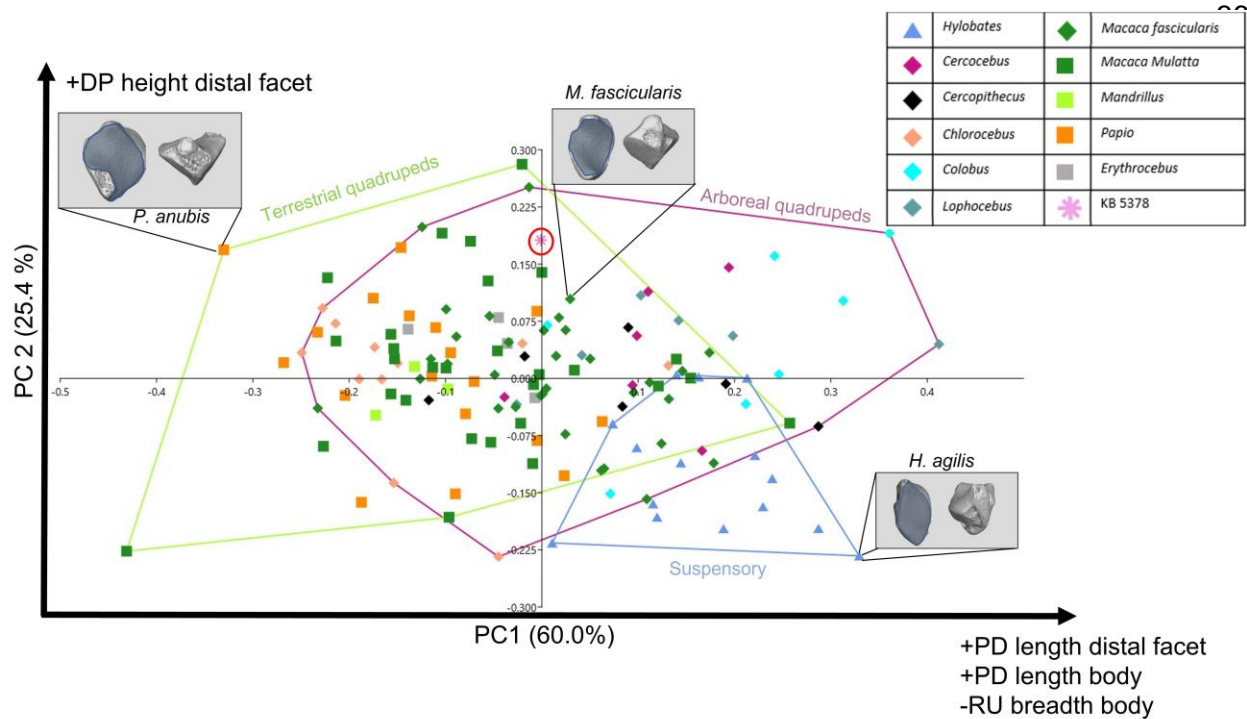


Fig 14: Within-group PCA results of the os centrale. Functional groups are each surrounded by labelled convex hulls. Surface models of representative taxa are included to demonstrate the morphology reflected at various points of the plot. Relevant facets on each surface model are shaded for clarification of the change in morphology along each axis.

PC2 describes 25.4% of the remaining variation and separates the suspensory taxa from most arboreal and terrestrial quadrupeds based on the DP height of the os centrales distal facet. Along PC2 KB 5378 is distinguished from suspensory taxa but is within the range of both arboreal and terrestrial quadrupeds in having a particularly DP tall distal facet, but is within range of both arboreal and terrestrial quadrupeds. In general, the PC plots for the os centrale indicate KB 5378 is unlike suspensory taxa and has shared morphology with both arboreal and terrestrial quadrupeds, but there is substantial overlap in os centrale morphology between these two functional groups.

### Lunate:

The lunate of KB 5378 reflects morphology intermediate between all functional groups, apart from knuckle-walkers (Fig 15). The body of KB 5378 lunate is most similar to *Ateles* and *Lagothrix* in RU breadth and to *Hylobates*, *M. mulatta*, and *Mandrillus* in DP height. It has a relatively small distal facet in both RU breadth and DP height. The reduced size of the distal facet combined with the average-sized radial facet (in both RU breadth and DP height), creates a lunate body which becomes gradually RU broader from distal to proximal end, similar to the morphology seen in *Mandrillus* and *Macaca mulatta*. Additionally, KB 5378 shows a PD and DP expanded triquetrum facet similar in height only to *Colobus* and *Lophocebus*, and in length to *Mandrillus*. Overall, the lunate of KB

5378 is distinct from knuckle-walking taxa and does not reflect similarities to any particular taxa within the arboreal and terrestrial functional groups, or the suspensory functional groups it frequently overlaps within.

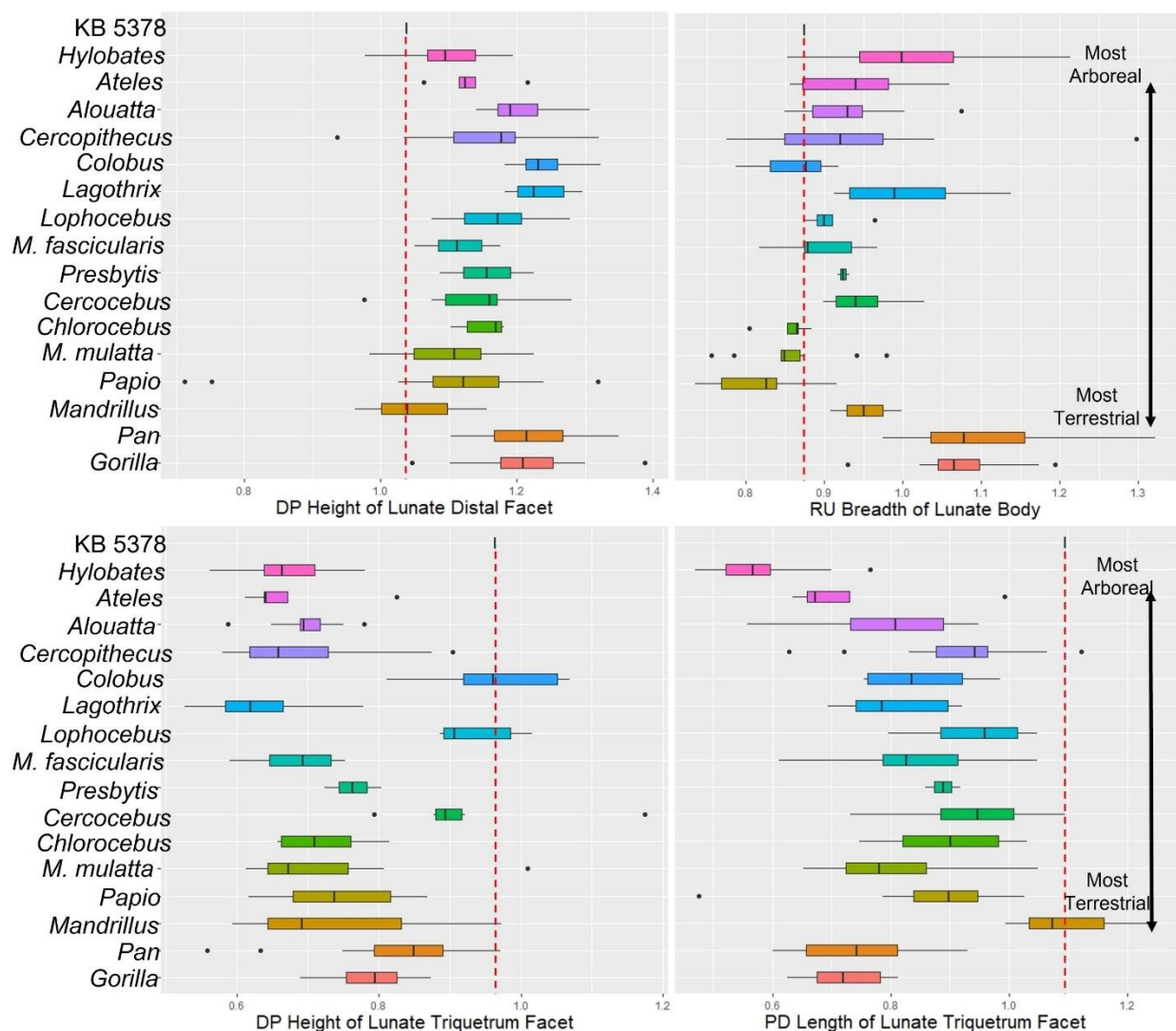


Figure 15. Box-and-whiskers plots of the Lunate distal facet, triquetrum facet and body.

Principal component analysis reveals similar trends in morphology to univariate analyses. PC1 (Fig 16) describes 27.5% of the variation of the lunate and does not clearly separate functional groups. Along PC1 KB 5378 falls within the range of both arboreal and terrestrial quadruped functional groups in having a relatively DP tall triquetrum facet and relatively PD short scaphoid facet, and outside the ranges of our suspensory and knuckle-walker groups. PC2 described 18.1% of the remaining variation within the lunate. Along PC2 KB 5378 is distinguished from knuckle-walking and suspensory taxa and falls within the range of both arboreal and terrestrial quadrupeds in having a DP lengthened

triquetrum facet, DP short body and a DP tall radial facet. Overall, the morphology of the lunate is distinct from that of knuckle-walker and suspensory taxa and can be described as similar to both arboreal and terrestrial quadrupeds.

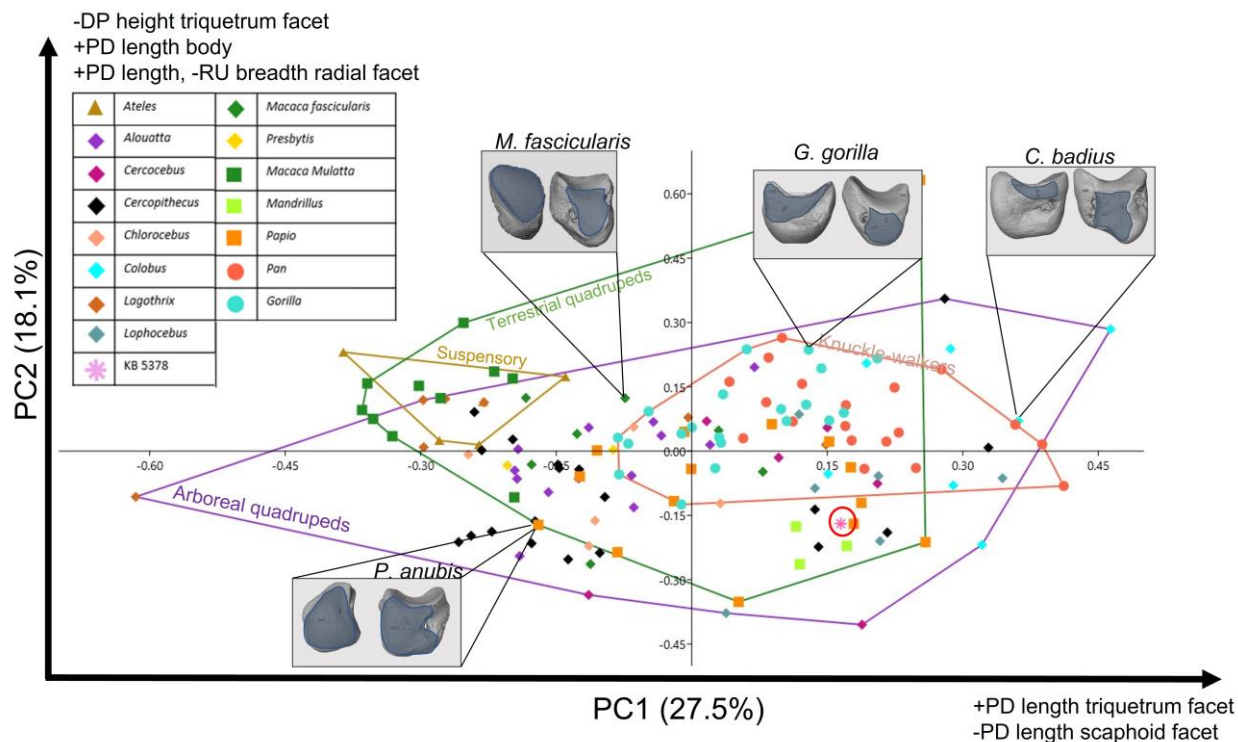


Figure 16: Within-group PCA results of the lunate. PC1 describes 27.5% of total variation, and PC2 describes 18.1%. Functional groups are each surrounded by labelled convex hulls. Surface models of representative taxa are included to demonstrate the morphology reflected at various points of the plot. Relevant facets on each surface model are shaded for clarification of the change in morphology along each axis.

## Trapezium:

The trapezium of KB 5378 has a body that is intermediate between, yet outside of the ranges of the arboreal and terrestrial quadrupeds, and the knuckle-walker functional groups in measurements including DP height and PD length (Fig. 17). However, all facets of its trapezium consistently measure closer to the morphology of knuckle-walkers than either group of quadrupedal monkeys. Notably, its Mc1 facet, the facet whose morphology qualitatively distinguishes a hominoid and monkey trapezium, is average in PD length, but above average in breath indicating a facet that stretches far further down the palmar surface of the body of the trapezium than is typical. Overall, univariate analysis indicates that the trapezium of KB 5378 is a bone with a unique combination of features of both knuckle-walkers and both groups of quadrupeds.

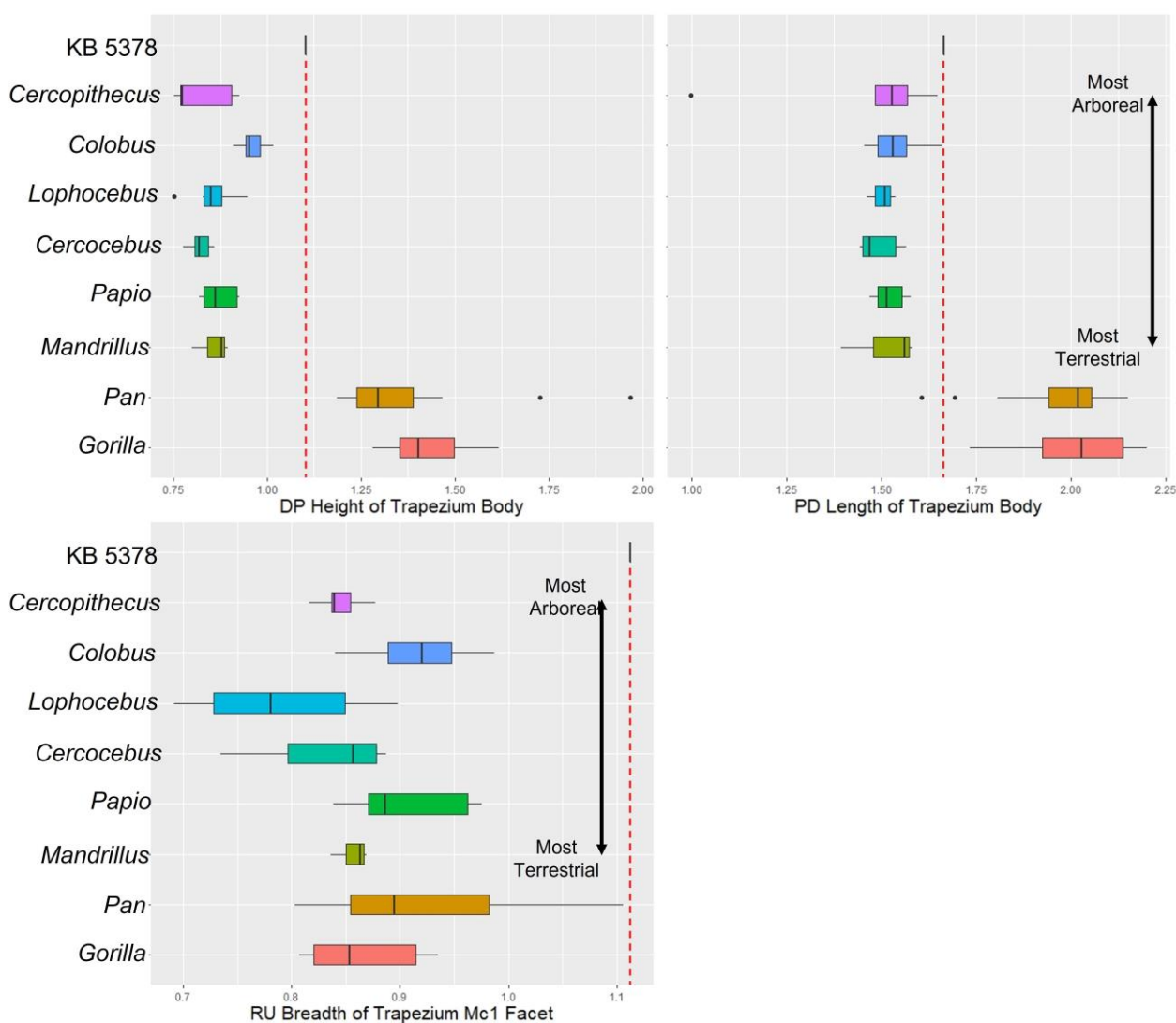


Figure 17. Box-and-whisker plots of the trapezium body and breadth of the trapezium Mc1 facet. All values are adjusted by geometric mean.

The PCA further support similarities in morphology between KB 5378 and knuckle-walking taxa (Fig. 18). PC 1 describes 35.5% of the variation within the trapezium. Along PC1, KB 5378 is distinguished from both the arboreal and terrestrial quadrupeds and overlaps with knuckle-walkers in having a DP tall body, a PD shortened trapezoid facet and similarly shortened total distal facet surfaces. PC2 describes 17.8% of variation within the trapezium. Along PC2 KB 5378 is distinct from terrestrial quadrupeds but overlaps with knuckle-walkers and some arboreal quadrupeds in having both a body and Mc1 facet of average PD length. Like the results of univariate analyses, principal component plots of the trapezium indicate similarity in morphology between KB 5378 and knuckle-walking taxa. However, PCA plots do not reflect the overlap between KB 5378 and terrestrial quadrupeds apparent in univariate analyses.

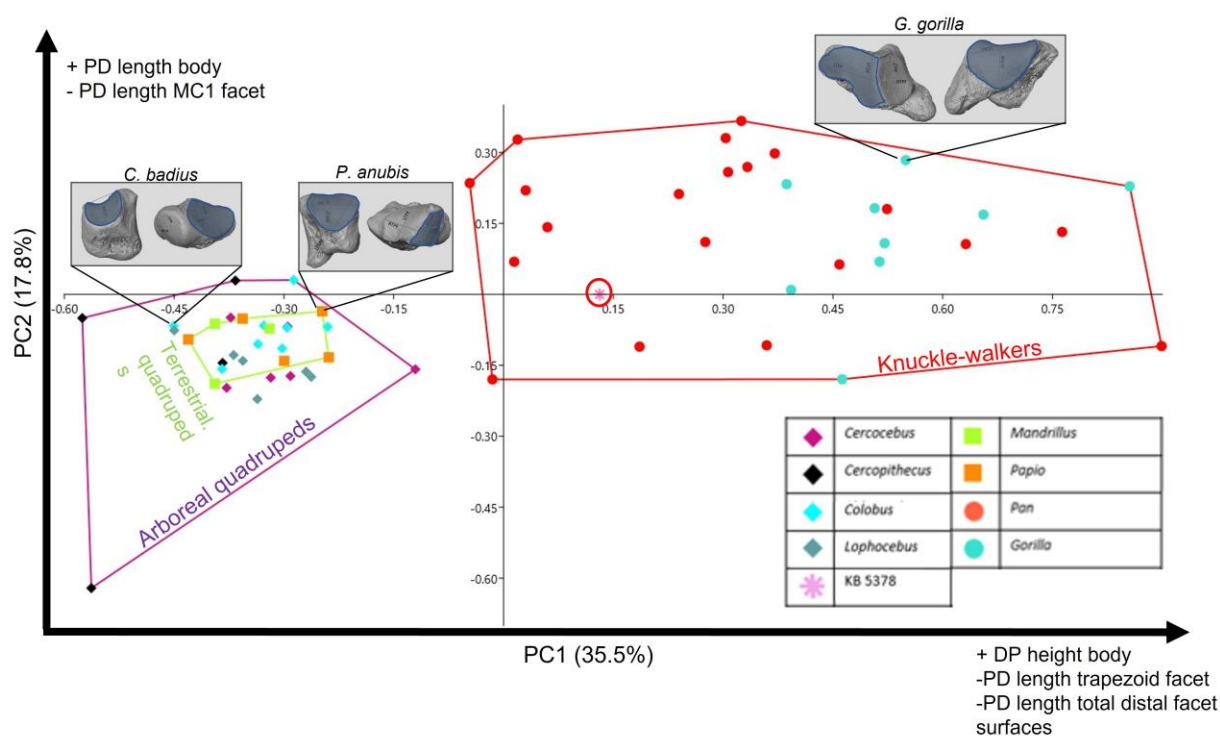


Figure 18: Within-group PCA results of the trapezium. Functional groups are each surrounded by labelled convex hulls. Surface models of representative taxa are included to demonstrate the morphology reflected at various points of the plot. Relevant facets on each surface model are shaded for clarification of the change in morphology along each axis.

### Trapezoid:

The KB 5378 trapezoid morphology shows significant overlap between each functional group in measures including DP height of the body, size of the dorsal surface, and size of the Mc2 facet (Fig 19). However, in PD length of its palmar surface and both PD length and DP height of its trapezium facet, KB 5378 falls within the ranges of *Papio* and knuckle-walkers but outside the ranges of all arboreal quadrupeds. This indicates that while the KB 5378 trapezoid is not particularly distinct, it does align more with the facet morphology of knuckle-walkers and the terrestrial quadrupeds. Particularly noteworthy is that the trapezium facet of the trapezoid of KB 5378 is similar to that of the knuckle-walkers, the functional group with whom KB 5378 seems to share the majority of its trapezium facet morphology.

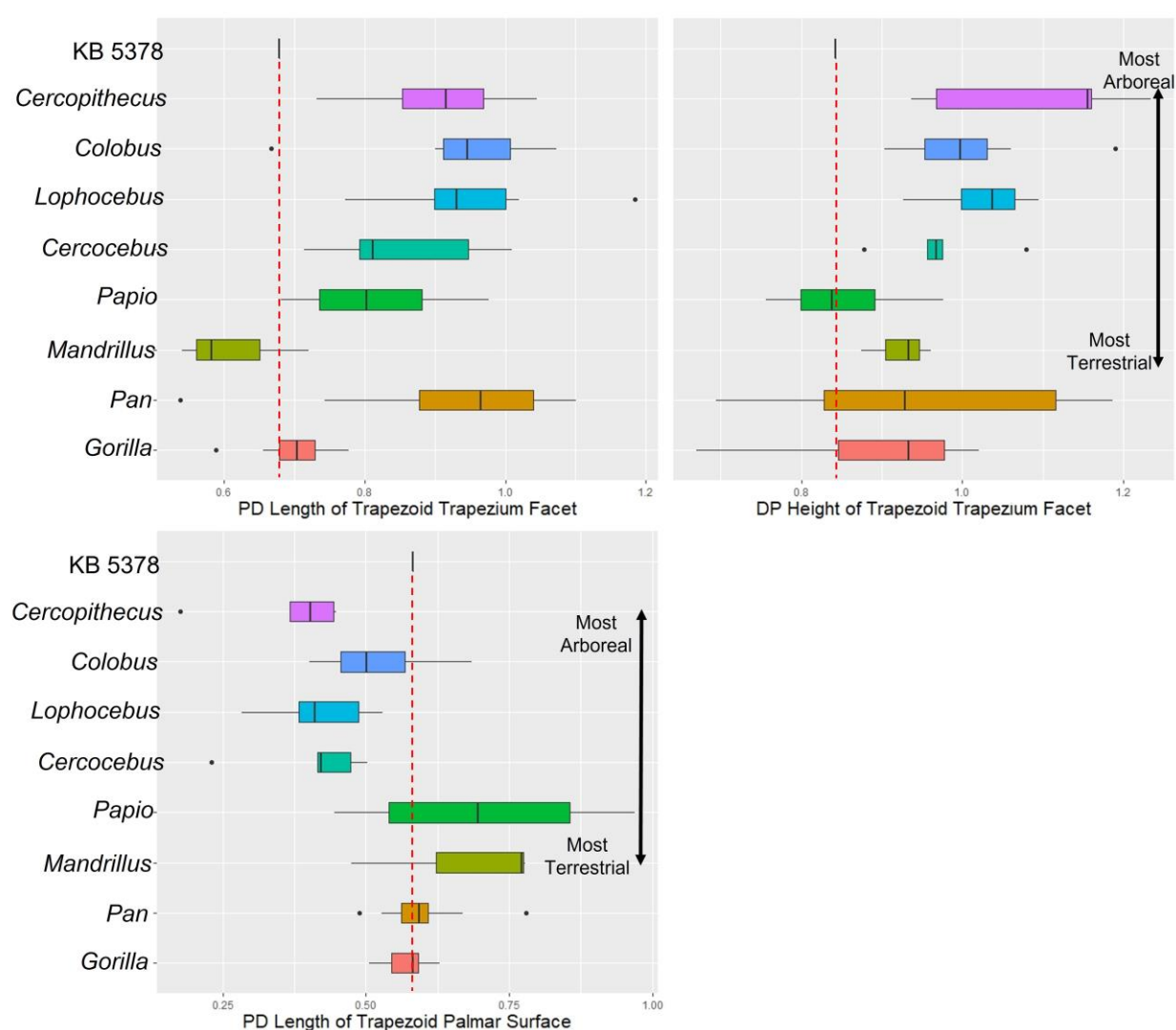


Figure 19. Box-and-whisker plots of the trapezoid trapezium facet and palmar surface. All values are adjusted by geometric mean.

Principal component analyses support the trends in morphology evidenced in univariate analyses. PC1 describes 34.8% of the variation of the trapezoid. Along PC1 KB 5378 is somewhat distinguished from the terrestrial quadrupeds and most arboreal quadrupeds (with the exception of several individuals of *Cercopithecus*) in having a relatively DP short body and PD short dorsal surface (Fig 20). PC2 describes 22.4% of the variation within the trapezoid. Along PC2 KB 5378 cannot be distinguished from any functional groups but falls closest to taxa including *Gorilla* and *Papio* in having a PD shortened distal surface and trapezium facet. Overall, the trapezoid of KB 5378 reflects *Gorilla*-like morphology but shares similarities with *Papio* as well.

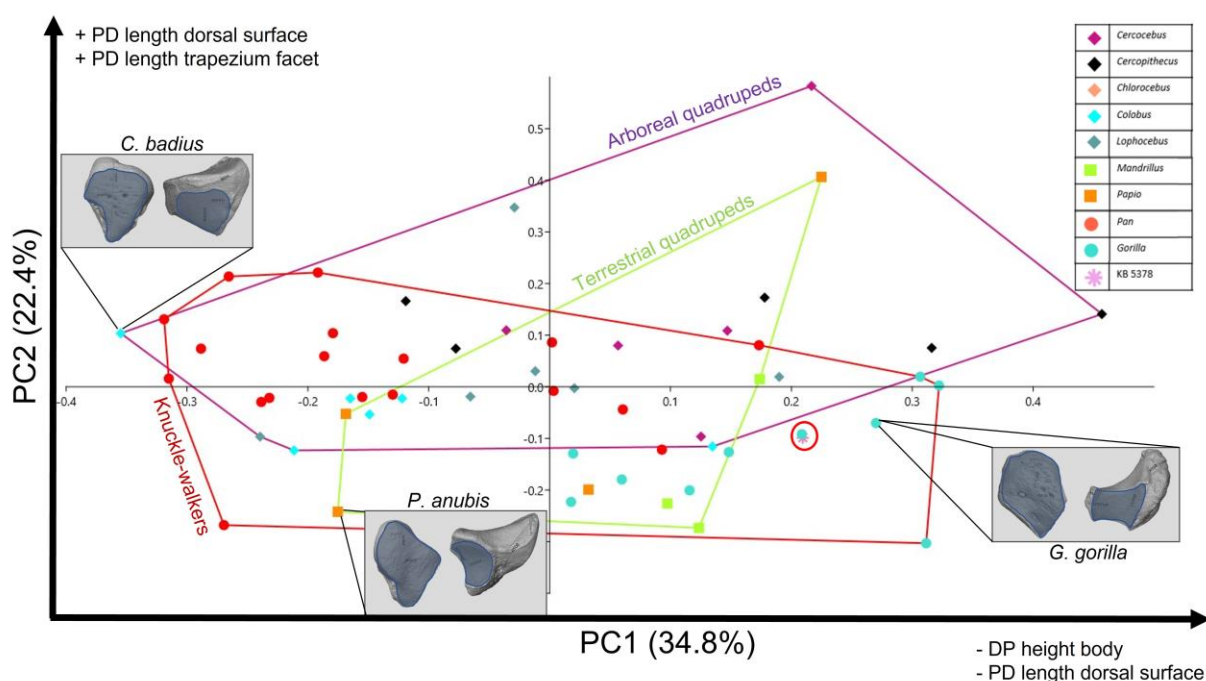


Fig 20: Within-group PCA results of the trapezoid. Functional groups are each surrounded by labelled convex hulls. Surface models of representative taxa are included to demonstrate the morphology reflected at various points of the plot. Relevant facets on each surface model are shaded for clarification of the change in morphology along each axis.

### Capitate:

The capitate of KB 5378 is characterized by a mosaic of features from all functional groups (Fig 21,22). Though it is of average PD length, the body of the KB 5378 capitate is particularly DP tall, and RU broad reflecting the general morphology of *Hylobates* and *Gorilla*. Meanwhile, the morphology of the proximal capitate facet is similar to that of suspensory taxa including *Ateles* and *Hylobates* by being both RU narrow and DP short. The hamate facet of KB 5378 is uniquely DP tall, falling above the ranges of all taxa, but below average in PD length similar to that of *Hylobates*. Thus, the morphology of the capitate of KB 5378 is most consistently similar to that of *Hylobates* and *Gorilla*.

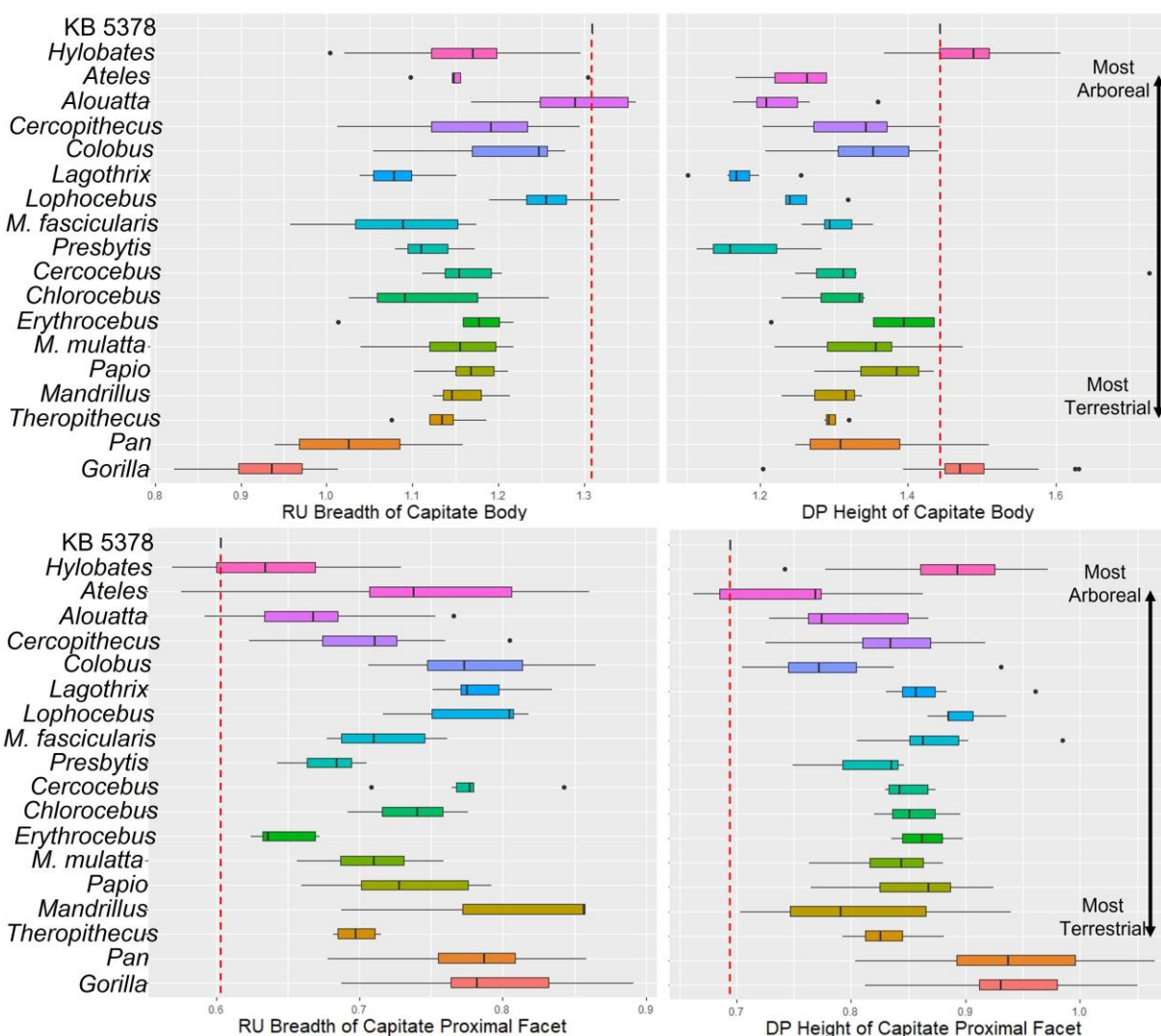


Figure 21. Box-and-whisker plots of the capitate body and proximal facet All values are adjusted by geometric mean.

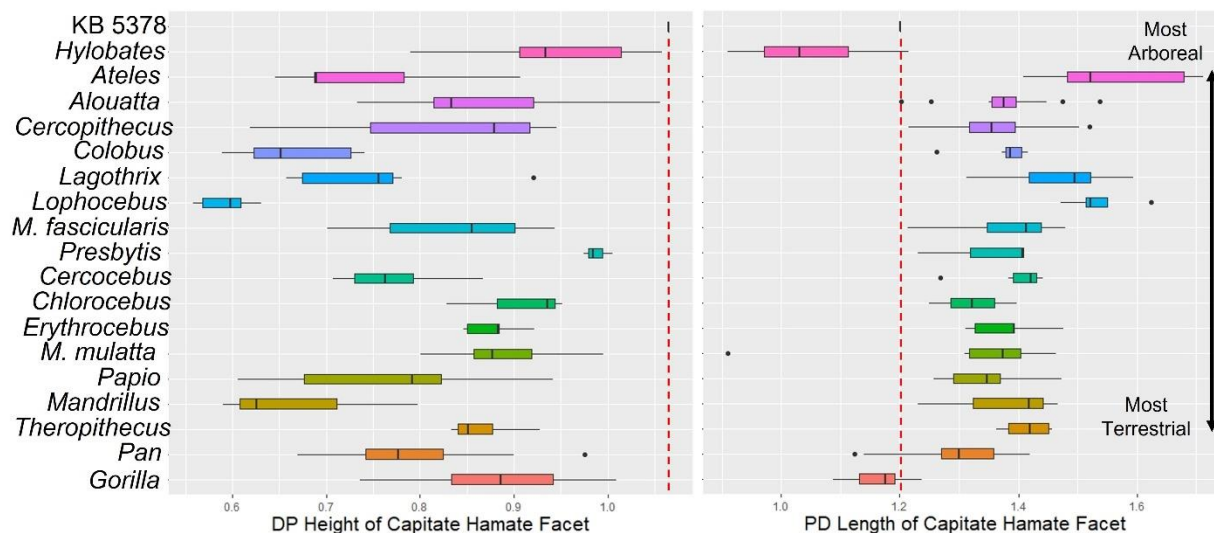


Figure 22. Box-and-whiskers plots of the capitate hamate facet. All values are adjusted by geometric mean.

Principal component analyses reveal additional trends in morphology not seen in univariate analyses (Fig. 23). PC1 describes 44.3% of variation of the capitate. Along PC1 KB 5378 is distinguished from suspensory taxa, and most similar to *Gorilla* and select individuals of *M. mulatta*, *Presbytis* and *Aloutta* in having a relatively PD short but DP tall hamate facet and a PD short body (fig 23). PC2 describes 17.1% of variation in the capitate. Along PC2 KB 5378 can again be distinguished from the suspensory functional group in having a relatively PD tall and RU narrow body and a PD and DP short hamate facet. This plot indicates that the capitate of KB 5378 reflects *Gorilla*-like morphology in its body and hamate facet and is distinct from suspensory taxa but does not align with any particular functional group.

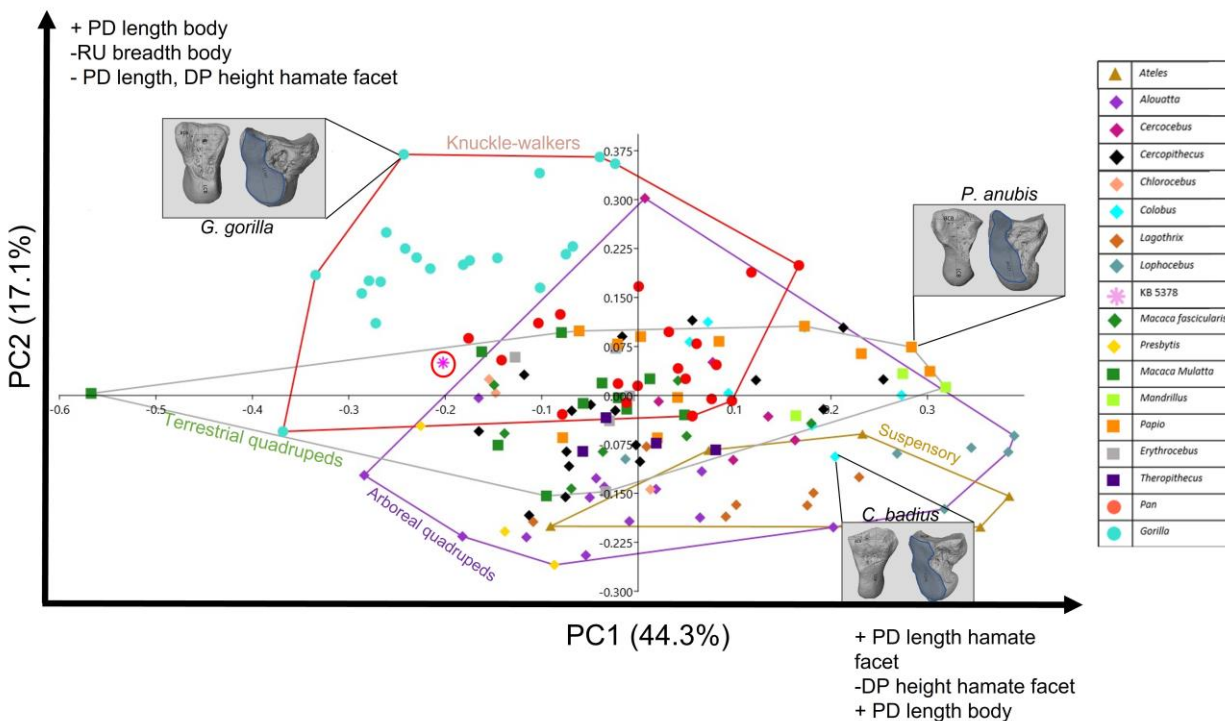


Figure 23. Within-group PCA results of the capitate. PC1 describes 44.3% of total variation, and PC2 describes 17.1%. Functional groups are each surrounded by labelled convex hulls. Surface models of representative taxa are included to demonstrate the morphology reflected at various points of the plot. Relevant facets on each surface model are shaded for clarification of the change in morphologies along each axis.

### Hamate:

The hamate of KB 5378 appears intermediate between all taxa in measurements of the PD length of its body and size of the capitate facet (Fig. 24). In DP height, the hamate of KB 5378 appears taller than average, though overlap occurs with *Hylobates*, the knucklewalkers and the uppermost ranges of quadrupedal monkey taxa.

However, the body of the hamate excluding the hamulus is DP short and PD long compared to other taxa. When the hamate is excluded, the hamate body is PD longer than all taxa except *Ateles*, *Hylobates* and the uppermost range of *Lophocebus* yet DP shorter than the median of every taxon apart from *Hylobates* though overlap occurs in the lower ranges between several taxa from all functional groups (Fig 24). This indicates that the hamulus of KB 5378 is above average in PD length and below average in DP height compared to other taxa in our sample. In univariate analyses the triquetrum facet of the hamate is DP short, overlapping with the lowest ranges of several quadrupedal taxa, and outside of the ranges of many arboreal quadrupeds. Conversely, this facet is relatively PD tall, though overlap between functional group does occur. Overall, the

morphology of the KB 5378 hamate does not align with any one functional group or taxon but is suggestive of generalized quadrupedal morphology.

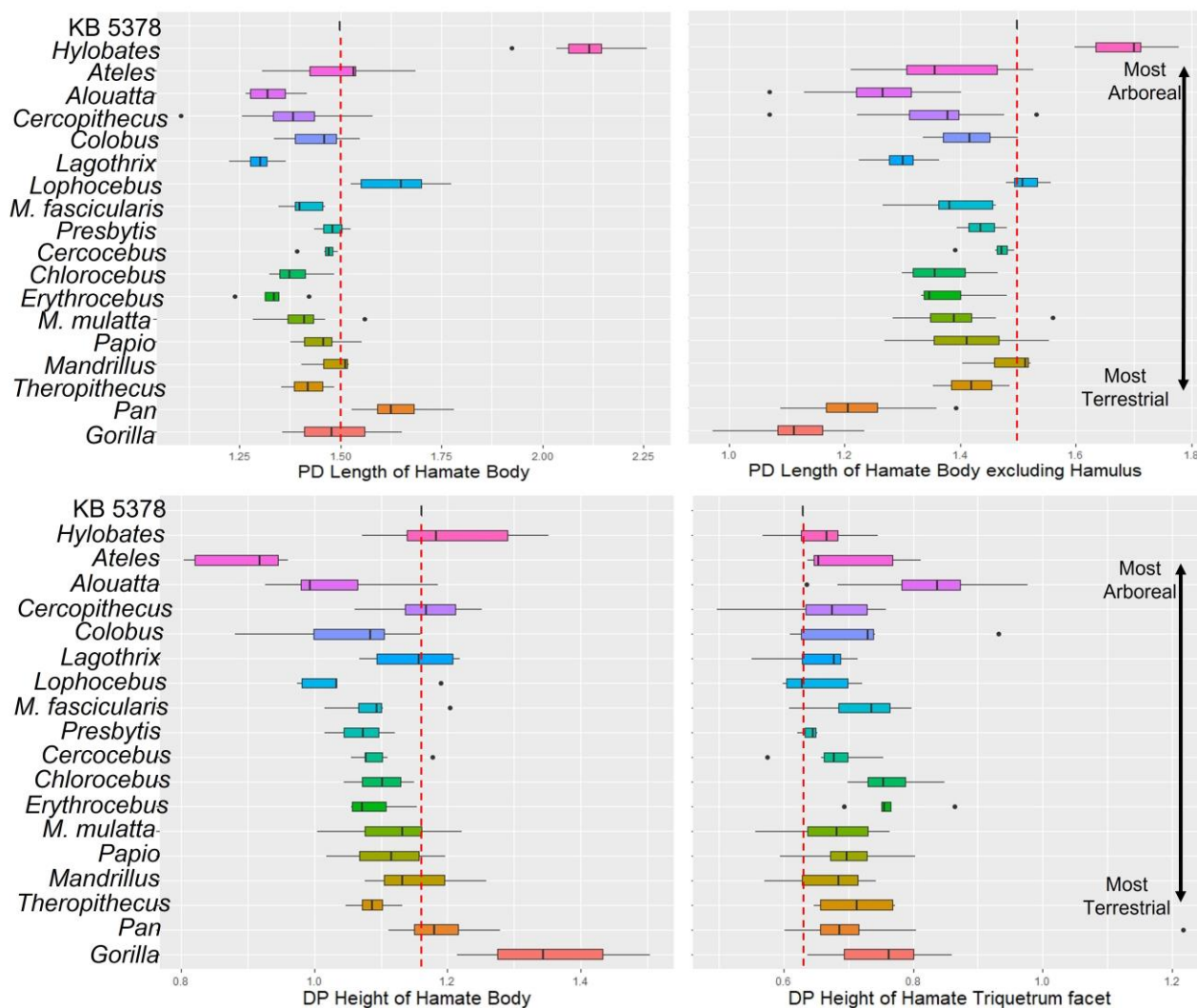


Figure 24. Box-and-whisker plots of the hamate body and triquetrum facet. All values are adjusted by geometric mean.

Principal component analyses agree with the findings of the univariate analyses (Fig. 25). PC1 describes 43.5% of the variation within the hamate. Along PC1 KB 5378 can be distinguished only from the suspensory group in having a relatively DP short and PD long capitate facet, and a PD long triquetrum facet (Fig 25). PC2 describes 21.5% of the variation in the hamate. Along PC2 KB 5378 can be distinguished only from the suspensory group in having a relatively PD long, RU narrow hamate body with a DP shortened triquetrum facet. PC1 and PC2 indicate that the hamate of KB 5378 does not reflect the morphology of a specific taxon or functional group, but that it is distinct from the morphology of suspensory taxa.

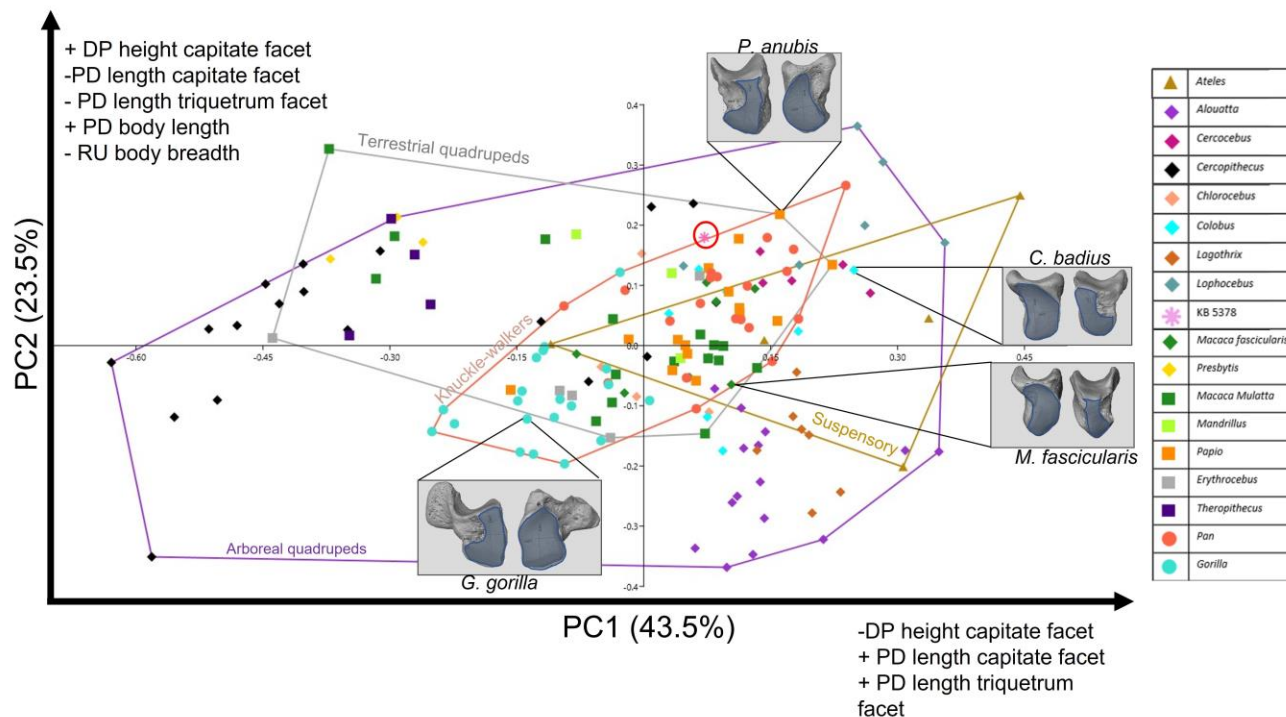


Figure 25. Within-group PCA results of the hamate. PC1 describes 43.5% of total variation, and PC2 describes 23.5%. Functional groups are each surrounded by labelled convex hulls. Surface models of representative taxa are included to demonstrate the morphology reflected at various points of the plot. Relevant facets on each surface model are shaded for clarification of the change in morphology along each axis.

### Comparison of absolute size in carpals:

Univariate analyses were performed using raw variables (i.e. not divided by the geometric mean) of overall PD length, RU breadth and DP height of each carpal to assess absolute size of KB 5378 relative to the comparative sample.

Overall, the KB 5378 carpal bones are most similar in size to *Mandrillus* and *Papio*. More specifically, they are consistently smaller than the range of variation of knuckle-walkers for every bone, and typically larger than all arboreal quadrupeds (Fig 26, 27). The only notable exceptions to this pattern are for the PD length of the hamate, which overlaps with the upper range of *Hylobates*, and the DP height of the trapezoid and RU breadth of the capitate that overlaps with the lowest range of variation of *Pan*.

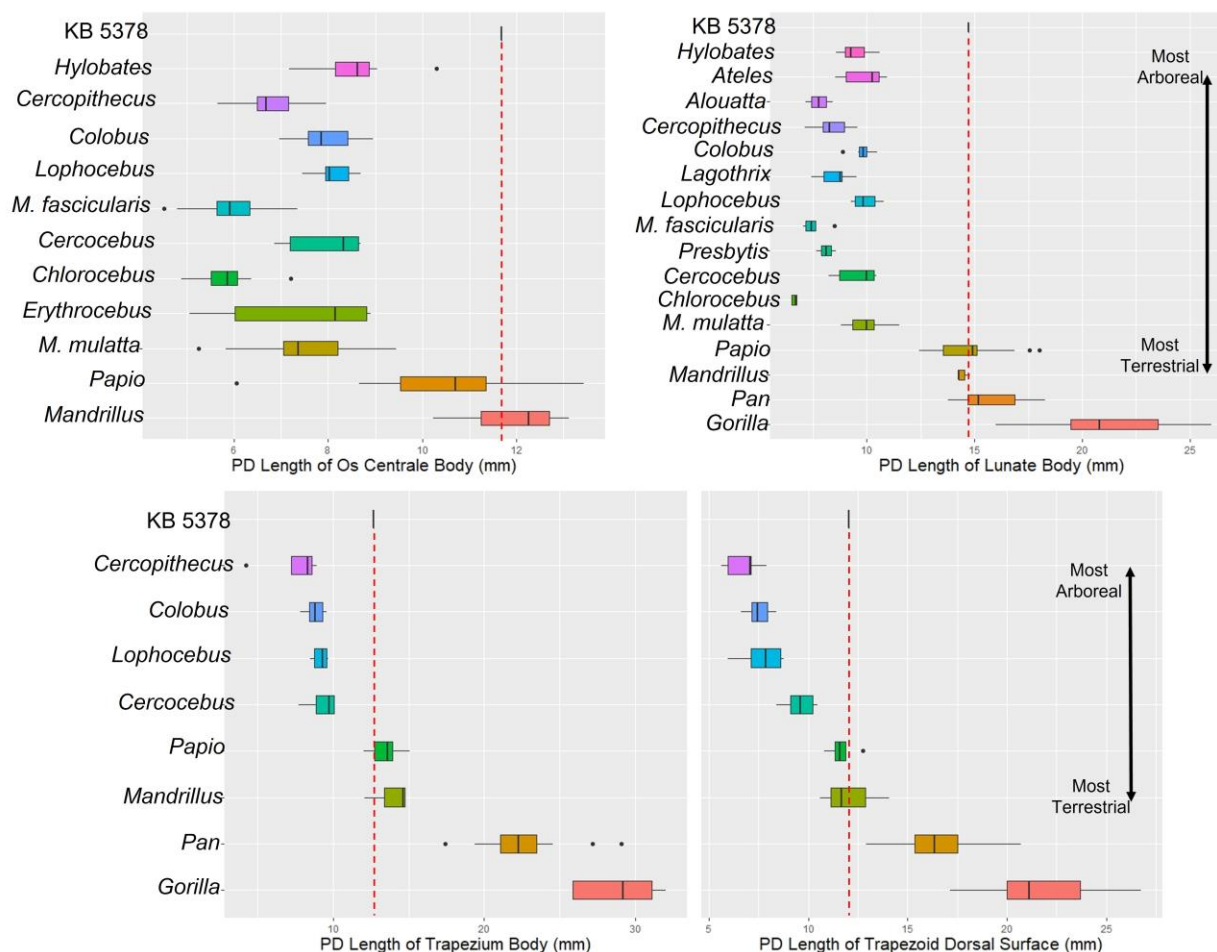


Figure 26. Box-and-whisker plots of the PD length (mm) of the os centrale, lunate and trapezium bodies and PD length (mm) of the trapezoid dorsal surface.

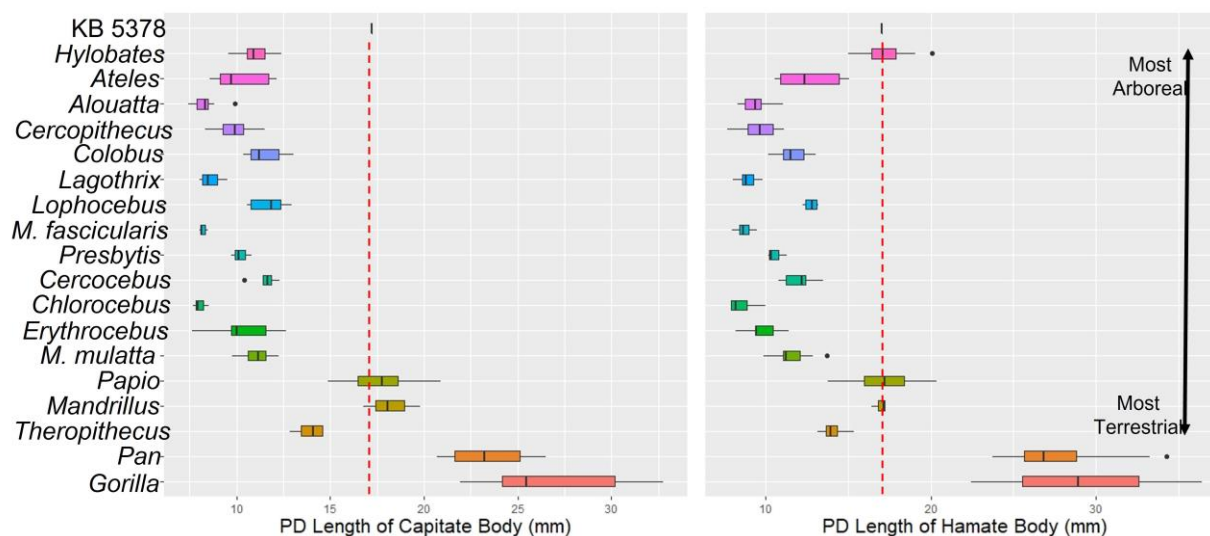


Figure 27. Box-and-whisker plots of the PD length (mm) of the capitata and hamate body.

#### Comparison of absolute size to metacarpals:

I also assess the maximum PD length of each metacarpal of select comparative taxa and the fossil metacarpals (Fig. 3) associated with KB 5378 (Fig. 28) to aid our understanding of the association between the KB 5378 carpals and metacarpals and taxonomic attribution. The length of KB 5378 Mc2-5 each fall within the range of variation seen in *Papio* and *Mandrillus* (Fig 28). However, the length of KB 5378 Mc1 falls well above that of most taxa in our sample and is only within the range of *Gorilla* indicating it has an exceptionally long Mc1. Overall, patterns in absolute size of the metacarpals reflect trends seen in the carpals, with the exception of Mc1.

To further investigate the potential association between the KB 5378 carpals and metacarpals, I assessed metacarpal PD length relative to PD length of the capitata, which was used as a proxy for overall carpus size. Bivariate plots for each metacarpal confirm that the KB 5378 Mc2-5 are similar in relative size to *Mandrillus* and *Papio*, but that the Mc1 is most similar to *Gorilla* (Fig 28, 29).

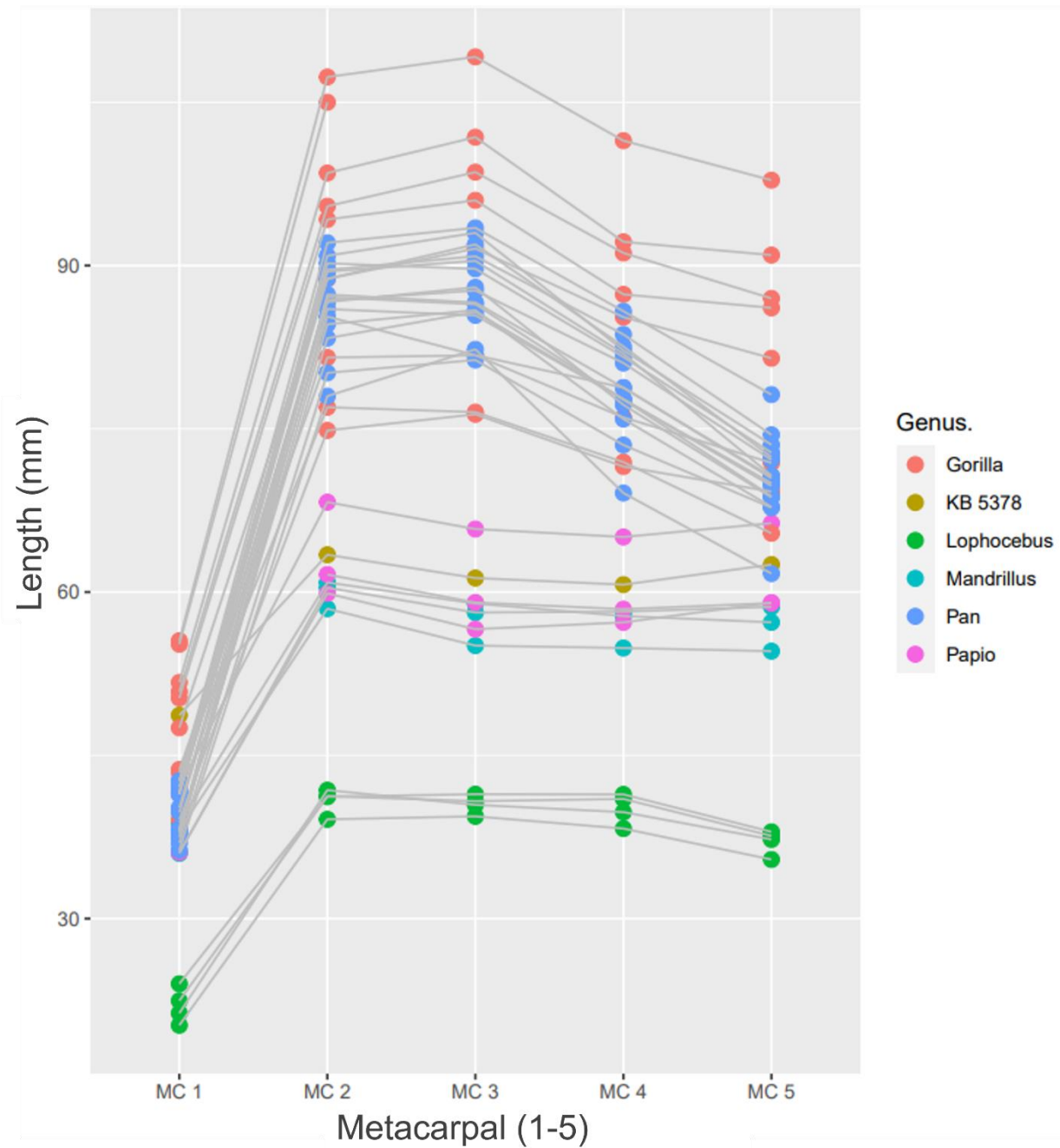


Figure 28. Comparative plot showing the absolute lengths of all metacarpals per individual. The metacarpals belonging to each individual are connected using grey lines to illustrate the actual angles created by varying lengths of each metacarpal.

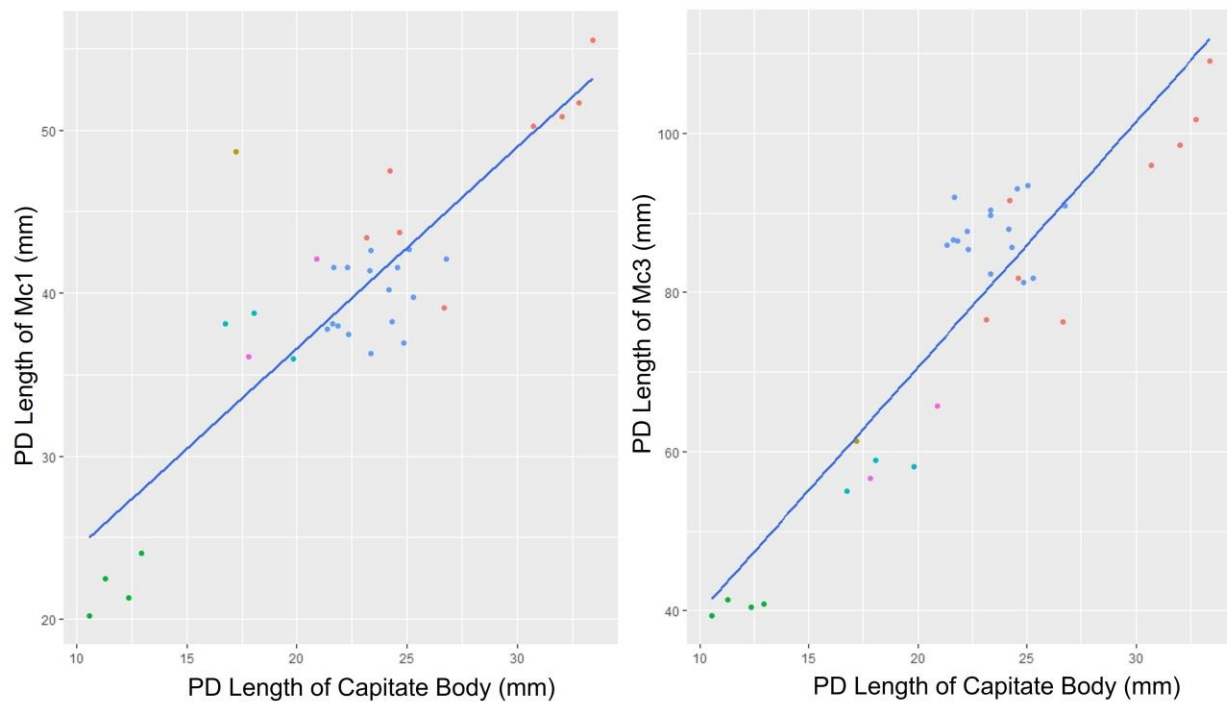


Figure 29. Bivariate plots comparing the PD length of the capitate body to the PD length of each metacarpal. A regression line is placed with a confidence interval of 95%.

## Discussion

Summarizing the quantitative results reveals that though there is substantial overlap across functional groups in our comparative sample, KB 5378 is most similar to terrestrial and arboreal cercopithecoids. More specifically, KB 5378 shares traits with *Papio* and *Mandrillus* both quantitatively and qualitatively in morphology and absolute size. Results are discussed below for each carpal in more detail.

### Comparative Morphology

#### Scaphoid:

The incomplete articular morphology preserved in the KB 5378 partial scaphoid, has morphology that is best described as reflecting generalized quadrupedalism. The flat, broad radial facet and a shallow os centrale facet suggest increased stability at the radiocarpal and midcarpal joints and are most similar to terrestrial quadrupedal taxa in our sample. However, limited preservation of scaphoid, including the lack of tubercle, prohibit further functional interpretation.

#### Os Centrale:

Results of our quantitative analyses reveal that the KB 5378 os centrale shares morphological traits with both arboreal and terrestrial quadrupeds but was distinct from suspensory taxa. Qualitatively, the KB 5378 has a distinct proximoulnar lunate facet (Fig. 7). This facet is absent in arboreal species including *Ateles* and *Pongo* and is more commonly found in papionines such as *Papio* and *M. mulatta* who frequently use

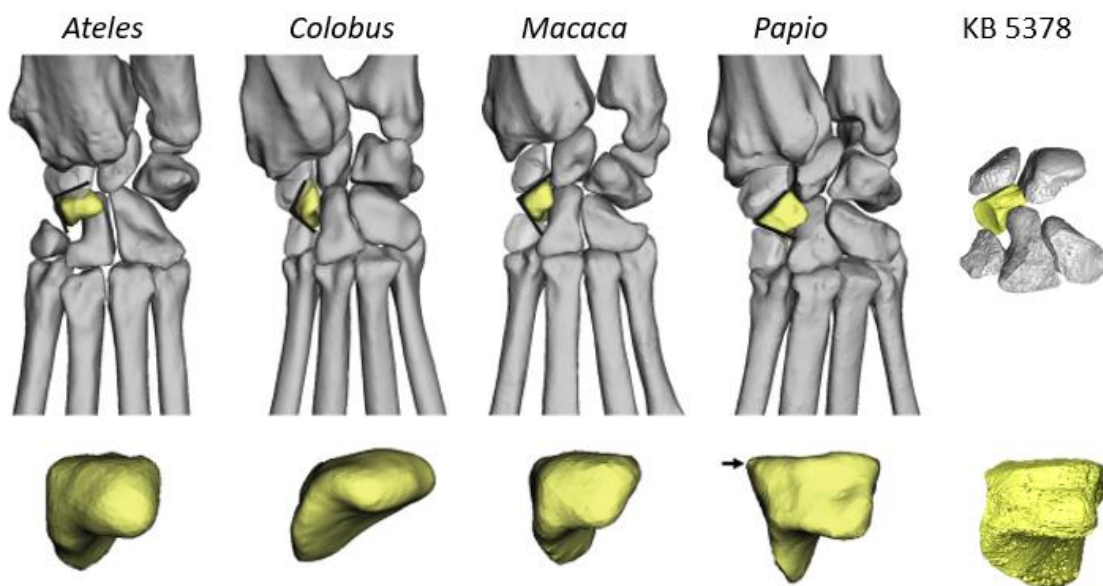


Fig 30. The angle and orientation of the scaphoid and trapezoid-trapezium facets of the os centrale shown ex and in situ. An arrow is included to indicate the joint between the scaphoid and trapezoid trapezium facet at which measurement was taken. Adapted from Orr, 2018.

terrestrial, digitigrade locomotion (Orr 2018). This facet, in tandem with the radially oriented trapezoid-trapezium facet, has been shown in a study using CT-based motion captures of cadaveric wrists to facilitate a form of rotation of the os centrale characterized by early contact with the capitate head during extension (Orr, 2018). This early contact improves joint congruence and load transfer through the joint, thus increasing stability during terrestrial quadrupedal locomotion (Orr, 2018).

The angle between the trapezoid-trapezium and scaphoid facets of the os centrale has also been shown to be informative about mobility and stability of the scapho-capitate-centrale joint (Orr, 2018). In KB 5378, the angle between the scaphoid and trapezoid-trapezium facet, taken at the approximate midpoint of each facet, is 88.1 degrees (Fig 30). In digitigrade species like *Papio* this angle is typically acute, while species that use a mix of digitigrade and palmigrade postures such as *M. mulatta* and those that utilize arboreal, palmigrade locomotion such as *Colobus* exhibit a right, or obtuse angle respectively between these facets (Orr, 2018). During extension, having an acute angle at these facets creates a more tightly packed articulation between the trapezoid, os centrale, and capitate that limits extension and further facilitates more effective transmission of forces through the joint during digitigrade locomotion (Orr, 2018). KB 5378 has a slightly acute angle between these facets, indicating an intermediate morphology between *Papio*, *Macaca* both of whom engage in terrestrial quadrupedal locomotion, but to varying degrees. This intermediate angle, along with the facet morphology described above suggests that KB 5378 had os centrale morphology most similar to a generalized quadruped, with specializations for terrestrial quadrupedalism.

#### Lunate:

The KB 5378 lunate morphology overlaps with several functional groups and taxa, but overall is most similar qualitatively and quantitatively to quadrupedal cercopithecoids and particularly terrestrial quadrupedal taxa. Results of our quantitative analysis reveal that the KB 5378 lunate body is relatively RU narrow (Fig 15,16), which is a morphology common in cercopithecoids and unlike the RU broader lunates of great apes (Lewis, 1989). The distal capitate facet of the KB 5378 lunate is unique in being both DP tall, and RU narrow. The reduced size of the articulation between the lunate and capitate suggests limited mobility but also limited surface area for transfer of load at the capitollunate joint.

The triquetrum facet of KB 5378 lunate is both PD long and DP tall relative to other taxa. The functional morphology of the lunate triquetrum facet has not yet been explored. However, in primates that regularly use postures like knuckle-walking and digitigrady (particularly *Papio* and *Pan*) the lunotriquetral joint is known to be planar which limits the range of extension at that joint (Orr, 2017). An expanded lunate triquetrum facet may impact the range of motion between these coplanar facets during extension. However, preservation of the KB 5378 triquetrum is needed to confirm these morphological predictions.

Finally, the radial facet is large and expands across the entire proximal aspect of the KB 5378 lunate and when articulated with the scaphoid creates a coplanar surface with the scaphoid's radial facet. The congruent orientation between the radial surfaces of the scaphoid and lunate is a feature often noted in knuckle-walkers and terrestrial quadrupeds to increase the stability of the radio-carpal joint (Kivell, 2016a).

Trapezium:

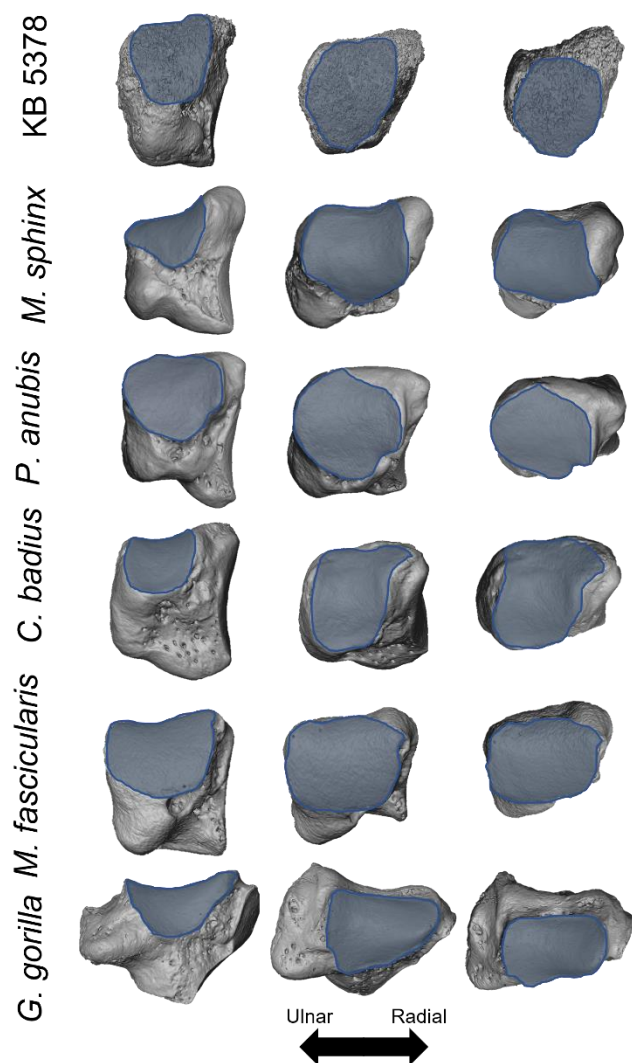


Fig 31: Surface models of trapezia of KB and representative comparative taxa are shown with a focus on the MC1 facet.

The KB 5378 trapezium has a mix of both knuckle-walking and arboreal/terrestrial quadruped morphology. Comparative quantitative results of the facet morphology group KB 5378 as similar to the knuckle-walking taxa in our sample (Fig. 17, 18). However, qualitatively the overall KB 5378 trapezium morphology is unlike knuckle-walkers and most similar to quadrupedal monkeys (Fig. 9). Extant cercopithecoids and great apes have a saddle-shaped Mc1 facet, which allows for rotation and opposition of the thumb (Tocheri et al., 2003; Tocheri et al., 2005). Conversely, platyrrhines and strepsirrhines often have a flat or cylindrical Mc1 facet that can reduce the mobility of the thumb by creating a more rigid hinge-like joint at the trapezium-Mc1 joint (Kivell, 2016a). The trapezium-Mc1 joint of KB 5378 is not saddle-shaped. Instead, it is oval-shaped, with a flat edge at its distal-most extreme and becomes convex as it expands palmarly down the palmar aspect of the bone (Fig 9, 31). In our sample, this morphology is unique to KB 5378 as even though many cercopithecoids had a flattened trapezium-Mc1 facet (see *Papio* and *Mandrillus* in Fig. 9), their facets were consistently more concave and therefore maintained some degree of

a saddle shape, than that of KB 5378. The trapezium-Mc1 facet of KB 5378 is additionally uniquely broad, expanding far further down the palmar surface of the body than in any other comparative taxa. This morphology suggests that KB 5378 may have had thumb mobility similar to that of the extant cercopithecoid taxa but with a greater degree of flexion.

Additionally, unlike the trapezia of African apes, the trapezium of KB 5378 does not show a clear facet for Mc2. The presence of an Mc2 facet was variable within our monkey sample, indicating that the lack of an Mc2 facet in KB 5378 may be a shared trait with extant monkeys. However, the orientation of the Mc2 facet on the trapezium has

been discussed in humans and some apes as an indicator of manipulative and gripping abilities, as well as for the distribution of force during locomotion across the carpus (Tocheri et al., 2003). In humans, the Mc2 facet of the trapezium is oriented sagittally, allowing a great degree of Mc2 pronation compared with African apes (Tocheri et al., 2003). If an Mc2 facet in apes and humans serves to increase mobility for Mc2, the lack of an Mc2 facet of the trapezium of KB 5378 may indicate that it had limited Mc2 mobility and perhaps only basic gripping abilities. The lack of a facet for Mc2 paired with the morphology of the facet for Mc1 on the trapezium indicates a hand with relatively limited mobility of the thumb, and perhaps the index finger.

Further differentiating the trapezium of KB 5378 from knuckle-walkers is a lack of a proximo-radial tubercle. In apes, this tubercle serves as an attachment point for flexor retinaculum, a fibrous band that protects and supports the flexor muscles of the forearm (Deak and Bordini, 2019). The lack of tubercle seen in KB 5378, and indeed in many of the other terrestrial cercopithecoids in our sample, creates a more shallow carpal tunnel (in combination with features of the hamate discussed below) which may imply a lack of support for the strong flexor muscles used in climbing, and consequently less reliance on climbing behaviors. This, in combination with the morphologies describe above, imply that the KB 5378 trapezium is best adapted for terrestrial quadrupedalism with little climbing and particularly limited thumb mobility compared to humans and apes, but possibly more thumb mobility than extant monkeys.

#### Trapezoid:

Quantitative measurements of the trapezoid generally reveal considerable overlap between all functional groups and KB 5378. However, the morphology of the trapezoid trapezium facet, and the PD length of the palmar surface of the trapezoid indicate that overall, the KB 5378 trapezoid is most similar in morphology to terrestrial cercopithecoids and knuckle-walkers (Fig. 19, 20). Unfortunately, complicating functional interpretations of this bone is a lack of foundational literature studying its morphology, especially in non-hominoid primates.

In arboreal quadrupedal strepsirrhines the proximal embrasure between the capitate and the trapezoid -that which articulates with the os centrale- is known to be wider dorsally to facilitate palmar rotation (pronation) during midcarpal rotation. Conversely, in leaping strepsirrhines the embrasure is wider palmarly to promote dorsal rotation (supination) during midcarpal rotation (Hamrick, 2007; Kivell, 2016a). In KB 5378, the capitate-trapezoid embrasure is wider dorsally indicating a midcarpal joint more capable of palmar rotation during midcarpal rotation and greater stability at that joint during quadrupedal locomotion. Additionally, the Mc2 facet of the trapezoid of KB 5378 is keeled in dorsal view (Fig. 10). In extant Old World monkeys and African apes, this keeling creates a tight articulation with a complementarily concave Mc2 proximal facet, which creates a more stable joint (Fig. 10) (Kivell, 2016a).

#### Capitate:

Quantitative comparison indicate the proximal capitate morphology of KB 5378 is hylobatid-like in being both extremely RU narrow and DP short (Fig 21, 22, 23). The capitate head is often discussed in the context of midcarpal joint mobility and stability (Daver et al., 2012; Kivell, 2016a; Lewis, 1989; Richmond, 2006). More specifically, the

capitate's proximal surface is broader in taxa that habitually use terrestrial quadrupedalism as this adds stability to a joint that experiences high forces during such locomotion (Daver et al., 2012; Kivell, 2016a). Conversely, taxa that typically use suspensory locomotion such as the hylobatids and *Ateles*, tend to have a RU narrow proximal head of the capitate, which, combined with broader proximal hamate, allows for greater mobility at the midcarpal joint (Kivell, 2016a; Lewis, 1989). The hylobatid-like KB 5378 capitate head is notably narrower than other cercopithecoids in our sample (Fig. 21). However, the proximal hamate is not hylobatid-like in its RU breadth (described further below), suggesting the KB 5378 midcarpal joint is not hylobatid-like overall. The relatively narrow capitate head in KB 5378 therefore suggests less stability than the RU broader capitate heads of terrestrial cercopithecoids and, together with the hamate (see below), a midcarpal joint morphology that is most similar to arboreal quadrupedal monkeys.

The metacarpal facets of KB 5378 capitate are smooth and overall planar (Fig 11). Unlike African apes, the small areas of concavity of the Mc3 facet are shallow and variable, with greater concavity dorsally than palmarly. In African apes, a complex and concavoconvex Mc3 facet- in addition to large interosseous ligaments- create a locking mechanism that limits axial rotation and sliding at that joint ((Lovejoy et al., 2009; Marzke, 1983; Rein and Harvati, 2013; Selby et al., 2016). Moreover, deeply concave Mc facets limit sliding and rotation of the metacarpals and consequently add stability to the joint (Marzke, 1983). The relative flatness of the Mc3 facet of KB 5378 is a shared trait to many Old World monkeys. A planar Mc3 articulation is less stable, as it cannot resist torsion or shear forces within the carpo-metacarpal joint (Lovejoy et al., 2009; Marzke, 1983). However, the Mc2 facet of KB 5378 is angled sharply radially, a trait commonly observed in knuckle-walking apes that allows the capitate to act as a buttress against torsional forces and increases the stability of the carpo-metacarpal joints (Lovejoy et al., 2009; Marzke, 1983; Selby et al., 2016). Overall, the Mc facets of KB 5378 reflect combined morphology of both a generalized joint and one specialized for stability during high force locomotion. The Mc facets do not reflect any suspensory morphology like the proximal facets seem to, further complicating functional interpretation of the capitate.

#### Hamate:

The hamate of KB 5378 is characterized by generalized monkey morphology in its overall size and shape. It is wedge shaped, and approximately equal in size to the capitate (for example, in PD length there is a difference of only 0.15 mm between the slightly larger capitate and the hamate). Quantitatively, KB 5378 hamate overlaps with taxa from all functional groups and is best described by the morphologies of a generalized quadruped. However, specific qualitative morphologies separate KB 5378 from suspensory taxa and arboreal quadrupedal monkeys including the orientation of its triquetrum facet and its relatively small hamulus.

The orientation of the triquetrum facet of the hamate can be used to interpret stability of the midcarpal joint. It is broad and proximally oriented in quadrupeds which limits radioulnar deviation and supination creating a more stable joint during extended carpus postures often used during digitigrade locomotion and creates a stable platform for the triquetrum (Daver et al., 2012; Kivell, 2016a; Lewis, 1989; O'Connor, 1975). In KB 5378, the triquetrum facet is proximally oriented creating a flatter and consequently more

stable midcarpal joint suggesting a midcarpal joint well suited for terrestrial quadrupedalism. (Fig. 12).

In addition to the angle of the triquetrum facet, the size of the hamate hamulus can be informative of both joint stability and associated soft tissue configuration (Kivell, 2016a; O'Connor, 1975; Ward et al., 1999; Ward, 2002). KB 5378 exhibits a PD long, and DP short hamulus when compared with extant taxa. However, the hamulus is overall considerably smaller than any ape included in our sample in both measurements (Fig 24). Having a smaller hamulus, particularly one with minimal distal projection, is a known adaptation to dorsiflexion that is normally limited by the extended hamulus in hominoids at the hamate-Mc5 joint and allows greater degree of dorsiflexion useful in palmigrade/digitigrade substrate contact (Kivell, 2016a; O'Connor, 1975; Ward et al., 1999; Ward, 2002). Additionally, the typically hominid trait of a large, pronounced hamulus has been associated with having a deep carpal tunnel capable of accommodating strong digital flexors of the forearm used during climbing and suspension (Kivell, 2016a; Ward et al., 1999; Ward, 2002). Therefore, the lack of large hamate hamulus and aforementioned proximo-radial trapezium tubercle suggest a shallow carpal tunnel and less pronounced digital flexor musculature of the forearm suggesting a de-emphasis of climbing and suspensory behaviors in KB 5378 during life.

#### Metacarpals: size, association, and development

The Mc1-Mc5 juvenile metacarpals have been associated with the KB 5378 carpus and have previously considered to come from the same individual (Vrba 1981). The metacarpal fossils were not available for study and thus I could not assess their functional morphology and limit my analysis to that of size only. Therefore, I tested the association between the carpals and metacarpals via an assessment of absolute size. Both bivariate and absolute length plots of KB 5378 metacarpals indicate that their size is consistent with the carpus of a primate roughly the size of *Papio* or *Mandrillus* (Fig. 28, 29), thus aligning well with the absolute size of the KB 5378 carpals. Therefore, this study confirms that the carpals and metacarpals assigned KB 5378 are likely to belong to the same individual.

The KB 5378 carpals reflect markers of adult morphology including smooth, homogenous cortical surfaces, clearly delineated articular facets, and a fully developed and a well-defined hamate hamulus (Kivell and Begun, 2007). Conversely, the metacarpals of KB 5378 display unfused metacarpal epiphyses indicating they are juvenile. Studies on the timing of epiphyseal fusion in metacarpals on non-hominoid primates are rare, and tend to focus only on large, long bones like the humerus, femur, and occasionally irregular bones such as the pelvis and scapula (Bolter and Zihlman, 2003; Michejda and Bacher, 1981; Newell-Morris et al., 1980; Van Wagenen and Asling, 1964). Studies of these taxa have shown that the rate of epiphyseal fusion from cartilage to fully ossified bone in different areas of the body are irregular, asynchronous, and often variable based on sex (Bolter and Zihlman, 2003; Michejda and Bacher, 1981; Newell-Morris et al., 1980; Van Wagenen and Asling, 1964). Limited studies on populations of members of the genus *Macaca* of known ages have found that while the lunate and capitate are fully matured between 5 and 6 years of age, their metacarpals do not fully mature until 5 to 8 years of age (Hamada, 1984; Kimura and Hamada, 1990). Whereas in larger bodied hominids full maturity of the carpus and metacarpus is reached at 10 to

12 years in *Pan* and 9 to 11 years in *Gorilla* (Kerley, 1966; Kivell and Begun, 2007; Newell-Morris et al., 1980). Although the KB 5378 preserved carpals appear fully adult, the specimens lacks preservation of the scaphoid tubercle and pisiform, two regions/bones that are typically last to fully ossify in the primate carpus (Kivell and Begun, 2007; Newell-Morris et al., 1980). Therefore, the association between the KB 5378 carpals and metacarpals is indeed possible from an ontogenetic perspective. I propose KB 5378 was likely a late juvenile individual whose carpus was potentially almost fully or fully developed before its metacarpals leaving the epiphyseal regions still cartilaginous enough to become fully disjunct (as seen in Fig 3) during the process of fossilization.

Additionally, the KB 5378 metacarpals reflect similar patterns of lengths of Mc2-5 often seen in terrestrial digitigrade primates (Etter, 1973; Patel, 2010a, b; Patel and Maiolino, 2016). This, in addition to morphologies in the carpus listed above, supports the likelihood that KB 5378 spent at least some time on the ground moving quadrupedally.

Interestingly, though Mc2-5 each consistently align KB 5378 with *Papio* and *Mandrillus* in analyses of size, both relative to each other and to the carpus, Mc1 is considerably above average in length. Some extant cercopithecoids are known to have an elongated Mc1, but none in our study exhibited lengthening to the degree seen in KB 5378 (Fig. 28, 29). *Theropithecus gelada* has been studied for its particularly elongated Mc1 that it uses in combination with a shortened first digit to finely pluck the roots and grasses that make up its diet (Etter, 1973; Patel and Maiolino, 2016). Interestingly, *Papio hamadryas* also displays an elongated MC1, though to a lesser degree than *T. gelada*, likely also related to some proportion of its diet consisting of fine grasses and roots (Etter 1973). The exceptional length of KB 5378 Mc1 may therefore be indicative of a diet consisting partly of grasses and roots like that of *T. gelada* and *P. hamadryas*. This, in combination with the results of our univariate analyses of the metacarpals, and qualitative morphologies described above support that KB 5378 had a hand adapted for terrestrial quadrupedalism.

### Overall carpal function

The carpus of KB 5378 presents an interesting mosaic of features representative of those found in arboreal and terrestrial monkeys, but that are typically distinct from knuckle-walking and suspensory taxa. The limited preservation of the scaphoid including its generally broad radial facet and shallow os centrale facet are adaptations to increasing stability of the radiocarpal and midcarpal joints often seen in terrestrial quadrupeds. The presence of a distoradial lunate facet, as well as the slightly acute angle between the scaphoid and trapezoid facets on the os centrale create a joint with improved congruency early on in extension which stabilizes the carpus. The morphology of the lunate tends to support an antebrachial joint built for stability proximally and ulnarly during terrestrial locomotion, but distally does not show traits associated with maximizing midcarpal stability. The trapezium of KB 5378 has unique morphology reflecting both knuckle-walkers and quadrupeds, taxa that are known to have entirely distinct qualitative morphology of their trapezia. The KB 5378 trapezium has a flat, broad, oval shaped Mc1 facet that extends particularly far palmarly and no Mc2 facet suggesting a lack of mobility at both the Mc1 and Mc2 joints. However, some degree of flexion may be regained due to its extremely RU broad Mc1 facet suggesting a more complicated thumb joint than seen in most cercopithecoid taxa. The dorsally wide capitate-trapezoid embrasure and keeled

Mc2 facet of the trapezoid each aid in creating a stable carpus by promoting pronation rather than supination during midcarpal rotation and decreasing radioulnar deviation at the carpo-metacarpal joint. The capitate of KB 5378 shows adaptations to contradictory locomotion types proximally and distally. The proximal head of the capitate is narrow, a trait often seen in suspensory or strictly arboreal primates that allows greater mobility at the midcarpal joint, whereas the distal metacarpal facets are indicative of a generalized midcarpal joint and one specialized for stability. Finally, the hamate of KB 5378 has morphology suggestive of general quadrupedal locomotion based on the proximal orientation of its triquetrum facet, with little climbing and suspensory behaviors indicated due to the diminutive size of its hamulus likely creating a shallow carpal tunnel incapable of accommodating the thick tendons of flexor muscles required for climbing behaviors.

Based on this collective carpal morphology, this study concludes that the most likely reconstruction of KB 5378 locomotor style is that of a generalized quadrupedal monkey, with specializations for digitigrade terrestrial quadrupedalism.

### Taxonomy

This study provides morphological and functional information that aids in potential taxonomic attribution of the KB 5378 fossils. Comparative analyses of overall size suggest that the KB 5378 carpals are too small to be attributed to *Gorgopithecus major*, the taxon originally suggested by Vrba (1981). Delson et al. (2000) estimate *Gorgopithecus* body size to be 30-37 kg, which is approximately the size of adult, female *Pan troglodytes* (c. 31 kg) or adult male *Pan paniscus* (c. 37-39 kg) (Rowe et al., 1996). In plots of absolute size (Fig 26, 27, 28, 29), KB 5378 falls consistently outside the range of variation of *Pan*. Instead, the absolute size of the KB 5378 carpals and metacarpals are most similar to *Papio* (12-37 kg) or *Mandrillus* (10-27 kg) (Rowe et al., 1996). While overlap in body mass ranges do occur between the maximum estimates of *Papio* and lowest estimate for *Gorgopithecus*, KB 5378 also overlaps with *Mandrillus*, a genus whose body mass range falls entirely below that estimated for *Gorgopithecus*. Due to this size discrepancy, I consider the taxonomic affiliation of KB 5378 as *Gorgopithecus* to be unlikely. Instead, known fossil cercopithecoids from Kromdraai and the surrounding contemporaneous fossil bearing sites that are estimated to have body masses within the extant *Papio* and *Mandrillus* size range include *Papio*, *Parapapio* or *Cercopithecoides*. Based on absolute size, I suggest that KB 5378 is more likely attributed to one of these fossil taxa.

Moreover, based on trends of external comparative morphology including mixed traits of a general quadruped, with some potential specializations to terrestrial quadrupedalism, in combination with the estimated size of KB 5378, a mixed arboreal/terrestrial locomotor repertoire is the most realistic reconstruction based on the carpus of KB 5378. This supports the likelihood that KB 5378 belongs to a species of *Papio*, or *Parapapio*, but may remove potential for identification as *Cercopithecoides* due to the exclusively terrestrial adaptations of that genus (Benefit, 1999; Leakey, 1982; Williams and Geissler, 2014).

### Limitations

There are several limitations to this study. Firstly, a lack of post cranial remains of closely related taxa- specifically of contemporaneous cercopithecoid primates- makes parsing the impacts of phylogeny on morphology from truly functional morphological traits difficult. It is well known that phylogeny impacts bony morphology. Studies specific to

primates often reveal symplesiomorphies in seemingly behaviorally distinct taxa (Szalay, 1981; Szalay and Dagosto, 1980; Vančata, 1991). As such, interpretation of behavior from isolated fossils in comparison to extant taxa must be done with phylogenetic impacts in mind. This study was unable to integrate phylogenetically adjusted statistics and as such may describe some traits that are in reality symplesiomorphies, or homologous traits retained from an ancestral state. Further studies on the phylogenetic history of Pleistocene cercopithecoids would enrich our understanding of such morphologies.

This lack in comparative fossil data additionally complicates taxonomic attribution. Carpal remains of fossil cercopithecoids are extremely limited, and for the purposes of this study proved inaccessible to comparative inclusion. Much would be gained in the future through inclusion of novel or known fossil cercopithecoid carpals.

### Conclusions:

This study aimed to report the external morphology of a partial, fossilized carpus belonging to an African Pleistocene cercopithecoid, KB 5378. Further, it then aimed to compare the morphology of each bone included in the partial carpus to identify the specimen within the fossil record and infer locomotor behaviors.

Using both quantitative and qualitative methods, this study revealed that both the carpals and metacarpals attributed to KB 5378 are likely too small to belong to the exceptionally large *Gorgopithecus major*. Instead, they may be attributed to a smaller bodied cercopithecoid from Kromdraai B such as *Papio* or *Parapapio*. Further, the results of this study indicate that the morphology of the KB 5378 carpus displays a mosaic of features from both arboreal and terrestrial quadrupedal monkeys, and that they overall suggest a generalized quadruped with some specializations for terrestrial quadrupedalism. This generalized morphology supports the likelihood that the KB 5378 carpus is likely to belong to *Papio*, *Parapapio* -genera known to have been mixed terrestrial/arborealists (Benefit, 1999; Bettridge and Dunbar, 2012; Ciochon, 1993a; Delson et al., 2000; Frost and Delson, 2002; Hartwig, 2002)

It is well known that drawing conclusions based on external morphology alone can be a challenging process. Ontological changes during life, development and phylogenetic factors can all influence the external morphology of bones making functional interpretation difficult (see Kivell (2016b) for a review). An interesting way to gain a deeper understanding of habitual behavior during life is the use of microCT to examine the internal bone structure of a specimen. These methods allow the researcher to view microscopic changes in bone structural anatomy known to indicate locomotor pattern in many postcranial elements of the primate skeleton (Barak et al., 2011; Bird et al., 2021; Dunmore et al., 2020; Stephens et al., 2018). Further investigations combining the external morphology described in this study with microCT studies of the internal anatomy may reveal a more definitive description of the functional anatomy of the KB 5378 carpus, and consequently aid in taxonomic identification therein.

### Acknowledgements:

I would like to thank the following institutions and individuals for access to comparative extant and/or fossil specimens: Mike Rose, the Ditsong National Museum of Cultural History, Kenyan national Museum, University of Toronto Biological Anthropology collections, Royal Ontario Museum, Museum of Comparative Zoology, Harvard, State

University New York, University of Toronto at Scarborough, Museum für Naturkunde, Berlin, Cleveland Museum of Natural History, Royal Museum for Central Africa, University of Toronto, Max Planck Institute for Evolutionary Anthropology, Tai chimp collection, Senckenberg Museum Frankfurt, Powell Cotton Museum, American Museum of Natural History, and the Smithsonian National Museum of Natural History. Additionally, I would like to thank both the internal and external examiners, Dr. Chris Dunmore and Dr. Chris Wuthrich, for their invaluable feedback and advisement. As well as Tracy Kivell, Matthew Skinner, and Theodore Smith for their assistance in all aspects of this study.

#### References cited

- Barak, M.M., Lieberman, D.E., Hublin, J.-J., 2011. A Wolff in sheep's clothing: trabecular bone adaptation in response to changes in joint loading orientation. *Bone* 49, 1141-1151.
- Benefit, B., 1999. Biogeography, dietary specialization, and the diversification of African Plio-Pleistocene monkeys. *African biogeography, climate change, and human evolution*, 172-188.
- Bettridge, C.M., Dunbar, R., 2012. Modeling the biogeography of fossil baboons. *International Journal of Primatology* 33, 1278-1308.
- Bird, E.E., Kivell, T.L., Skinner, M.M., 2021. Cortical and trabecular bone structure of the hominoid capitate. *Journal of Anatomy*.
- Bolter, D.R., Zihlman, A.L., 2003. Morphometric analysis of growth and development in wild-collected vervet monkeys (*Cercopithecus aethiops*), with implications for growth patterns in Old World monkeys, apes and humans. *Journal of Zoology* 260, 99-110.
- Bookstein, F.L., 2019. Pathologies of between-groups principal components analysis in geometric morphometrics. *Evolutionary Biology* 46, 271-302.
- Braga, J., Fourvel, J.-B., Lans, B., Bruxelles, L., Thackeray, J.F., Braga, J., Thackeray, J., 2016. Evolutionary, chrono-cultural and palaeoenvironmental backgrounds to the Kromdraai site: a regional perspective. *Kromdraai: A Birthplace of Paranthropus in the Cradle of Humankind*, 1-16.
- Braga, J., Thackeray, J.F., Bruxelles, L., Dumoncel, J., Fourvel, J.-B., 2017. Stretching the time span of hominin evolution at Kromdraai (Gauteng, South Africa): Recent discoveries. *Comptes Rendus Palevol* 16, 58-70.
- Brain, C., 1975. An interpretation of the bone assemblage from the Kromdraai australopithecine site, South Africa. *Paleoanthropology, morphology and paleoecology*, 225-243.
- Broom, R., 1940. The South African Pleistocene cercopithecoid apes. *Annals of the Transvaal Museum* 20, 89-100.
- Broom, R., Robinson, J., 1949. A new type of fossil baboon, *Gorgopithecus major*, *Proceedings of the Zoological Society of London*. Wiley Online Library, pp. 379-386.
- Bruxelles, L., Maire, R., Couzens, R., Thackeray, J.F., Braga, J., 2016. A revised stratigraphy of Kromdraai. *Kromdraai, a Birthplace of Paranthropus in the Cradle of Humankind*. SUN MeDIA MeTRO, Stellenbosch, South Africa, 31-47.
- Cant, J.G., 1988. Positional behavior of long-tailed macaques (*Macaca fascicularis*) in northern Sumatra. *American Journal of Physical Anthropology* 76, 29-37.

- Cant, J.G.H., 1986. Locomotion and feeding postures of spider and howling monkeys: field study and evolutionary interpretation. *Folia Primatologica* 46, 1-14.
- Carlson, K.J., Patel, B.A., 2006. Habitual use of the primate forelimb is reflected in the material properties of subchondral bone in the distal radius. *Journal of Anatomy* 208, 659-670.
- Ciochon, R., 1993a. Evolution of the cercopithecoid forelimb. Phylogenetic and functional implications from morphometric analyses. University Of California Press, Berkeley, CA.
- Ciochon, R.L., 1993b. Evolution of the cercopithecoid forelimb: phylogenetic and functional implications from morphometric analyses. University of Iowa.
- Daver, G., Berillon, G., Grimaud-Hervé, D., 2012. Carpal kinematics in quadrupedal monkeys: towards a better understanding of wrist morphology and function. *Journal of Anatomy* 220, 42-56.
- Deak, N., Bordoni, B., 2019. Anatomy, Shoulder and Upper Limb, Wrist Flexor Retinaculum.
- Defler, T.R., 2000. Locomotion and posture in *Lagothrix lagotricha*. *Folia Primatologica* 70, 313-327.
- Delson, E., Terranova, C.J., Jungers, W.L., Sargis, E.J., Jablonski, N.G., 2000. Body mass in Cercopithecidae (Primates, Mammalia): estimation and scaling in extinct and extant taxa. *Anthropological papers of the AMNH*; no. 83.
- Dunbar, R., Dunbar, E., 1974. Ecological relations and niche separation between sympatric terrestrial primates in Ethiopia. *Folia Primatologica* 21, 36-60.
- Dunmore, C.J., Bardo, A., Skinner, M.M., Kivell, T.L., 2020. Trabecular variation in the first metacarpal and manipulation in hominids. *American Journal of Physical Anthropology* 171, 219-241.
- El-Zaatari, S., Grine, F.E., Teaford, M.F., Smith, H.F., 2005. Molar microwear and dietary reconstructions of fossil Cercopithecoidea from the Plio-Pleistocene deposits of South Africa. *Journal of Human Evolution* 49, 180-205.
- Etter, H., 1973. Terrestrial adaptations in the hands of Cercopithecinae. *Folia Primatologica* 20, 331-350.
- Fleagle, J., 1978. Locomotion, posture and habitat utilization in two sympatric Malayan leaf monkeys. *Ecology of arboreal folivores*.
- Fleagle, J.G., 1976. Locomotion and posture of the Malayan siamang and implications for hominoid evolution. *Folia Primatologica* 26, 245-269.
- Fleagle, J.G., 1998. *Primate Adaptation and Evolution*. Elsevier.
- Fourvel, J.-B., Brink, J., O'regan, H., Beaudet, A., Pavia, M., 2016. Some preliminary interpretations of the oldest faunal assemblage from Kromdraai. Kromdraai, a Birthplace of Paranthropus in the Cradle of Humankind. SUN MeDIA MeTRO, Stellenbosch, South Africa, 71-104.
- Freedman, L., 1957. The fossil cercopithecoidea of South Africa. *Annals of the Transvaal Museum* 23, 121-262.
- Frost, S.R., Delson, E., 2002. Fossil Cercopithecidae from the Hadar Formation and surrounding areas of the Afar Depression, Ethiopia. *Journal of Human Evolution* 43, 687-748.

- Frost, S.R., Gilbert, C.C., Pugh, K.D., Guthrie, E.H., Delson, E., 2015. The hand of *Cercopithecoides williamsi* (Mammalia, Primates): earliest evidence for thumb reduction among colobine monkeys. *PLoS one* 10, e0125030.
- Gear, J., 1926. A preliminary account of the baboon remains from Taungs. *South African Journal of Science* 23, 731-747.
- Gebo, D.L., Chapman, C.A., 1995. Positional behavior in five sympatric Old World monkeys. *American Journal of Physical Anthropology* 97, 49-76.
- Gebo, D.L., Sargis, E.J., 1994. Terrestrial adaptations in the postcranial skeletons of guenons. *American Journal of Physical Anthropology* 93, 341-371.
- Hamada, Y., 1984. Age changes of the carpal bones in macaques: application of the Fourier analysis on the radiographs. *Primates* 25, 485-506.
- Hamrick, M.W., 1996. Locomotor adaptations reflected in the wrist joints of early Tertiary primates (Adapiformes). *American Journal of Physical Anthropology: The Official Publication of the American Association of Physical Anthropologists* 100, 585-604.
- Hamrick, M.W., 2007. Evolvability, limb morphology, and primate origins, *Primate origins: Adaptations and evolution*. Springer, pp. 381-401.
- Hartwig, W.C., 2002. *The primate fossil record*. Cambridge University Press Cambridge.
- Hunt, K.D., 1991. Positional behavior in the Hominoidea. *International Journal of Primatology* 12, 95-118.
- Jungers, W.L., Falsetti, A.B., Wall, C.E., 1995. Shape, relative size, and size-adjustments in morphometrics. *American Journal of Physical Anthropology* 38, 137-161.
- Kerley, E.R., 1966. Skeletal age changes in the chimpanzee. *Tulane Studies Zool.* 13, 71-82.
- Kimura, T., Hamada, Y., 1990. Development of epiphyseal union in Japanese macaques of known chronological age. *Primates* 31, 79-93.
- Kivell, T.L., 2016a. The primate wrist. *The evolution of the primate hand*, 17-54.
- Kivell, T.L., 2016b. A review of trabecular bone functional adaptation: what have we learned from trabecular analyses in extant hominoids and what can we apply to fossils? *Journal of Anatomy* 228, 569-594.
- Kivell, T.L., Begun, D.R., 2007. Frequency and timing of scaphoid-centrale fusion in hominoids. *Journal of Human Evolution* 52, 321-340.
- Leakey, M.G., 1982. Extinct large colobines from the Plio-Pleistocene of Africa. *American Journal of Physical Anthropology* 58, 153-172.
- Lee-Thorp, J., Sponheimer, M., Luyt, J., 2007. Tracking changing Pliocene environments of the South African hominin sites using stable isotopes in faunal tooth enamel. *Journal of Human Evolution* 53, 595-601.
- Lewis, O.J., 1989. *Functional morphology of the evolving hand and foot*. Oxford University Press, USA.
- Lovejoy, C.O., Simpson, S.W., White, T.D., Asfaw, B., Suwa, G., 2009. Careful climbing in the Miocene: the forelimbs of *Ardipithecus ramidus* and humans are primitive. *science* 326, 70-70e78.
- Marzke, M.W., 1983. Joint functions and grips of the *Australopithecus afarensis* hand, with special reference to the region of the capitate. *Journal of Human Evolution* 12, 197-211.

- McCrossin, M.L., Benefit, B.R., Gitau, S.N., Palmer, A.K., Blue, K.T., 1998. Fossil evidence for the origins of terrestriality among Old World higher primates, *Primate locomotion*. Springer, pp. 353-396.
- McGraw, W.S., 2004. Diversity of guenon positional behavior, *The guenons: Diversity and adaptation in African monkeys*. Springer, pp. 113-131.
- Michejda, M., Bacher, J., 1981. Skeletal age as a determinant of gestation in *Macaca mulatta*: a radiographic study. *Journal of Medical Primatology* 10, 293-301.
- Mittermeier, R.A., 1978. Locomotion and posture in *Ateles geoffroyi* and *Ateles paniscus*. *Folia Primatologica* 30, 161-193.
- Morbeck, M.E., 1977. Positional behavior, selective use of habitat substrate and associated non-positional behavior in free-ranging *Colobus guereza* (Rüppel, 1835). *Primates* 18, 35-58.
- Nakatsukasa, M., 1994. Morphology of the humerus and femur in African mangabeys and guenons: functional adaptation and implications for the evolution of positional behavior. *African study monographs. Supplementary issue*. 21, 1-61.
- Newell-Morris, L., Tarrant, L.H., Fahrenbruch, C.E., Burbacher, T.M., Sackett, G.P., 1980. Ossification in the hand and foot of the pigtail macaque (*Macaca nemestrina*). II. Order of appearance of centers and variability in sequence. *American Journal of Physical Anthropology* 53, 423-439.
- O'Connor, B.L., 1975. The functional morphology of the cercopithecoid wrist and inferior radioulnar joints, and their bearing on some problems in the evolution of the Hominoidea. *American Journal of Physical Anthropology* 43, 113-121.
- Orr, C.M., 2018. Kinematics of the anthropoid os centrale and the functional consequences of scaphoid-centrale fusion in African apes and hominins. *Journal of Human Evolution* 114, 102-117.
- Patel, B.A., 2010a. Functional morphology of cercopithecoid primate metacarpals. *Journal of Human Evolution* 58, 320-337.
- Patel, B.A., 2010b. The interplay between speed, kinetics, and hand postures during primate terrestrial locomotion. *American Journal of Physical Anthropology: The Official Publication of the American Association of Physical Anthropologists* 141, 222-234.
- Patel, B.A., Maiolino, S.A., 2016. Morphological diversity in the digital rays of primate hands, *The evolution of the primate hand*. Springer, pp. 55-100.
- Queen, J.P., Quinn, G.P., Keough, M.J., 2002. *Experimental design and data analysis for biologists*. Cambridge university press.
- Rein, T.R., Harvati, K., 2013. Exploring third metacarpal capitate facet shape in early hominins. *The Anatomical Record* 296, 240-249.
- Richmond, B.G., 2006. Functional morphology of the midcarpal joint in knuckle-walkers and terrestrial quadrupeds, *Human origins and environmental backgrounds*. Springer, pp. 105-122.
- Rodman, P.S., 1979. Skeletal differentiation of *Macaca fascicularis* and *Macaca nemestrina* in relation to arboreal and terrestrial quadrupedalism. *American Journal of Physical Anthropology* 51, 51-62.
- Rose, M., 1973. Quadrupedalism in primates. *Primates* 14, 337-357.
- Rowe, N., Goodall, J., Mittermeier, R., 1996. *The pictorial guide to the living primates*. Pogonias Press New York.

- Schmitt, D., 2003. Mediolateral reaction forces and forelimb anatomy in quadrupedal primates: implications for interpreting locomotor behavior in fossil primates. *Journal of Human Evolution* 44, 47-58.
- Selby, M.S., Simpson, S.W., Lovejoy, C.O., 2016. The functional anatomy of the carpometacarpal complex in anthropoids and its implications for the evolution of the hominoid hand. *The Anatomical Record* 299, 583-600.
- Stephens, N.B., Kivell, T.L., Pahr, D.H., Hublin, J.-J., Skinner, M.M., 2018. Trabecular bone patterning across the human hand. *Journal of Human Evolution* 123, 1-23.
- Szalay, F.S., 1981. Phylogeny and the problem of adaptive significance: the case of the earliest primates. *Folia Primatologica* 36, 157-182.
- Szalay, F.S., Dagosto, M., 1980. Locomotor adaptations as reflected on the humerus of Paleogene primates. *Folia Primatologica* 34, 1-45.
- Thackeray, J.F., 2017. Kromdraai: A birthplace of *Paranthropus* in the cradle of humankind. *AFRICAN SUN MEDIA*.
- Tocheri, M.W., Marzke, M., Liu, D., Bae, M., Jones, G., Williams, R., Razdan, A., 2003. Functional capabilities of modern and fossil hominid hands: three-dimensional analysis of trapezia. *American Journal of Physical Anthropology: The Official Publication of the American Association of Physical Anthropologists* 122, 101-112.
- Tocheri, M.W., Razdan, A., Williams, R., Marzke, M., 2005. A 3D quantitative comparison of trapezium and trapezoid relative articular and nonarticular surface areas in modern humans and great apes. *Journal of Human Evolution* 49, 570-586.
- Tuttle, R., 1969. Terrestrial trends in the hands of the Anthropeidea. A preliminary report. CR Carpenter (Ed.) *Recent Advances in Primatology*, New York and Basel (S. Karger) 1969, pp. 187-191.
- Tuttle, R.H., 1967. Knuckle-walking and the evolution of hominoid hands. *American Journal of Physical Anthropology* 26, 171-206.
- van der Spuy Mollett, O., 1947. Fossil mammals from the Makapan valley, Potgietersrust, I. *Primates. South African Journal of Science* 43, 295-303.
- Van Wagenen, G., Asling, C., 1964. Ossification in the fetal monkey (*Macaca mulatta*). Estimation of age and progress of gestation by roentgenography. *American journal of anatomy* 114, 107-132.
- Vančata, V., 1991. Evolution of femur and tibia in higher primates: Adaptive morphological patterns and phylogenetic diversity. *Human evolution* 6, 1-47.
- Vanhoof, M.J., Galletta, L., De Groote, I., Vereecke, E.E., 2021. Functional signals and covariation in triquetrum and hamate shape of extant primates using 3D geometric morphometrics. *Journal of Morphology* 282, 1382-1401.
- Vrba, E., 1981. The Kromdraai australopithecine site revisited in 1980; recent investigations and results. *Annals of the Transvaal Museum* 33, 17-60.
- Ward, C., Leakey, M., Brown, B., Brown, F., Harris, J., Walker, A., 1999. South Turkwel: a new Pliocene hominid site in Kenya. *Journal of Human Evolution* 36, 69-95.
- Ward, C.V., 2002. Interpreting the posture and locomotion of *Australopithecus afarensis*: where do we stand? *American Journal of Physical Anthropology: The Official Publication of the American Association of Physical Anthropologists* 119, 185-215.
- Williams, F.L.E., Geissler, E., 2014. Reconstructing the diet and paleoecology of Plio-Pleistocene *Cercopithecoides williamsi* from Sterkfontein, South Africa. *Palaos* 29, 483-494.

